INVESTIGATION OF MASS WASTING IN THE VICINITY OF KHAO KHO, CENTRAL THAILAND USING TIME – SERIES INSAR TECHNIQUE

Mr. Nuttavit Kumvijairat

จุฬาลงกรณ์มหาวิทยาลัย
CHULALONGKORN UNIVERSITY

A Thesis Submitted in Partial Fulfillment of the Requirements
for the Degree of Master of Science in Earth Sciences
Department of Geology
FACULTY OF SCIENCE
Chulalongkorn University
Academic Year 2022

การตรวจสอบการเคลื่อนที่ของมวลในพื้นที่เขาค้อ ภาคกลางของประเทศไทยด้วยเทคนิคอนุกรม
เวลาอินซาร์

นายนัทวิชญ์ คุ้มวิจัยรัตน์

วิทยานิพนธ์นี้เป็นส่วนหนึ่งของการศึกษาตามหลักสูตรปริญญาวิทยาศาสตรมหาบัณฑิต
สาขาวิชาโลกศาสตร์ ภาควิชาธรณีวิทยา
คณะวิทยาศาสตร์ จุฬาลงกรณ์มหาวิทยาลัย
ปีการศึกษา 2565

Thesis Title	INVESTIGATION OF MASS WASTING IN THE VICINITY OF KHAO KHO, CENTRAL THAILAND USING TIME – SERIES INSAR TECHNIQUE
By	Mr. Nuttavit Kumvijairat
Field of Study	Earth Sciences
Thesis Advisor	Professor PITSANUPONG KANJANAPAYONT, Dr.rer.nat.

Accepted by the FACULTY OF SCIENCE, Chulalongkorn University in Partial Fulfillment of the Requirement for the Master of Science

.... Dean of the FACULTY OF SCIENCE
(Professor POLKIT SANGVANICH, Ph.D.)

THESIS COMMITTEE

.... Chairman
(Professor SRILERT CHOTPANTARAT, Ph.D.)
.... Thesis Advisor
(Professor PITSANUPONG KANJANAPAYONT, Dr.rer.nat.)
.... Examiner
(Professor SANTI PAILOPLEE, Ph.D.)
.... External Examiner
(Assistant Professor Krit Won-in, Ph.D.)

นัทวิชญ์ คุ้มวิจัยรัตน์ : การตรวจสอบการเคลื่อนที่ของมวลในพื้นที่เขาค้อ ภาคกลางของประเทศไทยด้วยเทคนิค อนุกรมเวลาอินซาร์ . (INVESTIGATION OF MASS WASTING IN THE VICINITY OF KHAO KHO, CENTRAL THAILAND USING TIME – SERIES INSAR TECHNIQUE) อ.ที่ปรึกษาหลัก : ศ. ดร.พิษณุพงศ์ กาญจนพยนต์

การสำรวจระยะไกลแบบอนุกรมเวลาอินซาร์ได้นำมาใช้เพื่อการวิเคราะห์อัตราการเคลื่อนที่ของมวลบริเวณพื้นที่เขา ค้อ และพื้นที่โดยรอบตามแนวเทือกเขาเพชรบูรณ์ การศึกษานี้มีวัตถุประสงค์เพื่อการตรวจสอบการเคลื่อนที่ของพื้นผิวดิน และ นำผลลัพธ์จากการตรวจสอบมาใช้จำแนกประเภทของการเคลื่อนที่ของมวล ในงานศึกษานี้ใช้ข้อมูลโทรสัมผัส ที่มีระบบบันทึก แบบมีพลัง โดยอาศัยภาพถ่ายดาวเทียมเรดาห์ช่องเปิดสังเคราะห์ จากดาวเทียม Sentinel-1A และ Sentinel-1B ระหว่างปี ค.ศ. 2015 จนถึง ค.ศ. 2018 ผลจากการวิเคราะห์ได้จำนวนจุดภาพที่ใช้เป็นจุดตรวจสอบจำนวน 7,354 จุด สำหรับบวงโคจรดาวเทียมเดินทางจากทิศใต้สู่ทิศเหนือ และ 8,984 จุด สำหรับบวงโคจรดาวเทียมเดินทางจากทิศเหนือสู่ทิศใต้ โดยมีค่าเฉลี่ยอัตราการเคลื่อนตัวจากจุดตรวจสอบสำหรับบวงโคจรดาวเทียมเดินทางจากทิศใต้สู่ทิศเหนือ 65.19 มิลลิเมตรต่อปี และ 13.97 มิลลิเมตรต่อปี เมื่อนำอัตราการเคลื่อนตัวที่ได้รับมาจำแนกตามมาตรฐานการแบ่งเกณฑ์การเคลื่อนที่ของมวลจาก งานวิจัยอื่น พบว่ากษณะการเคลื่อนที่ของมวลที่ได้ตรวจสอบได้อยู่ในลักษณะการเคลื่อนที่แบบคืบคลานเป็นหลักโดยเฉพาะจุด ตรวจสอบส่วนใหญ่อยู่บริเวณพื้นที่เมืองที่มีสิ่งปลูกสร้างจำนวนมาก และเมื่อนำผลลัพธ์ที่ได้นี้ไปเปรียบเทียบกับผลลัพธ์การ วิเคราะห์พื้นที่อ่อนไหวการเกิดดินถล่มของกรมทรัพยากรธรณี, เสถียรภาพความลาดชันในพื้นที่, พื้นที่อ่อนไหวตะกอนไหล ถล่มและน้ำปนตะกอนบ่า จะเห็นว่าผลลัพธ์ที่ได้จากงานค้นคว้านี้สอดคล้องกับข้อมูลพื้นที่อ่อนไหวค่อนข้างมาก แต่ค่อนข้างมี ความแตกต่างกันมากสำหรับพื้นที่อ่อนไหวการเกิดดินถล่มของกรมทรัพยากรธรณี, พื้นที่อ่อนไหวตะกอนไหลถล่มและน้ำปน ตะกอนบ่า และบันทึกดินถล่มในอดีต เนื่องจากผลลัพธ์ที่เกิดจากการเคลื่อนตัวที่ช้าอย่างการคืบคลานของมวลกับการเคลื่อนที่ แบบฉับพลันอย่างดินถล่มและตะกอนไหลถล่มมีสาเหตุการเกิดที่แตกต่างกัน ทำให้การกระจายตัวของจุดไม่อยู่ในตำแหน่ง เดียวกันแตกอาจแสดงในรูปแบบตำแหน่งรอบข้างแทน

สาขาวิชา	โลกศาสตร์	ลายมือชื่อนิสิต ....
ปีการศึกษา	2565	ลายมือชื่อ อ.ที่ปรึกษาหลัก ....

6071954023 : MAJOR EARTH SCIENCES

KEYWOR D: InSAR, PSInSAR, Time-series InSAR, Mass wasting, Microwave remote sensing, Remote sensing

Nuttavit Kumvijairat : INVESTIGATION OF MASS WASTING IN THE VICINITY OF KHAO KHO, CENTRAL THAILAND USING TIME – SERIES INSAR TECHNIQUE . Advisor: Prof. PITSANUPONG KANJANAPAYONT, Dr.rer.nat.

The application of time-series InSAR has been employed for investigation of mass wasting in the Khao Kho and Phetchabun mountain range. The objective of this study is to Investigation of mass wasting by SAR data between 2015 to 2018 and classification of mass wasting by displacement rate millimeter/year. This study using active remote sensing data, which is Synthetic Aperture Radar (SAR) satellite imagery from Sentinel-1A and Sentinel-1B satellites. Result from PSInSAR analysis yielded a total of 7,354 PS points for ascending orbit, and 8,984 PS point for descending orbit. The average ground displacement rate result from ascending orbit is 65.19 millimeters per year, while displacement rate from ascending orbit is 13.97 millimeters per year. The classifying obtained displacement rates using the criteria for categorizing mass wasting type by other research, it was found that the observed mass wasting characteristics in study area dominant by Creep movement, particularly PS points in urban areas. Then, the result of this study comparing with landslide susceptibility data, slope stability map, debris flow-flood susceptibility data and Landslide inventory. This research result presents a correspond with the slope stability map. in the other hand, landslide susceptibility data, debris flow-flood susceptibility data and Landslide inventory give a little of relation due to velocity and factor of occurring between Creep and landslide are quite different.

จุฬาลงกรณ์มหาวิทยาลัย

CHULALONGKORN UNIVERSITY

Field of Study:	Earth Sciences	Student's Signature
		....
Academic Year:	2022	Advisor's Signature
		....

ACKNOWLEDGEMENTS

TABLE OF CONTENTS

LIST OF TABLES

LIST OF FIGURES

Chapter 1   Introduction

1.1 Introduction

Mass wasting is a movement along a sloped surface by the gravitational effects of large amounts of soil, rock, and organic materials. Although the movement is a geomorphologic process, which typically occurs on the Earth's surface, the movement can hurt human life, building, and agricultural area. High-intensity rainfall is the most crucial trigger of mass wasting because water can increase surface material's weight, improving the gravitational effect. Mass wasting occurs with high water volume and long-time rainfall and could develop into critical hazards such as debris floods. Thailand has a tropical climate in the Köppen climate classification. The amount of rainfall depends on monsoon wind, especially the South-west monsoon (May-October), which brings the rainy season to most regions of Thailand. That describes how often and the potential of mass wasting in Thailand, especially high slope areas along the mountain.

The new study of mass wasting applies spatial data analysis technology, including Remote sensing, Geographic Information System (GIS) and Global Positioning System (GPS) to measurement, investigation, and monitoring. The information obtained by those techniques is important for understanding the behavior of surface movement, which take advantage of hazard risk assessment. Earth Observation satellite is an easy way to approach information in interesting areas with the capacity to collect wide-area images, which make the facility to approach information cover interesting area. Remote sensing is divided into two types active and passive remote sensing. Passive remote sensing uses a sensor to measure sunlight energy reflected from the Earth's surface. So, passive remote sensing can only work when sunlight is available.

On the other hand, Active Remote sensing uses the energy transmitted from the sensor to illuminate the image. Therefore, Active remote sensing can obtain the image from an interested area even have no

sunlight in that area. Active remote sensing is suitable for monitor phenomenal on the Earth or hazard.

The most populated sensor of active remote sensing is Real aperture radar (RAR), a system that uses microwave wavelength. RAR have an advantage for monitoring the earth phenomenon or military objective. Although RAR has been very widely used for earth monitoring, but it has some disadvantages, such as low-resolution pixels of RAR images, that make important limits to applying the RAR image for some Earth observation work. Later, the RAR data was used widely, and the researcher developed new technology to resolve the RAR disadvantage: Synthetic aperture radar (SAR) or SAR. SAR was developed to resolve the low-resolution problem of RAR data.

InSAR is the process of SAR image which uses differential microwave phase or find the interferometric phase from different acquisition times. The character of the InSAR technique, which measures a difference of two times or two images of SAR data, is a chance to use for observing the Earth's surface phenomenon of the natural hazard. The initial period of using InSAR for earth observation focused on analysing interferometric phase to estimate the Earth's surface deformation. That reach facilitatively to the quantitative of Earth surface deformation, Differential interferometry SAR (DInSAR) can provide deformation rates of the Earth's surface and process with a low number of SAR images. Although DInSAR is a convenient and fast method for estimating deformation by SAR images, the result of this method depends on the characteristic of the study area properties. The coherence value is representative of the correlation between each SAR image. Coherence loss may cause by the different surface between 2 times the acquisition of SAR, especially temporal decorrelation and atmospheric effects as example, if the study area is located at dense vegetation area, that have a low correlation value between 2 SAR image. Thus, uncorrelated temporal can be removed by using Time-series analysis SAR images to avoid the coherence value loss, Permanent scattterer interferometric synthetic aperture radar (PSInSAR), this technique employs multitemporal SAR data, and InSAR approaches estimate to find average better coherence point, that point is identified to be stability pixel or PS pixel. PS pixels

achieve from the one stable scatterer, which is reduced background pixel is stable phase might be an echo from a large rock or man-made building. scatterers to be small enough to enable extraction of the deformation signal.

The purpose of this study focuses on two targets. Firstly, the investigation of surface displacement velocity by Permanent Scatterers Interferometric Synthetic Aperture Radar (PSInSAR) technique. The PSInSAR technique is one type of time-series analysis that can detect and investigate Earth surface displacement along the Line of Sight (LOS) direction. Secondly, the Classification of mass wasting uses the results from the first purpose, displacement rate or LOS velocity, which is the proportion between distance and time displacement. That result is available to help regional and urban planners for mitigate injury from mass wasting.

1.2 Objective of Research

1. The main objective of this study is investigation of mass wasting in KHAO KHO sub water shade and PHETCHABUN mountain range using Time-series InSAR technique.

2. Classification of mass wasting type criteria by mass displacement rates.

1.3 Scope and Limitation

This study investigates surface displacement on the Phetchabun mountain range boundary with the intersection between Sentinel-1A (Ascending orbital direction) and 1B (Descending orbital direction) image acquisition scene. The area of interest is about 1,400 square kilometers, covering travel and economic activity area, including Phu Thap Boek and Khao Kho district.

The investigation of mass wasting will carry out by The Sentinel Application Platform (SNAP) and PSInSAR technique using Stanford Method for Persistent Scatterers (StaMPS) algorithm (Hooper et al., 2012). The result of PSInSAR will generate Permanent scatterer point

(PS point), which contains displacement value in millimeters per year (mm/yr) accuracy. SAR data used in this study were acquired in December 2015 to 2018 both ascending and descending orbital directions. The displacement rate from PS point will be classified by mass wasting velocity scale from International Union of Geological Sciences Working Group on landslide, 1995 and United States Geological Survey (USGS).

1.4 Expected Results

1. The surface displacement map with PS pixel.

2. The mass wasting type report will be classified by displacement rates.

1.5 Characterization of the study area

The study area is between Phetchabun and Phitsanulok provinces. The special character of the area is the high steep slope along with the Phetchabun range (Figure 1.1). The Phetchabun mountain range is once part of the Lieo-Phtchabun mountain range, which is covered by the Korat plateau. The Phetchabun range has controlled by Nan-Uttaradit Ophiolite. The high elevation and steep slope area in the Phetchabun mountain range were forced by plate tectonics between the Shan-Thai plate and Indochina plate from late Permian and uplifted in the late Cretaceous until Tertiary. The mountain range is oriented north-south along with Petchabun Fault Zone.

The area has Earth activity, especially the erosion process, that is the main cause of slope, including the geological hazard as mass wasting. The study area is significant to the economy because the favoured travel place in Phetchabun province KHAO KHO and PHU THAP BOEK located in this range. Thus, arriving to those places requires a road which builds on the mountain. This study area interests on Phetchabun mountain range, covering approximately 1,400 square kilometres. This mountain setting on the Korat plateau margin along a north-south trend, therefore the mountain slope faces to the east and west direction, is shown in (figure 1.2).
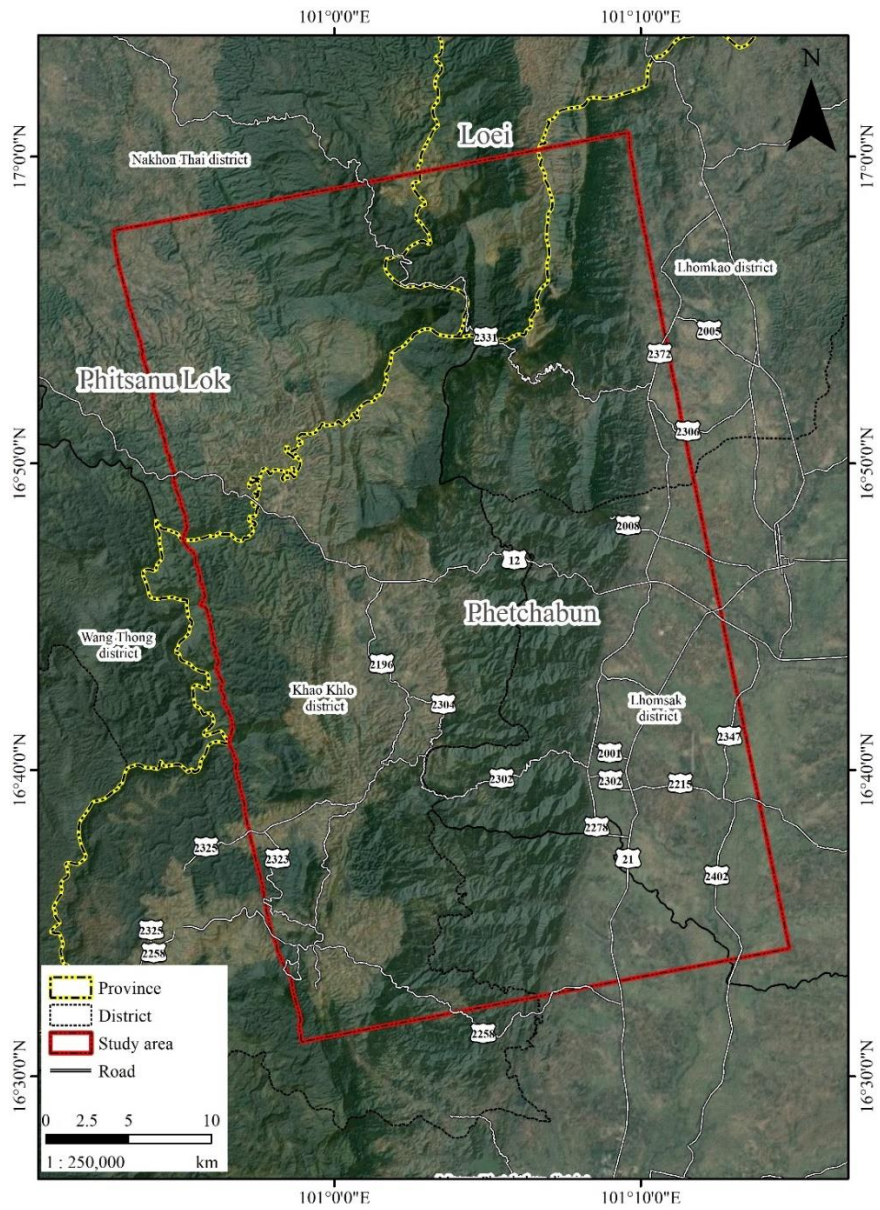
Figure 1.1 High resolution satellite image of study area
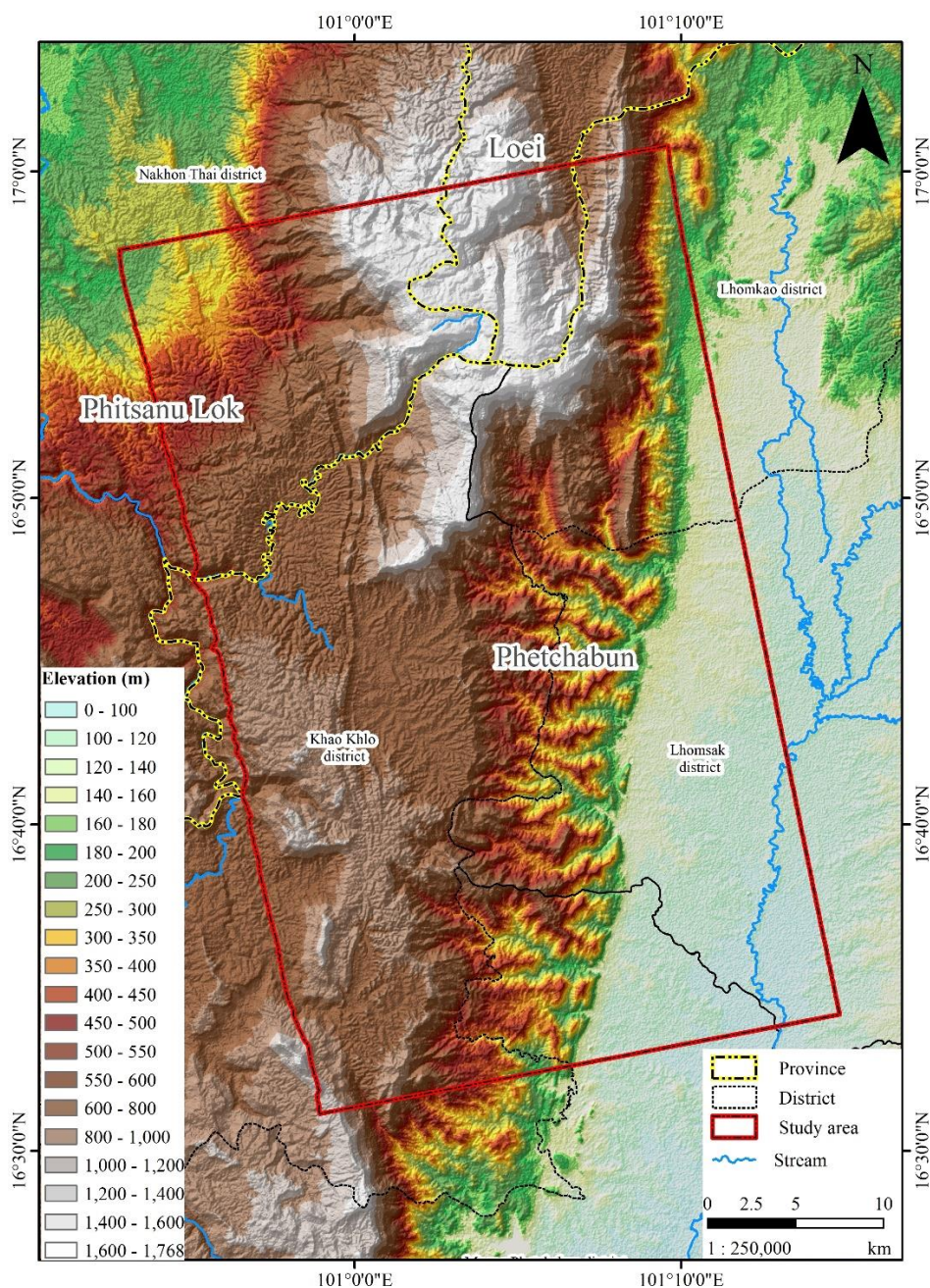
Figure 1.2 Topography of the study area

The weather at the study area is separated into 3 seasons, including summer, rainy season, and winter. Seasons in the Phetchabun province depend on 2 monsoons, those are summer monsoon and winter monsoon. The south-west or summer monsoon cover the Thailand between February to October and north-east or winter monsoon cover between October to January. According to 2 major monsoon, Thailand and Phetchabun province can divide seasons in three seasons as follow.

1)   Summer season is on February - May when the study area is affected by the south-west monsoon and weak northeast monsoon. The average temperature about higher that 29 ℃, especially, April is the highest temperature of years because Sun ray be perpendicular to around Thailand.

2)   Rainy season is on middle May – middle October when the study area is affected by the southwest monsoon or rainy monsoon. Humidity and rain are emanated from Andaman Sea and Bengal gulf. The average annual rainfall in rainy season is 1,300 to 1,700 mm per years, whereas the highest rainfall is in September.

3)   Winter season is in October to February, the season is caused by high pressure or cold weather from north - east monsoon from China-Siberia, the average temperature in study area of this season is 23.9 to 29.3 ℃. January is the lowest temperature of year.

Average temperature of Phetchabun province is 27.0 ℃, highest temperature of each year is around 33.5 ℃, the peak temperature can be recorded is 43.3 ℃ in April, lowest temperature of each year is around 23.9 ℃ and the lowest has been recorded temperature can be record is 2 ℃ on January

The Phetchabun province has a complex geography, that cause to amount rainfall in study area. The average annual rainfall 1,200 – 1,300 millimeter in Chondan, Nongpai, Wangpong and Vichangburi. About 1,000 – 1,200 in another district. The month with highest amount rainfall is September about 207.5 millimeter.
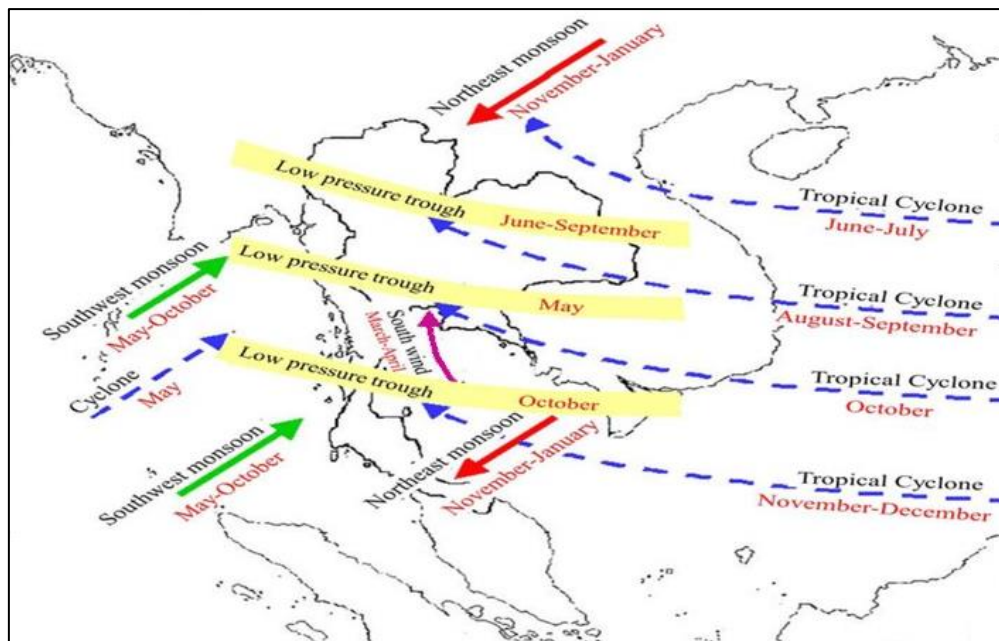
Figure 1.3 Monsoons and Tropical cyclones effect to Thailand amount rainfall
(Jampanil, 2017)

1.6 A brief guide to the thesis

The thesis provides InSAR technique for estimate the displacement rate of mass wasting and classified types of mass wasting at vicinity of Khao Kho. The thesis combines with 6 chapters, including:

Chapter I - Introduction, objective, characterization of the study area, expect results and limitation of this research.

Chapter II – Literature Review, overview of mass wasting, technical aspects of Interferometric SAR and Permanent Scatterer Interferometric SAR

Chapter III – Methodology, experiment process includes InSAR step and mass wasting classification process.

Chapter IV – Firstly, the displacement rates map will be showed deformation estimated PS pixel along the LOS direction and along slope. secondary, interpretation mass movement type base on displacement rate.

Chapter V – Discussion

Chapter 2   literature review

2.1 Mass wasting type definition

The classification system of mass wasting has developed for a long time. The most popular classification system Cruden and Varnes (1996), which applied type of movement and surface material type (Figure 2.1).

Type of Movement		Type of Material		
		Bedrock	Engineering Soils	
			Predominantly Coarse	Predominantly Fine
Fall		Rock Fall	Debris Fall	Earth Fall
Topples		Rock Topple	Debris Topple	Earth Topple
Slide	Rotational	Rock Slide	Debris Slide	Earth Slide
	Translational			
Lateral Spreads		Rock Spread	Debris Spread	Earth Spread
Flows		Rock Flow (Deep Creep)	Debris Flow	Earth Flow
			Soil Creep	
Complex		Combination of Two or more Principal Types of Movement		

Figure 2.1 Type of mass wasting (Cruden and Varnes, 1996)

2.1.1 Fall movement

Fall movement is the phenomenon that occurs from a high steep slope surface which low or no shear displacement. Fall of mass (including rock and soil) commonly appears on vertical slopes or steep slopes and areas damaged by hydrology erosion, such as coastal areas and rocky banks of rivers and streams. Falls often present very rapidly to extremely rapid displacement. However, in some areas, the movement may be represented by rolling and bouncing depending on the slope angle.

2.1.2 Slide movement

Slide is a downward movement along the slope surface of rock or soil mass. Most sliding events are trigged by water (i.e., after long and high-intensity rainfall). This movement can divide into two characters.

1) Rotational slide or Slum is a curved upward movement like a spoon shape. The rotation of mass occurs most frequently in homogeneous materials, especially landslides, most occurring in "fill" materials. This slide character has Extremely slow to moderately fast to rapid.
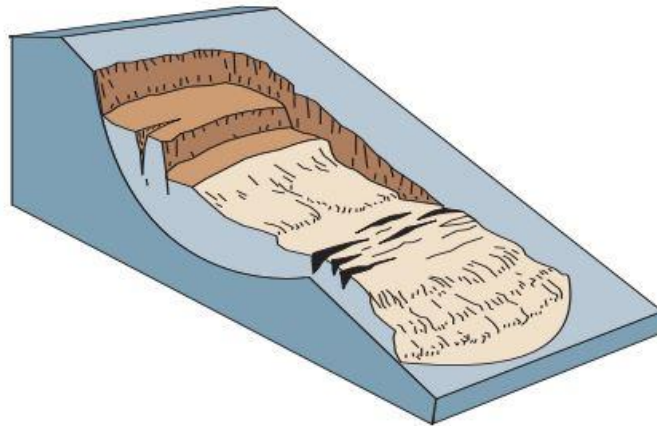
Figure 2.2 Schematic of a rotational slide (Highland & Bobrowsky, 2008)

2) Translational slide is a movement of material parallel along a planar surface. The translational slide mainly involves structural features like fault, joint, and rock bedding plane. The movement can damage at low to critical.
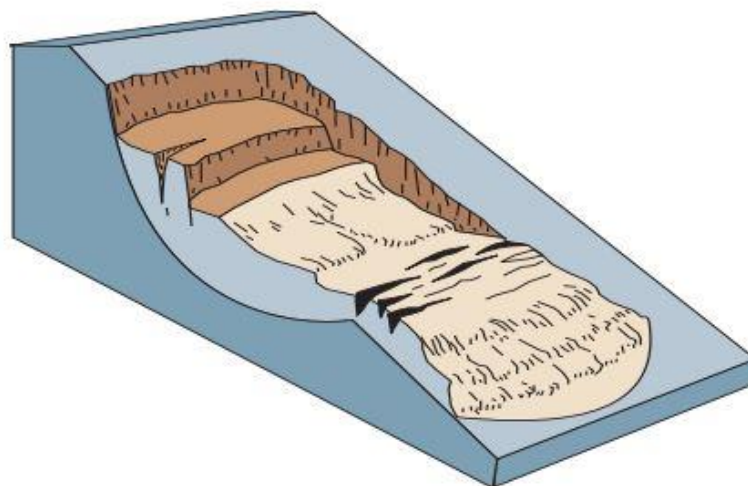
Figure 2.3 Schematic of a Translational slide (Highland & Bobrowsky, 2008)

2.1.3 Flows movement

Flows are a spatially continuous movement. The movement properties of the Flows type resemble a viscous liquid. The flow phenomenon can often be evolved from slides relating to the movement's water content and mobility. Flows can separate into five basic categories depending on surface materials.

1) Debris flow is mass wasting, a combination of loose soil, rock, organic matter, and water. They often occur during high-intensity rainfall on slope areas or mountains, especially steep gully channel on slope. Debris flows can be deadly as they can be extremely rapid velocity and may contain material to long distances.
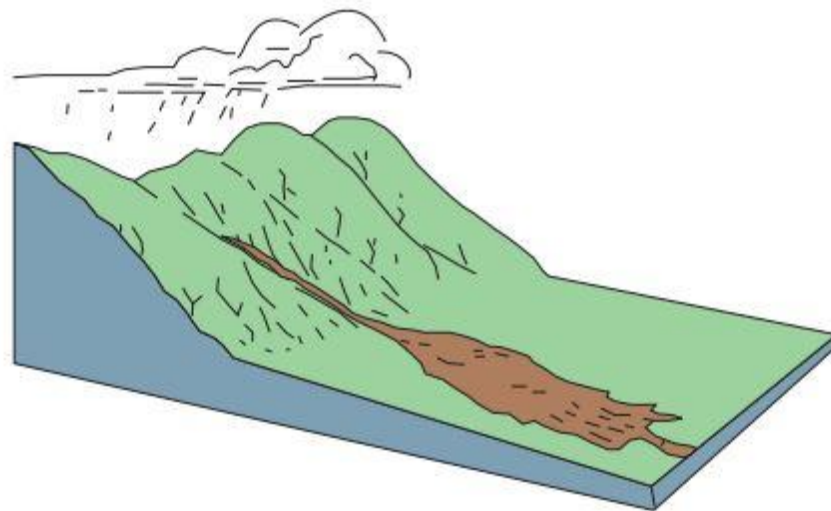
Figure 2.4 Schematic of a debris flow (Highland & Bobrowsky, 2008)

2) Debris avalanche is dominate by extremely rapid velocity and sudden movement by large volumes of sediment cover widely areas.
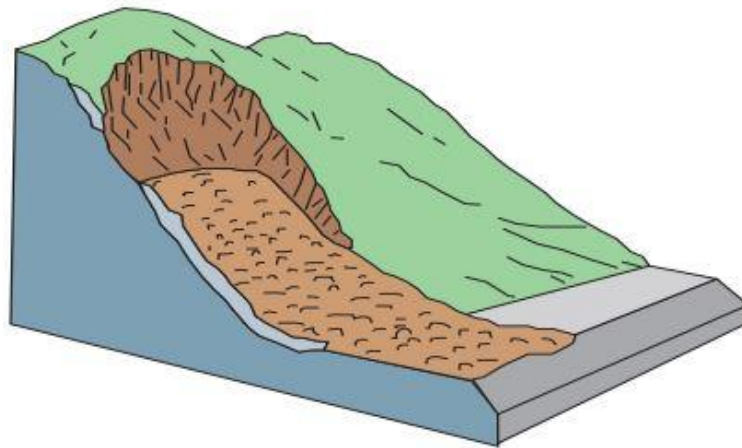
Figure 2.5 Schematic of a debris avalanche (Highland & Bobrowsky, 2008)

3) Earthflows usually occur by fine-grained soil, commonly clay or silt, on a medium slope and saturated surface material. The moving of Earthflows resembles a plastic or viscous flow with strong internal deformation. Earthflow may be developed from slides or lateral spreads. The velocity of Earthflow can range from very slow to rapid and disastrous.
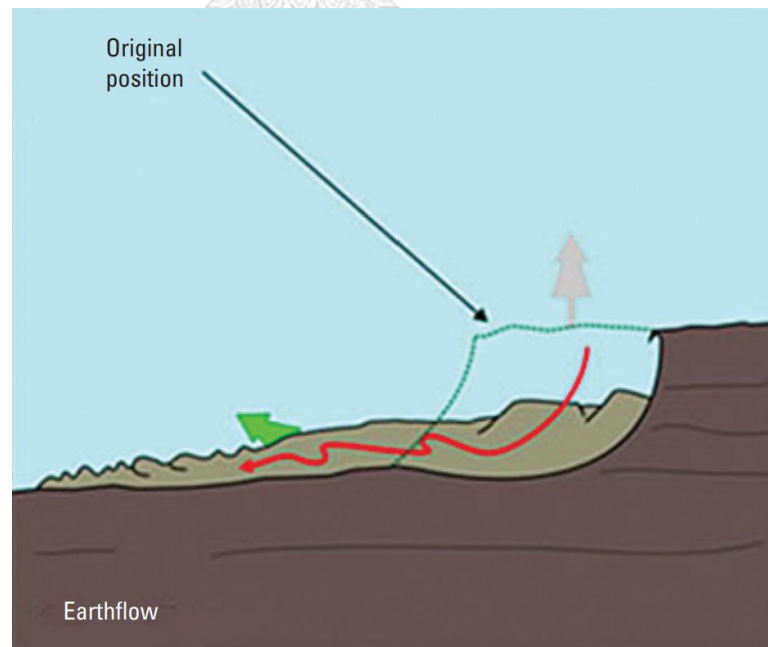
Figure 2.6 Schematic of an earthflow (Highland & Bobrowsky, 2008)

4) Creep is one of the slow earthflow categories, which involves the mass moving petty slow, steady velocity of soil or rock materials along a sloped surface. They can observe tilted poles, curved trees, fences out of alignment, and other human structures on a slope. Creep movement is characterized by internal shear stress sufficient to make moving but not enough to fail. The dominant feature of Creep is a relatively slow process, which is typically measured in millimeters per year.
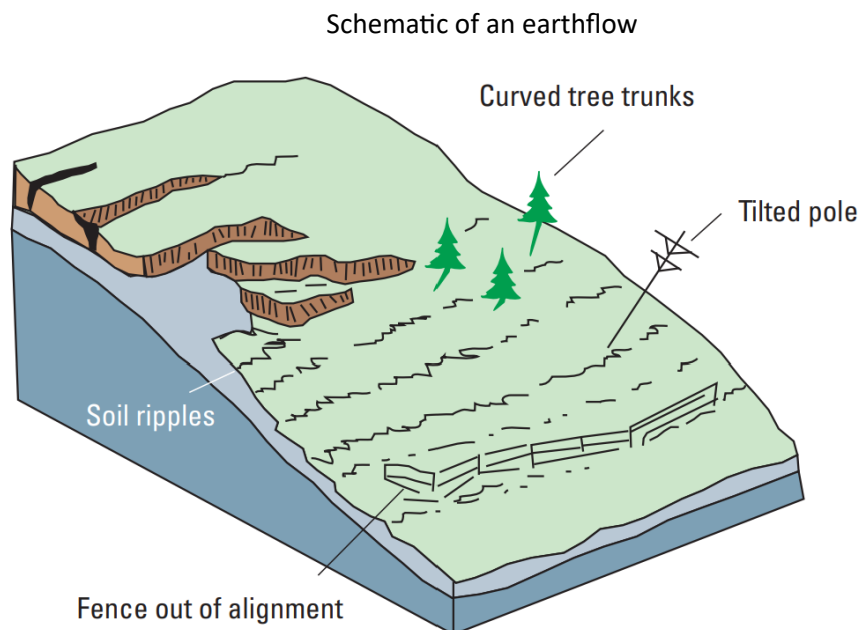
Figure 2.7 Schematic of soil creep or slow earthflow (Highland & Bobrowsky, 2008)

2.1.3 Topple movement

Topple refer to mass of soil or rock rotate forward out of slope. Topple generally occurrence on columnar-jointed volcanic terrain as well as steep slope of channel bank.

2.2 Interferometric Synthetic Aperture Radar (InSAR)

InSAR is an application of the interferometry method, finding a different wave phase. Typically, the different phase is related to different acquisitions combined with more than two antenna positions and different acquisition times. Interferometry calculations employ either sensor-to-ground distance, antenna angle and wavelength (i.e. microwave; 30 cm to 1 mm) for generated differential or interferometric phases. A represented

interferometric phase is an interferogram, which is produced by multiplying pixels between SAR images. The interferometric phase can be used in several ways, the popular application of interferometric phase study has been focusing on generated DEM and investigating the Earth's surface change. Regarding using the InSAR technique, researchers can generate large-area surface change maps with millimeter precision and better for a difficult accessed area. Figure 2.7 shows an image acquisition geometry for the InSAR technique, which use to find topography. Two SLC SAR images collected over the same focus area with approximate geometry acquisition can be used to generate an interferogram, which is an image of the differential phase between the two SAR images. The first phase value result of each pixel in a SAR image can be obtained as a Master image. Another phase value result of each pixel in SAR images can be obtained as Slave images.
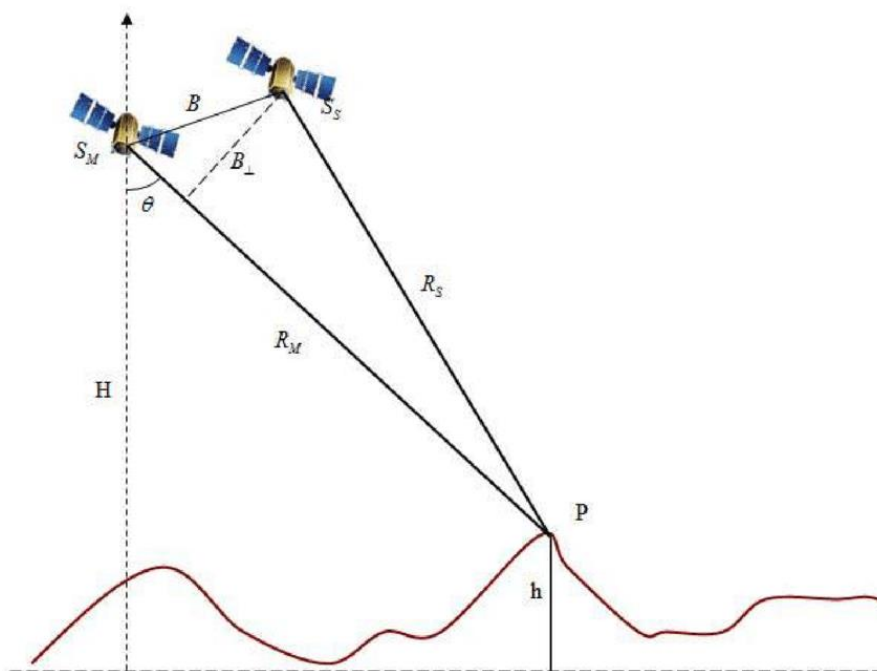
Figure 2.8 The principle of SAR data acquisition geometry for InSAR analysis to generating DEM

2.2.1 Synthetic Aperture Radar (SAR)

Radio Detection and Ranging (Radar) is a type of Earth Observation (EO) satellite data. In recent years, Studies expected the applicability of radar for slope instability investigations, which is about

the violent transformation of topography, such as mass wasting, land subsidence, and volcanic eruption. Although satellite image data can provide at night and daytime, including covering large areas, Real Aperture Radar (RAR) radar image is low resolution for investigating the Earth's surface deformation. The high-resolution radar data is called Synthetic Aperture Radar (SAR), which is an active remote sensing method that used a microwave frequency device potent for observation by electromagnetic resonance backscattered from the Earth's ground. SAR data is mostly acquired in a single-look complex platform consisting of wave amplitude data and wave phase value. The high-resolution SAR use side-looking geometry of radar antenna mounted on satellite and aircraft. The SAR antenna uses a moving antenna for receiving signals, which can obtain many backscattered signals from the Earth's surface. That technique can increase azimuth resolution.

2.2.2 Amplitude and wave phase of SAR data

The component of SLC includes amplitude and wave phase. The amplitude of the radiation reflected showed a composition image of bright and dark pixel values. This pixel value depends on the roughness of the earth's surface, particularly, outcrop rocks and urban areas show higher amplitude than flat surfaces such as bare soil and water basin. The high amplitude pixel is shown in brighter pixels, but the lower amplitude is shown in darker pixels (Ferretti et al., 2007).
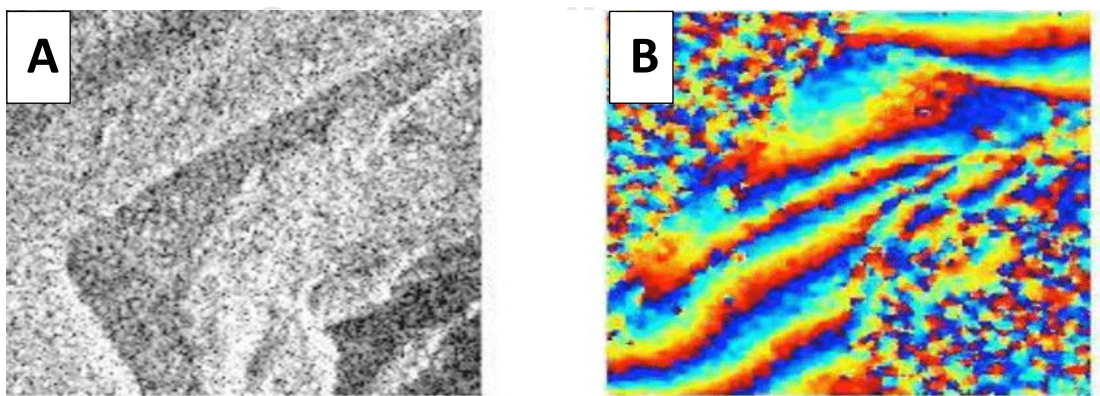
Figure 2.9 A) amplitude data of SAR image the bright pixel showing high value and darkness pixel show low value B) differential of wave phase between two or more SAR data.

The radiation of the microwave sensor of the satellite travel to the scatterers on the earth's surface and come back to the satellite antenna for generated the SAR image. The phase depends on the wave frequency and time of signal travel, normally, A sinusoidal function sin is periodic of a wave phase 2π radian period. The property of wave phase travel is a two-way travel distance that is smaller than the transmitted wavelength (Ferretti et al., 2007).

2.2.3 Differential Interferometric Synthetic Aperture Radar (DInSAR)

DInSAR is the result of interferograms or interferometric phase, after the removed topographic phase. DInSAR is a once technique applied to SAR images, which measures ground deformation or earth surface displacement by the acquisition of repeat-pass interferometry. DInSAR, there are several methods to create differential interferogram. The first is a two-pass method which uses an interferogram pair to subtract the deformation phase. A second method is the three-pass DInSAR, the used two pair interferogram method, both are deformation pair (topography, deformation, atmosphere, wrapped phase) and topographic pair (no deformation assumed, absolute phase).
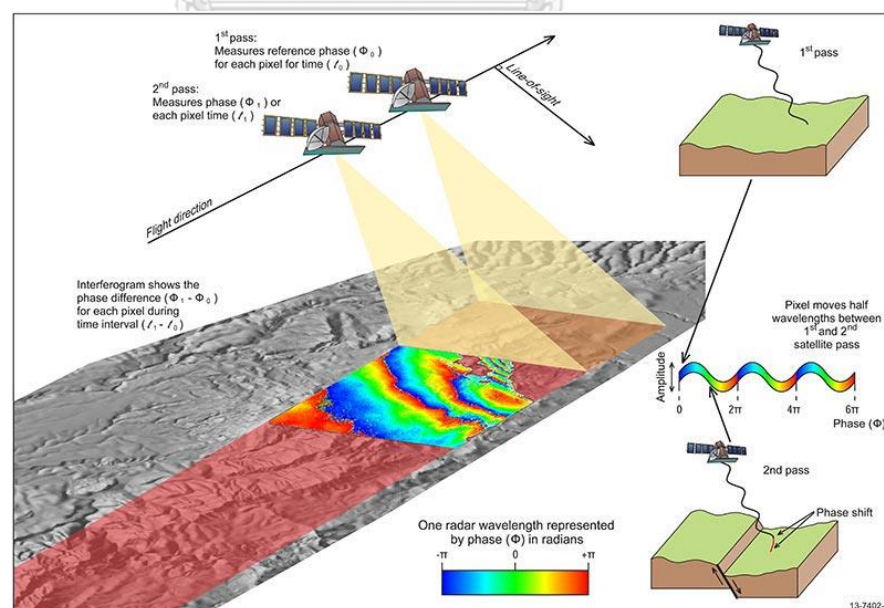
Figure 2.10 The schematics of DinSAR by muti pass 2-time acquisition
(Garthwaite et al., 2015)

DInSAR can be applied in various earth observation and geologic hazards investigation, such as landslide, subsidence, earthquake and volcanic activity. The result of the DInSAR is represented by a displacement map in LOS direction. But DInSAR still has many limitations, especially the limitations from atmospheric and vegetation cover.

2.2.4 Permanent Scatterer InSAR

Persistent Scatterer InSAR (PSInSAR) is an application of conventional DInSAR techniques, which focus on the noise of decorrelation and atmospheric delay. The distribution of scattering centers on the observation area affects the degree of decorrelation. In a SAR image, sum of individual wavelets scattered from scatterers pixel is the reflected wave from a resolution cell. Normally, the phase and amplitude of each pixel are varied by the interference of the wavelet, scattering value determined randomly to each pixel (Figure 2.10) between the $\pm\pi$ radians range and make spatial decorrelation. In contrast, the scatterer is brighter than the other scatterers, which gives the largest contributor to be a representative value pixel. Because of the high dominant scatterer, any movement of the scatterer covers up the movement of the other scatterer and can be readily measured by the phase of the radar echo.

Acquisition
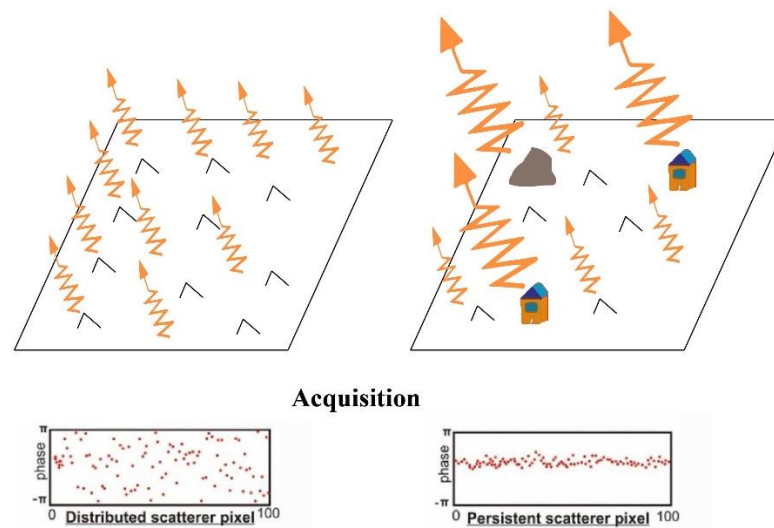
Figure 2.11 the difference between a dispersed scatterer pixel and a permanent scatterer pixel

As mentioned above, the scatterer which represented the phase of a pixel and reduce the decorrelation to zero, thus good interferograms are formed. Normally, the PS pixel might be, the building, a non-leaves and branches tree truck, large outcrop. All image pairs use the same image, which call the "master" scene by same path, azimuth width and range width with all the images. A criterion for choosing the Master images for PSInSAR use a low temporal baseline compared with all used images (Figure 2.11).
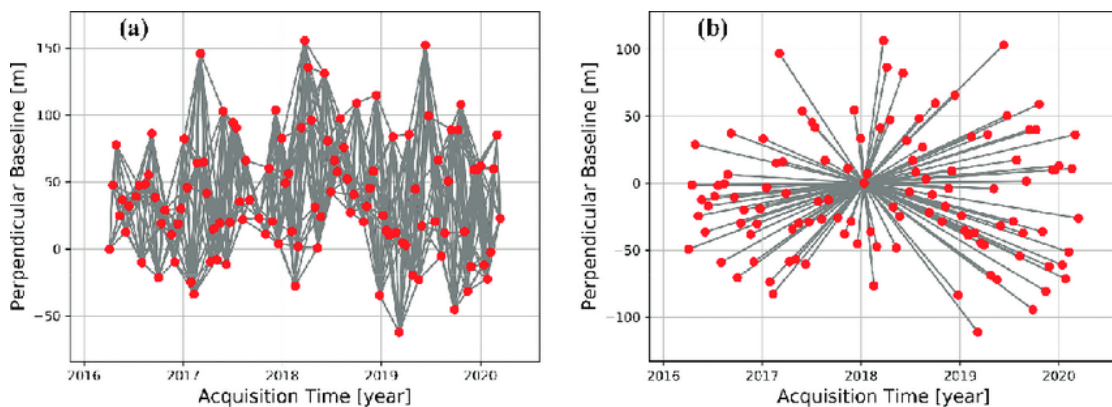
Figure 2.12 A) Example of pairing SAR image for generate interferogram by small baseline technique, which can be muti master images B) Example of pairing SAR image by chosen the shortest time distant to be a master image (Bui et al., 2021)

The first algorithm to accomplishment PS pixels was achieved by (Ferretti et al., 2001) in the permanent scatterers technique. The phase in PS pixels is used to present how to displacement varies with time. Obviously, this method has been very successful for InSAR analysis in densely building or man-made structures, which often make high reflectors and high dominated background scattering.

PS pixels or PS point are identified by a functional model of temporal displacement, which depend on behavior of phenomenon displacement. Generally, deformation or displacement is assumed to be steady state in nature. However, many deformation cases were non-steady movement such as volcanoes, landslide, fault movement. The area with a non-steady displacement has no permanent scatterers point, despite there are many man-made structures within the area.

2.3 Previous works

Mass wasting is a natural disaster, which significant damage to both human lives and the economy worldwide. For Thailand, the impact of the southwest monsoon, which brings continuous heavy rainfall during the monsoon season. The most slope failure in Thailand occur by the shallow mass movement covering small area and mass depth about 0.5-3 m. (Jotisankasa & Vathananukij, 2008). There are many researchers tried using remote sensing data for analysis, detection, and monitoring mass wasting. For the Phetchabun mountain range, remote sensing was associated with GIS for studying mass wasting factor and landslide risk assessment. (Yumuang, 2006) employ GIS to describe cause of the debris flow and debris flood pheomenon on 11 August 2001 which damage to Nam Ko Yai village. That research, using muti-spectral Landsat 7 detected mass wasting evidence in study area by combination of Normalized Difference Vegetation Index (NDVI) change and orthophotograph. The result from that research found that, debris flow-flood in Nam Ko area was caused by other factor furthermore longtime heavy rainfall, especially natural landslide dam forming within stream. That explain how movement of Nam Ko debris flow-flood to be critical hazard.

The previous works on mass movement rate investigation show many techniques using. In this study focus on investigation of mass wasting by PSInSAR technique, that applied and developed of DInSAR technique, so some important and related literatures about PSInSAR technique and using movement rate to classified type of mass movement have been briefly reviewed below order to be the background information. PSInSAR can apply to other term related earth surface deformation such as Earthquake, Landslide, ground subsidence. Hence, the algorithm for achieve the result of PSInSAR can be compatible using together between each studied term. The first period of using SAR data or InSAR to measure slope movement occurred for the landslide at La Clapiere, near Saint Etienne de Tinee.

Later that, InSAR technique is using differential phase between SAR images to measure earth surface deformation or terrain elevation.

(Carnec et al., 1996) applied InSAR technique on displacement fields of small spatial extent at La Clapiere. From the study, he analyzed different phase value between SAR images to investigating surface deformation. The study focuses on interpreting fringe cycle of interferogram, which generated by InSAR technique or image, which represent different phase value. Each fringe pattern is characterized by wavelength and travel time. He summarized that the interpretation of fringe pattern image for measure deformation is working well, is not suitable for high deformation with short time on steep sloping terrains. He suggested using shorter temporal baseline or shot time revisit satellite and sharper resolution image. The study described significance of correlation between 2 imageries, which directory effect to quality of interferogram images.

Once of technique to improving InSAR application for surface deformation investigate that presented by (Ferretti et al., 2001). He presented a new technique which developed from conventional DInSAR to reduce the decorrelation of interferometric pair including temporally decorrelation, geometrical decorrelation, and atmospheric disturbances. Time – series analysis is a key of PSInSAR technique for resolve decorrelation InSAR results. Atmospheric disturbances create an atmospheric phase screen (APS) to all SAR images and hard to detect it in the interferogram coherence map. The main procedure of PSInSAR is Permanent scatterer selection that is step for finding permanent pixels (high correlation). He concluded that, urban areas and rocky terrain have high potential to be PS pixel because of low Amplitude Dispersion, therefore PSInSAR technique can investigate deformation in the surface cover by building, road, bare soil, outcrop, which given many number of PS pixel to deformation estimating.

Ferretti et al., 2007 exploit PSInSAR technique for monitor Landslide and tectonic motion. His research brought surface deformation rate from PSInSAR comparing with value from optical leveling. 61 ERS images only generated 820 PS were in the sliding area and around sliding area. He summarized comparison result that deformation rate of the Ancona landslide from PSInSAR closer to optical leveling, that showed on performance of PSInSAR technique for landslide monitoring. He said PSInSAR technique can apply and respond for landslide monitoring

excellently. However, their study used LOS velocity from the PSInSAR technique to estimate the velocity of deformation that might be potential to be landslide. Although PSInSAR provided accurate deformation rates result, the technique can generate only deformation along LOS only.

The major problem of PSInSAR for investigate mass wasting, the technique provide PS pixel contain displacement rate along LOS only. For mass wasting, which move of mass of sediment downward steep slope surface. (Colesanti & Wasowski, 2006), they used both PSInSAR and conventional technique as DinSAR for investigate the sliding area of the Trisenberg-Triesen landslide. The slope failure cover 4.2 square kilometer. Their PS point fell within the sliding zone around 95% from 1.7 x 2.2 square kilometer. For PS analysis show displacement rate about more than -10 mm/yr. along LOS direction. Then, displacement rate along LOS was projected to slope direction by combination of slope aspect, LOS displacement rate, inclination angle between LOS and interesting ground.

Meisina et al., 2008 presented the geological interpretation of PSInSAR data at regional scale process. The process was significant advantage for mitigation and urban planning to protect human life, building. Their study has an extension of 25,000 sq.km and it is combination with geological context. They suggested that PSInSAR result interpretation (deformation rates) had required a GIS integration method and GIS data (DEM, landslide inventory, topographic and aerial orthophotos). the GIS data was a good choice for accuracy precision. Their PSInSAR results point combine with positive and negative value (toward and outward displacement dimension), so a landslide detecting needed to avoid the positive value that might represent an upfit deformation, thus the positive value was deleted.

Chapter 3   Methodology

The objectives of this research are an investigation of mass wasting using TIME-SERIES InSAR technique by PSInSAR method and classification of the mass wasting type by movement velocity. PS-InSAR method most used for detection and investigation velocity of earth surface deformation phenomenon. Previously, most researchers who interest in applying InSAR technique for investigation and monitoring of the Earth's surface deformation phenomenon. DinSAR have had some disadvantage by high decorrelation between master and slave images and an area characterized limitation, those problem may affect to the subtracted deformation phase process. Consequently, TIME-SERIES InSAR has resolved the phase decorrelation. This chapter describes all process of PSInSAR to appreciate displacement rate results both ascending and descending orbit direction. Later that, the LOS velocity (V_{LOS}) from PSInSAR will convert to the slope velocity (V_{slope}) by the C value.

3.1 Method of Interferometry SAR (InSAR)

The principle of Interferometry SAR, that application the phase of SAR data This topic will tell you about all process for approach the Interferometry SAR. Figure 3.1 demonstrate flow chart of PSInSAR method, which cover how to select data and description them, image preparations, coregistration, interferogram creation.
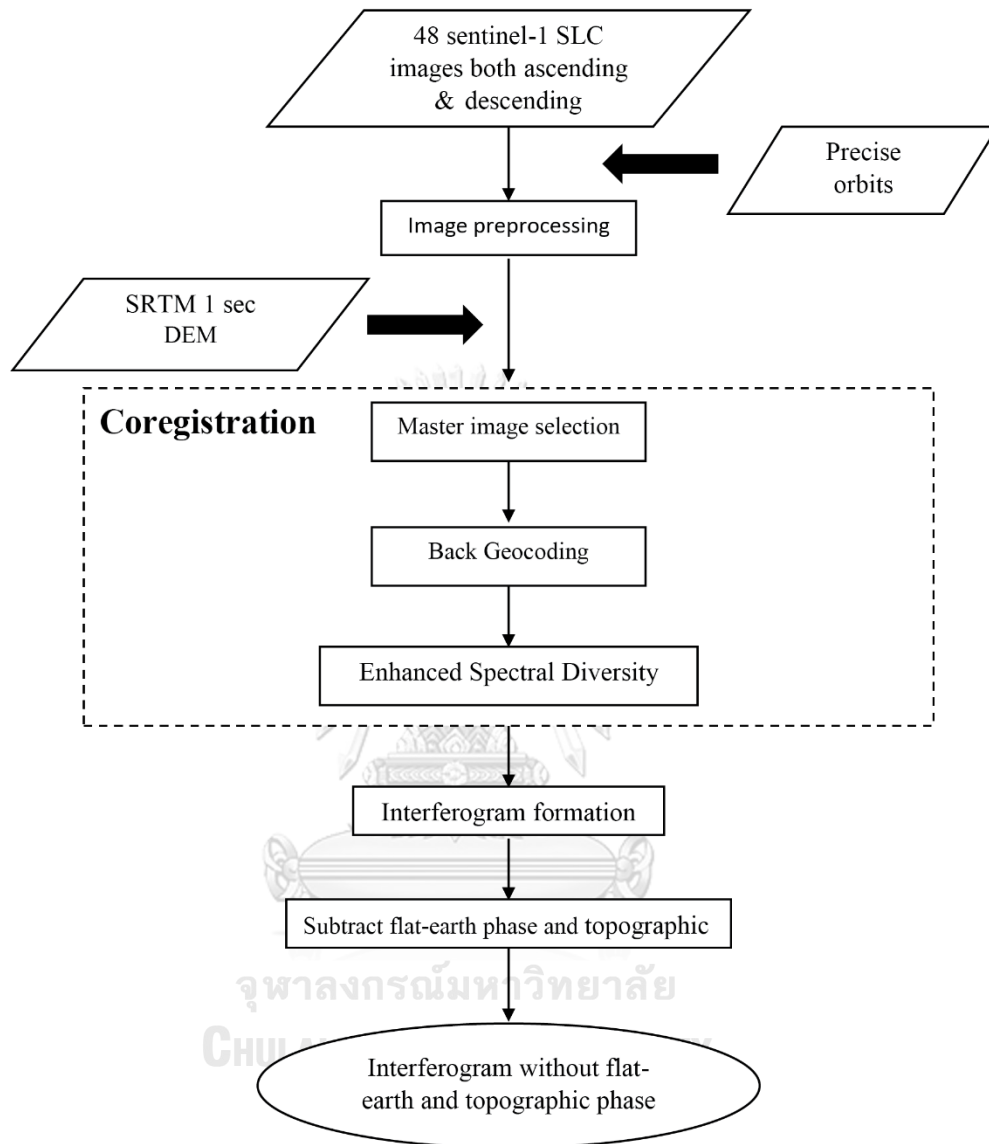
Figure 3.1 The Sentinel-1 InSAR workflow scheme

3.1.1 Data selection

In this work, the sentinel-1 products were selected for processing. Those images were acquisition year around 2015 to 2018. All Sentinel-images were downloaded from Alaska Satellite Facility (Figure 3.2). All the images are Level-1 Single look Complex (SLC) which contain both amplitude and phase of the image. The images collected with IW acquisition mode. IW mode scan image to three sub-swaths

(Figure 3.3) using Terrain Observation with Progressive Scan SAR (TOPSAR), therefore a tool for preparation SAR image, co-registration, interferogram generated request an ability for TOPSAR data. Figure 3.4 is showing SAR images extent both ascending and descending. The ascending direction collected at path 99 frame 57, and path 62, Frame 537 for descending direction.
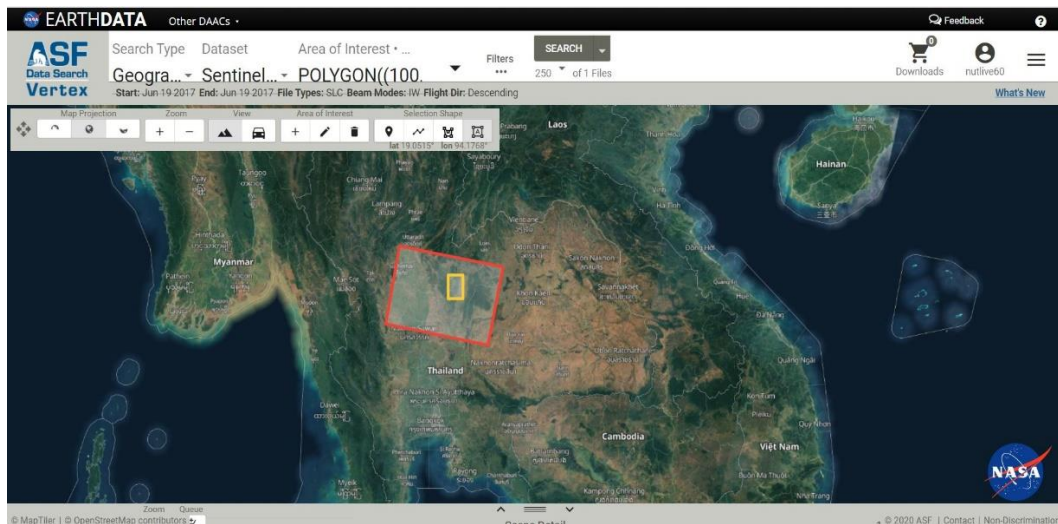
Figure 3.2 The SAR image data catalog from Alaska Satellite Facility
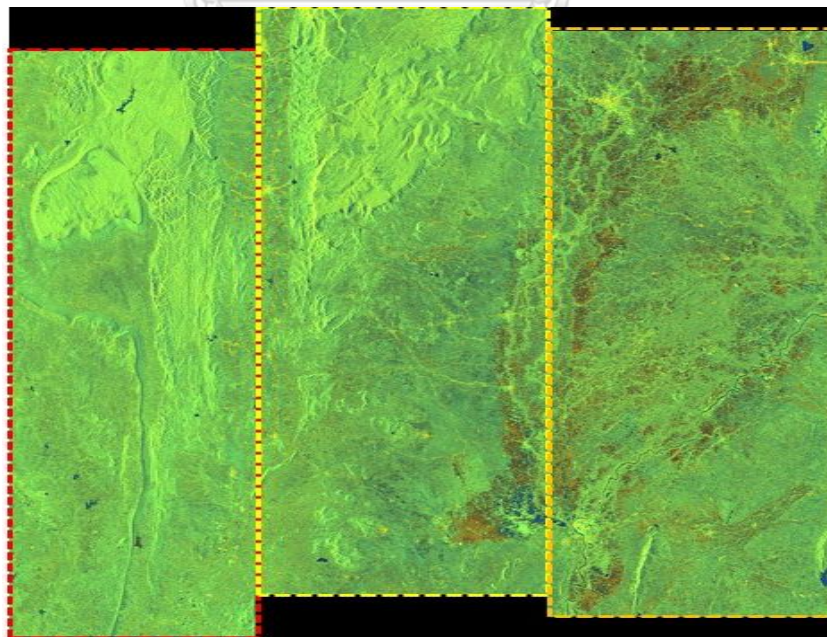
Figure 3.3 TOPSAR image data sub-swath before data preparation
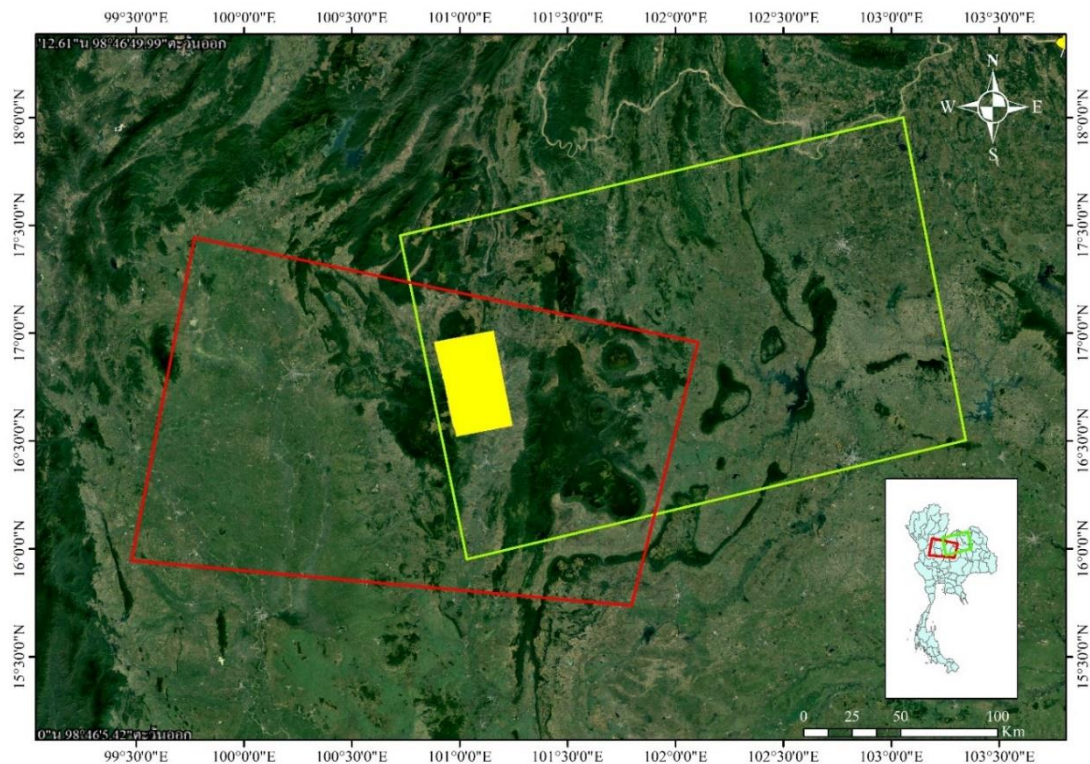
Figure 3.4 the sentinel-1 footprint over study area (yellow polygon), red border shows descending orbit data footprint and green border showing ascending orbit data footprint

3.1.2 Data preparation

After the data downloading and data selection, this topic is telling you about the data preparation before InSAR process and PSInSAR process. SAR image preparation is extremely important for the InSAR process because each SAR image files have unnecessary values for InSAR process. First, the Sentinel 1 orbit value are adjusted by the Sentinel 1 precise obit value. After That, each SAR images with adjusted orbital value, then separated their sub-swath and polarization of electrometric wave (the dimension of wave transmitted and reflected) by split step.

Sentinel-1 TOPSAR Split, it is the first process of SAR images preparation. According to Sentinel 1 data description in chapter 2, A Sentinel 1 C band downloaded with complex data, which is Single Look Complex (SLC) product. SLC product contain 2 data of SAR including amplitude and phase images. Each SLC image consist with three sub-

swaths (Figure 3.6). So, this step offers an easy way to split each IW or sub swath for reduce data size and other processing time. Furthermore, this step must choose a plane of electromagnetic wave or polarization (figure ภาพpolar). Sentinel 1 used 2 polarizations between VH (vertical transmit and receive horizontal) or VV (vertical transmit and receive vertical) for wave travel. In this study use VV (Vertical and Vertical), that is the single polarized. In Fact, 2 polarizations were not significant different for estimate earth surface displacement or other InSAR processing(อ้างอิง). IW 1 was chosen for ascending orbit direction (Figure 3.6), but IW 2 was chosen for descending orbit direction, because images both ascending and descending located overlay zone. Figure 3.7 all IW and all burst both ascending and descending orbits.

A precise orbit adjusting step. Generally, SAR data files consist of orbit value which are position and velocity of satellite while acquired an image. Orbit value can be offered from Sentinel 1 metadata. The origin orbit value can be used immediately for SAR application which does not request high accuracy of SAR transmit geometry. Nevertheless, InSAR technique request high accuracy of wave travel geometry because of baseline between data acquisitions including master and slave pixels correlation. Thus, accuracy of InSAR results extremely depend on correct acquired geometry data.
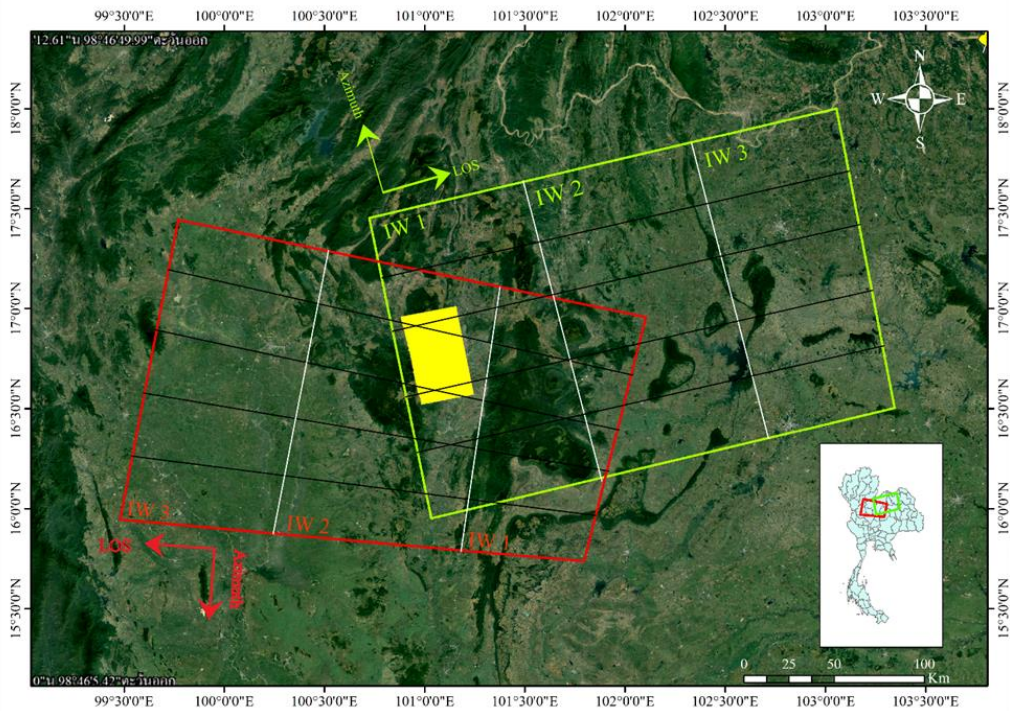
Figure 3.5 Showing component of TOPSAR data including image sub-swaths and burst in the image footprint border

3.1.3 Coregistration

After the SAR image preparation process, All of SAR data both descending and ascending direction will pairs by Co-registration process. The co-registration step will generate SAR data stack which be correlation between master and slave pixel images. So, this step need be done before interferogram generation.

The coregistration step have 3 step including Master image selection, Back Geocoding and Enhanced Spectral Diversity (ESD). Firstly, Master image selection was operated by equation 3.1.

$$\gamma^m = \frac{1}{K}\sum_{k=0}^{K} g\left(B_{prep}^{k,m}, 1200\right) \times g(T^{k,m}, 5) \times g(f_{dc}^{k,m}, 1380) \quad\text{......(Eq 3.1)}$$

Where γ^m is the modeled coherence

$B_{prep}^{k,m}$ is the perpendicular baseline between images m and k

$T^{k,m}$ is the temporal baseline between images m and k

$f_{dc}^{k,m}$ is the mean Doppler centroid frequency difference

Table 3.1 The ascending SAR images list

Mst/Slv	Acquisition	Image Track	Orbit	Perpendicular baseline [m]	Temporal baseline[days]	Modeled Coherence
Master	9-Aug-17	99	17846	0	0	1
Slave	18-Mar-17	99	15746	-32.19	144.00	0.84
Slave	30-Mar-17	99	15921	-6.58	132.00	0.87
Slave	11-Apr-17	99	16096	-67.18	120.00	0.84
Slave	5-May-17	99	16446	-135.00	96.00	0.81
Slave	4-Jul-17	99	17321	31.75	36.00	0.94
Slave	14-Sep-17	99	18371	-83.89	-36.00	0.90
Slave	8-Oct-17	99	18721	-25.53	-60.00	0.92
Slave	20-Oct-17	99	18896	25.16	-72.00	0.91
Slave	1-Nov-17	99	19071	-20.85	-84.00	0.91
Slave	31-Dec-17	99	19946	112.69	-144.00	0.79
Slave	12-Jan-18	99	20121	25.34	-156.00	0.84
Slave	25-Mar-18	99	21171	40.26	-228.00	0.76
Slave	30-Apr-18	99	21696	19.31	-264.00	0.75
Slave	24-May-18	99	22046	-93.22	-288.00	0.68
Slave	17-Jun-18	99	22396	15.94	-312.00	0.71
Slave	23-Jul-18	99	22921	-30.42	-348.00	0.66
Slave	30-Dec-15	99	9271	-61.74	588.00	0.44
Slave	23-Jan-16	99	9621	31.30	564.00	0.47
Slave	11-Mar-16	99	10321	8.59	516.00	0.52
Slave	4-Apr-16	99	10671	-67.54	492.00	0.52
Slave	22-May-16	99	11371	16.72	444.00	0.59
Slave	15-Jun-16	99	11721	-48.26	420.00	0.59
Slave	2-Aug-16	99	12421	-44.28	372.00	0.64

Table 3.2 The descending SAR images list

Mst/Slv	Acquisition	Track	Orbit	Perpendicular baseline [m]	Temporal baseline [days]	Modeled Coherence
Master	19-Jun-17	62	17109	0.00	0.00	1.00
Slave	8-Jan-16	62	9409	15.34	528.00	0.51
Slave	25-Apr-16	62	10984	-10.65	420.00	0.61
Slave	15-Dec-15	62	9059	11.81	552.00	0.49
Slave	20-Mar-16	62	10459	29.98	456.00	0.57
Slave	11-Aug-16	62	12559	-53.46	312.00	0.68
Slave	2-Jan-17	62	14659	29.94	168.00	0.82
Slave	12-Jun-16	62	11684	-10.16	372.00	0.65
Slave	21-Dec-16	62	14484	-15.36	180.00	0.82
Slave	7-Feb-17	62	15184	21.88	132.00	0.86
Slave	20-Apr-17	62	16234	7.55	60.00	0.93
Slave	27-Mar-17	62	15884	17.30	84.00	0.90
Slave	13-Jul-17	62	17459	-44.50	-24.00	0.94
Slave	30-Aug-17	62	18159	-13.62	-72.00	0.92
Slave	23-Sep-17	62	18509	-19.96	-96.00	0.89
Slave	6-Aug-17	62	17809	25.67	-48.00	0.93
Slave	17-Oct-17	62	18859	-25.58	-120.00	0.87
Slave	10-Nov-17	62	19209	-30.64	-144.00	0.84
Slave	28-Dec-17	62	19909	-85.27	-192.00	0.77
Slave	21-Jan-18	62	20259	26.07	-216.00	0.78
Slave	10-Mar-18	62	20959	-95.20	-264.00	0.69
Slave	14-Feb-18	62	20609	38.22	-240.00	0.75
Slave	9-May-18	62	21834	7.47	-324.00	0.70
Slave	15-Apr-18	62	21484	-10.30	-300.00	0.72

If image have high coherence value, that will be chosen to be the master image of project. However, the estimated coherence of this processing used information from image metadata only that do not cover spatial decoration. So, coherence will estimate again within interferometry step. This study was selected SAR images on 8 August 2017 for ascending orbit direction and 19 June 2017 for descending orbit direction (Table 3.1 and Table 3.2). Figure 3.7 display how slave images pair to the same mater image, that pairing method is requested for PSInSAR. Then, TOPS coregistration processing or Back-geocoding step operate by resampling between master and all slave image pixel. This

step requested 1-sec SRTM (Shuttle Radar Topography Mission) DEM, which was downloaded from the Earthexplorer. 1-sec SRTM project observation cover between 60º north to 56º south latitude, which work in and control by the National Geospatial-Intelligence Agency (NGA) and the National Aeronautics and space administration. 1-sec SRTM DEM (Figure 3.8) have resolution about 30 x 30 meter. DEM was an important parameter for resampling all slave image pixel to be correlation with master image pixel. In this study, applied the nearest neighbor interpolation method. Nearest neighbor method performs by align slave image pixels to master image pixels. This method does not affect to SAR pixel value, therefore nearest neighborhood reasonable using for InSAR technique. Outputs of coregistration provided 23 data stack per orbit direction, that stack contain 1 pair between master and slave images.
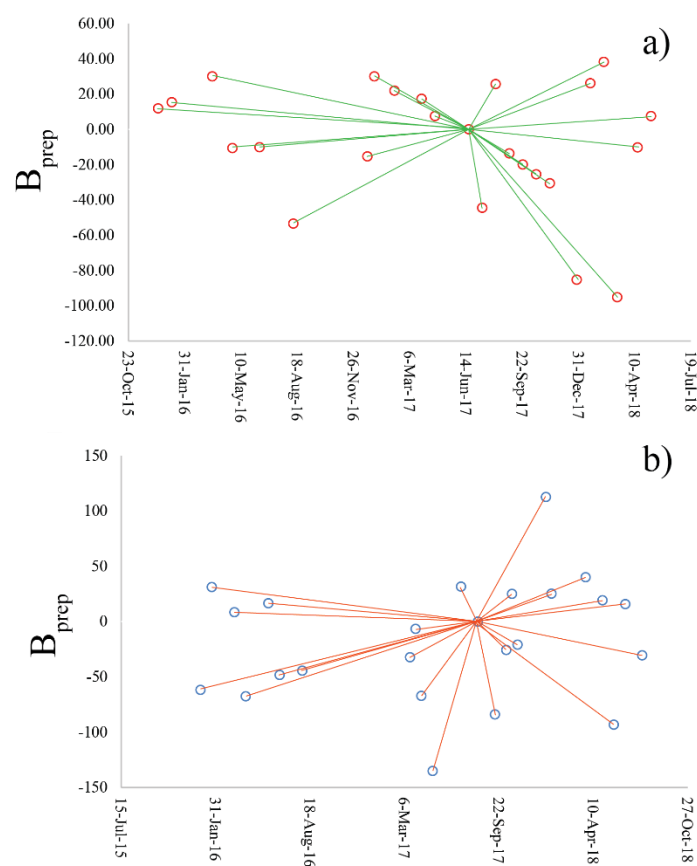

Figure 3.6 A) the paring baseline of slave images to a master image of ascending orbit B*)* the paring baseline of slave images to a master image of descending orbit
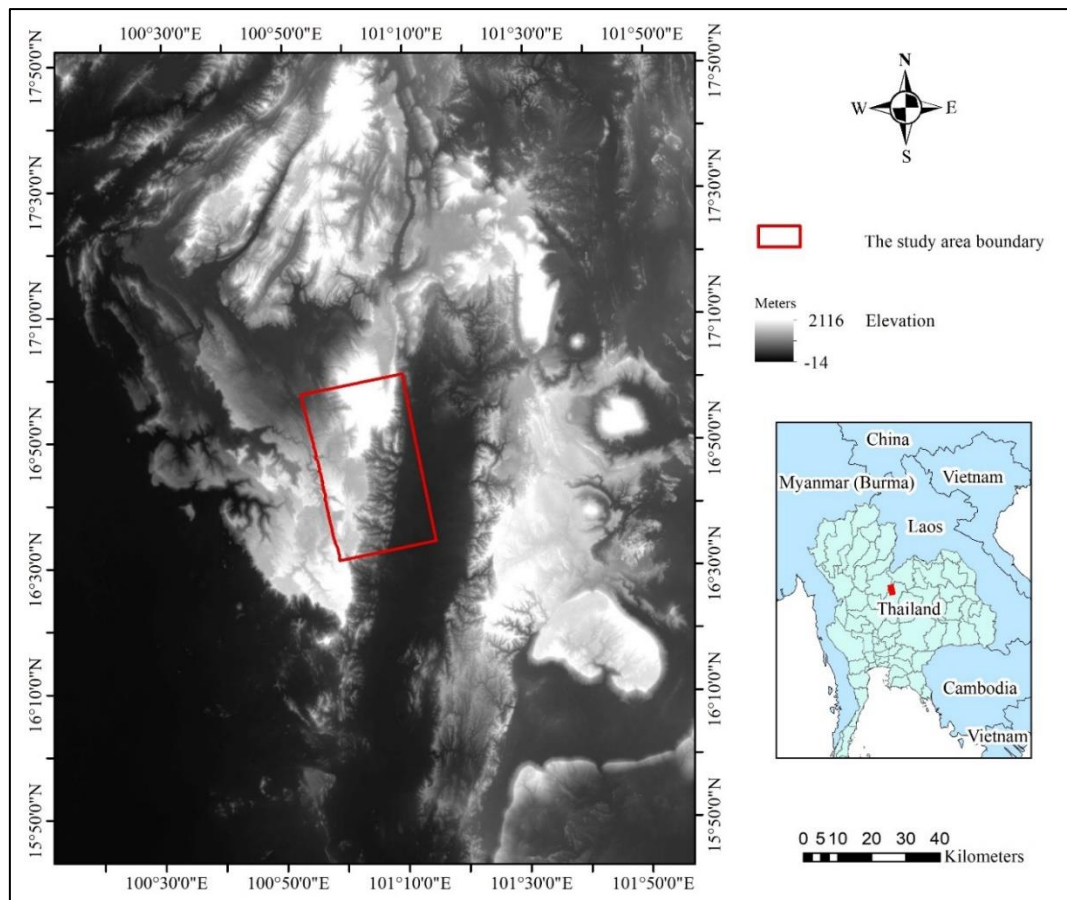
Figure 3.7 1-sec SRTM DEM, which using for images Coregistration

3.1.4 Interferometric pairs and Interferogram formation

This step is too important of normal InSAR and PSInSAR processing. Interferometric pairs or interferogram formation defined to generate the interferogram which representative of total differential phase of wave travel between master and slave images. This step also operated on SNAP platform, which the specific software for analysis satellite data from ESA project. Information is requested for interferogram formation including image stack from obtained by coregistration step, DEM and precise orbit. Interferogram formation processed 46 times follow by image quantity.

Interferogram formation was computed by pixel x pixel between master and slave images. At the mention in CHAPTER 2, interferogram is a result of total phase differential between 2 images, which include topographic phase (ϕtopo), Earth surface displacement phase (ϕdisp),

atmospheric effect phase (ϕatm), the flat-earth phase(ϕflat) and other noise(ϕnoise) that was shown in Equation 3.1.

$$\phi = \phi_{topo} + \phi_{flat} + \phi_{disp} + \phi_{atm} + \phi_{noise} \dots\dots\dots \text{(Eq 3.1)}$$

In this step also estimated fine the coherence image (Figure 3.8 to 3.10 for ascending orbit and Figure 3.11 to 3.13 for descending orbit) which is an indicator of the phase value. The coherence value depends on spatial and temporal correlation between mater and slave image. High coherence usually appears with bright pixel. In the other hand, Low coherence usually appears dark pixel.

Figure 3.8 the coherence images of ascending orbit between 30 December 2015 to 18 Mar 2017

Figure 3.9 the coherence images of ascending orbit between 30 Mar 2017
to 01 November 2017

Figure 3.10 the coherence images of ascending orbit between 31 December 2017 to 23 July 2018
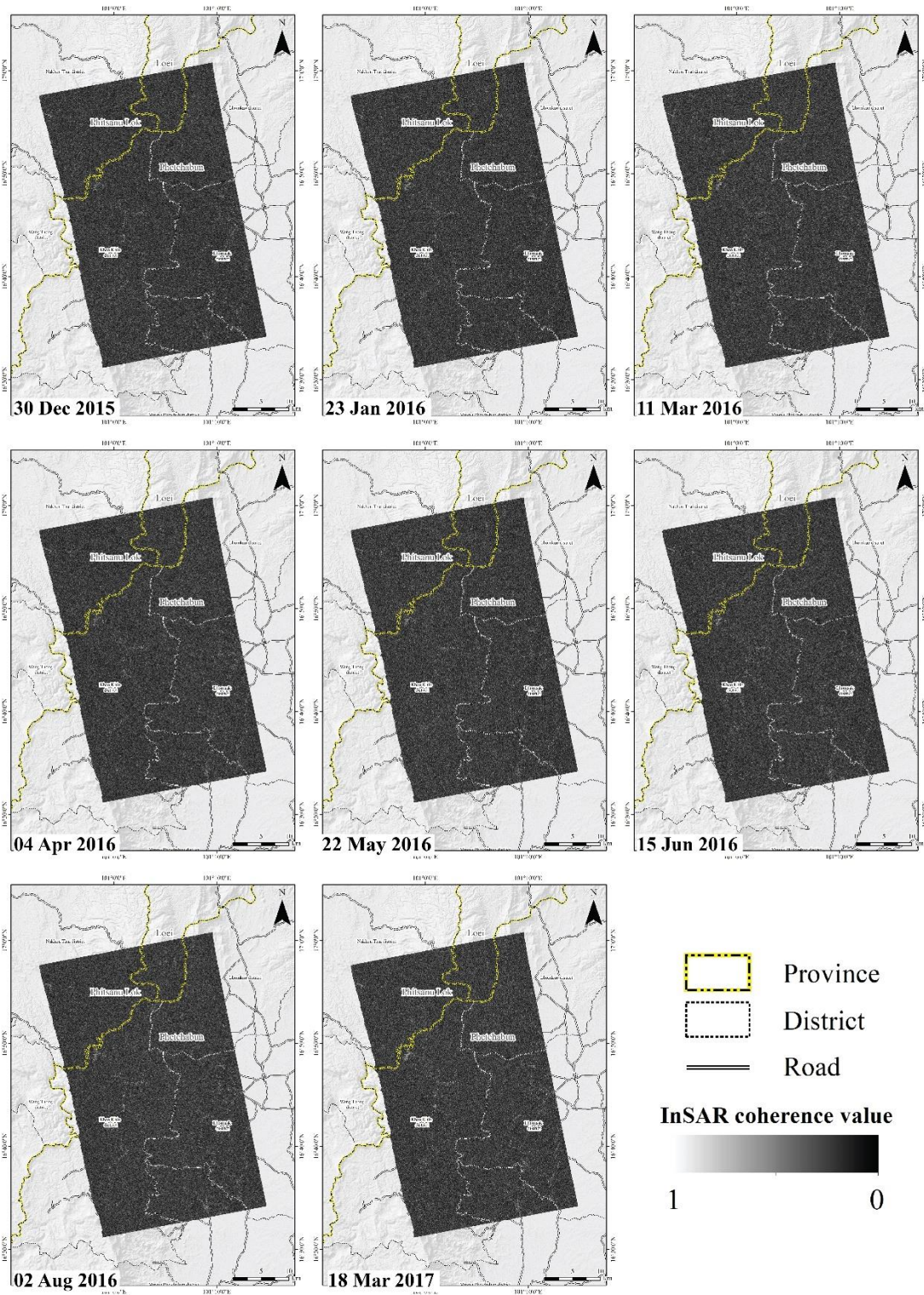
Figure 3.11 The coherence images of descending orbit between 15 December 2015 to 02 January 2017
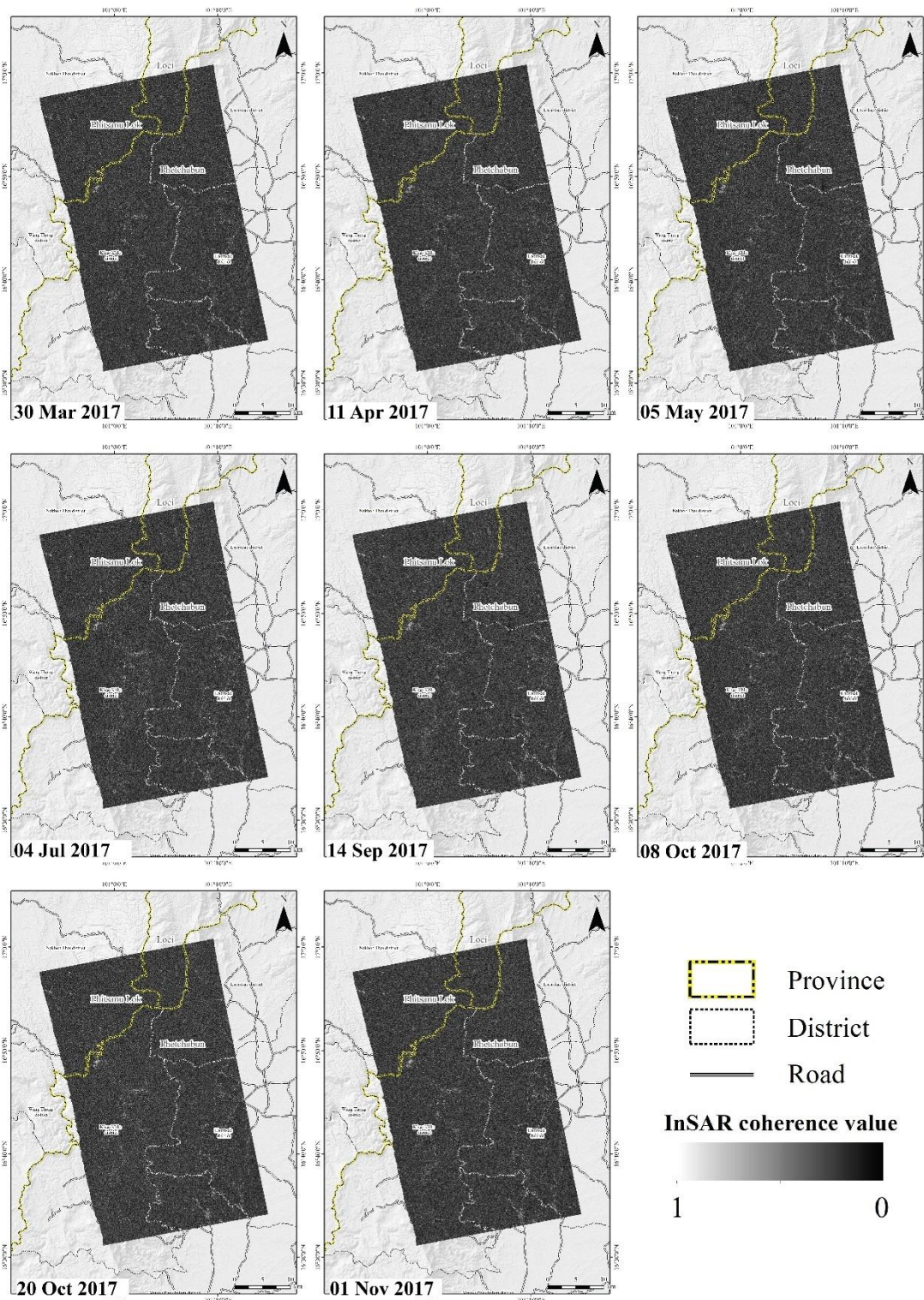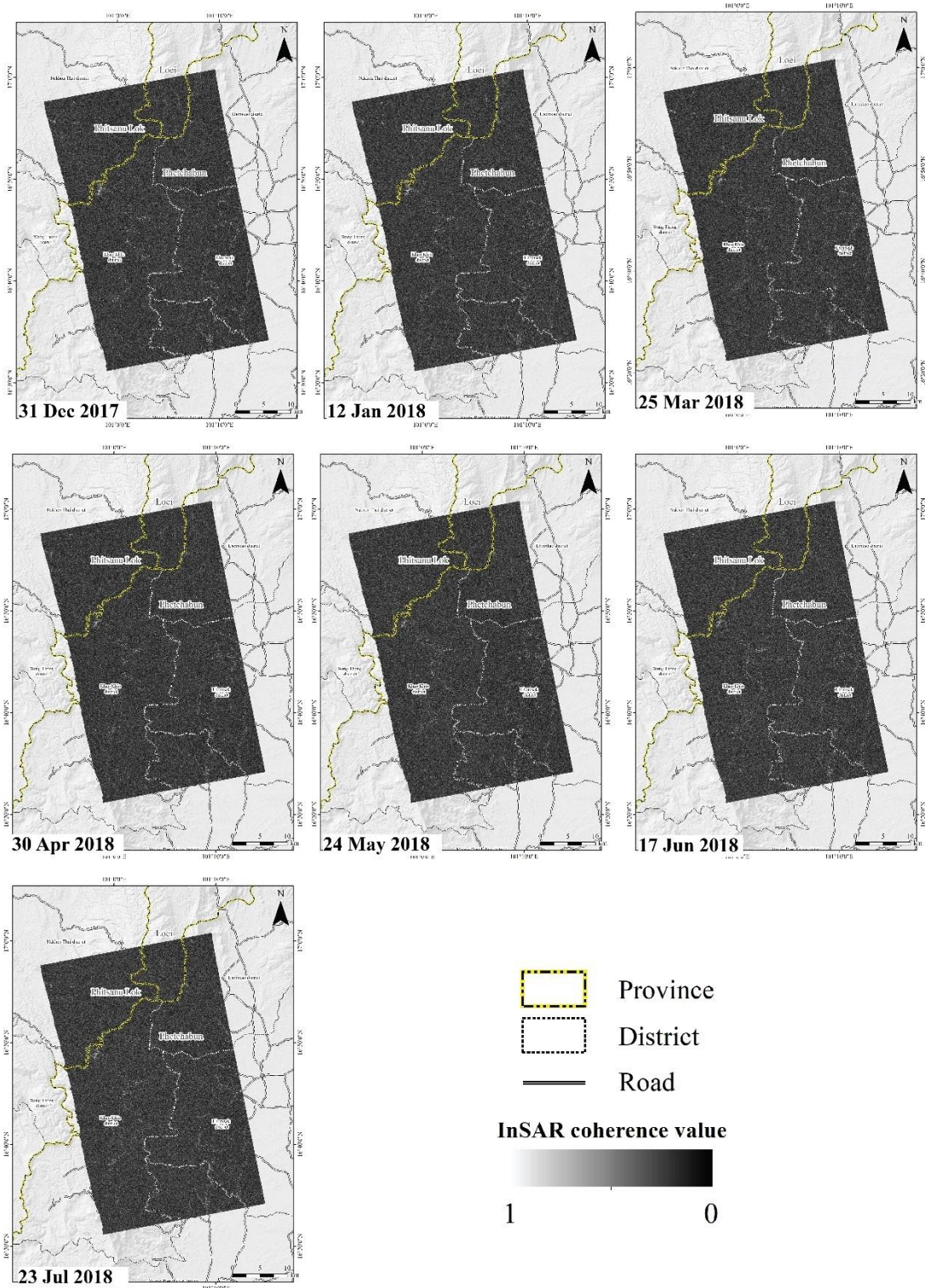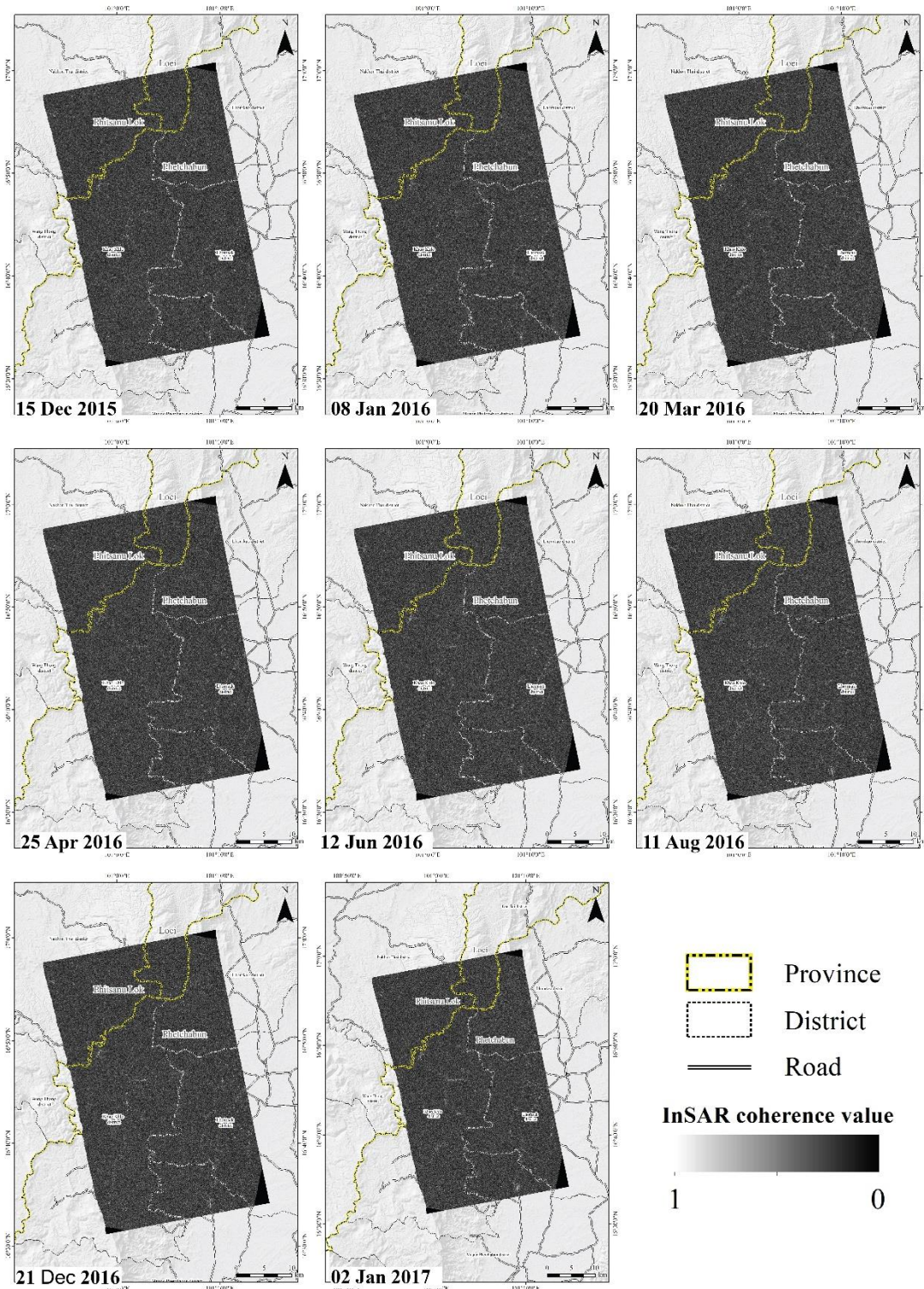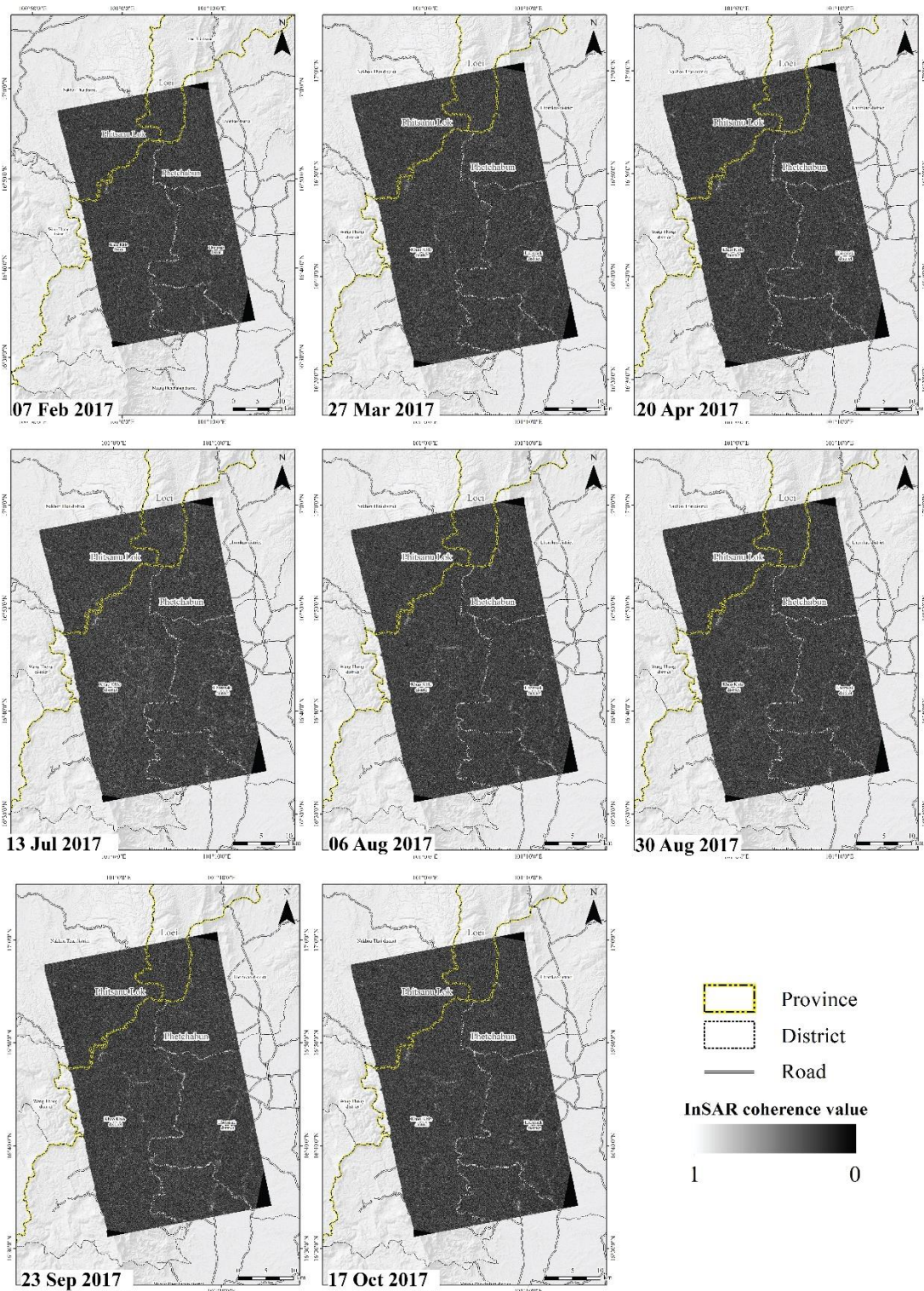
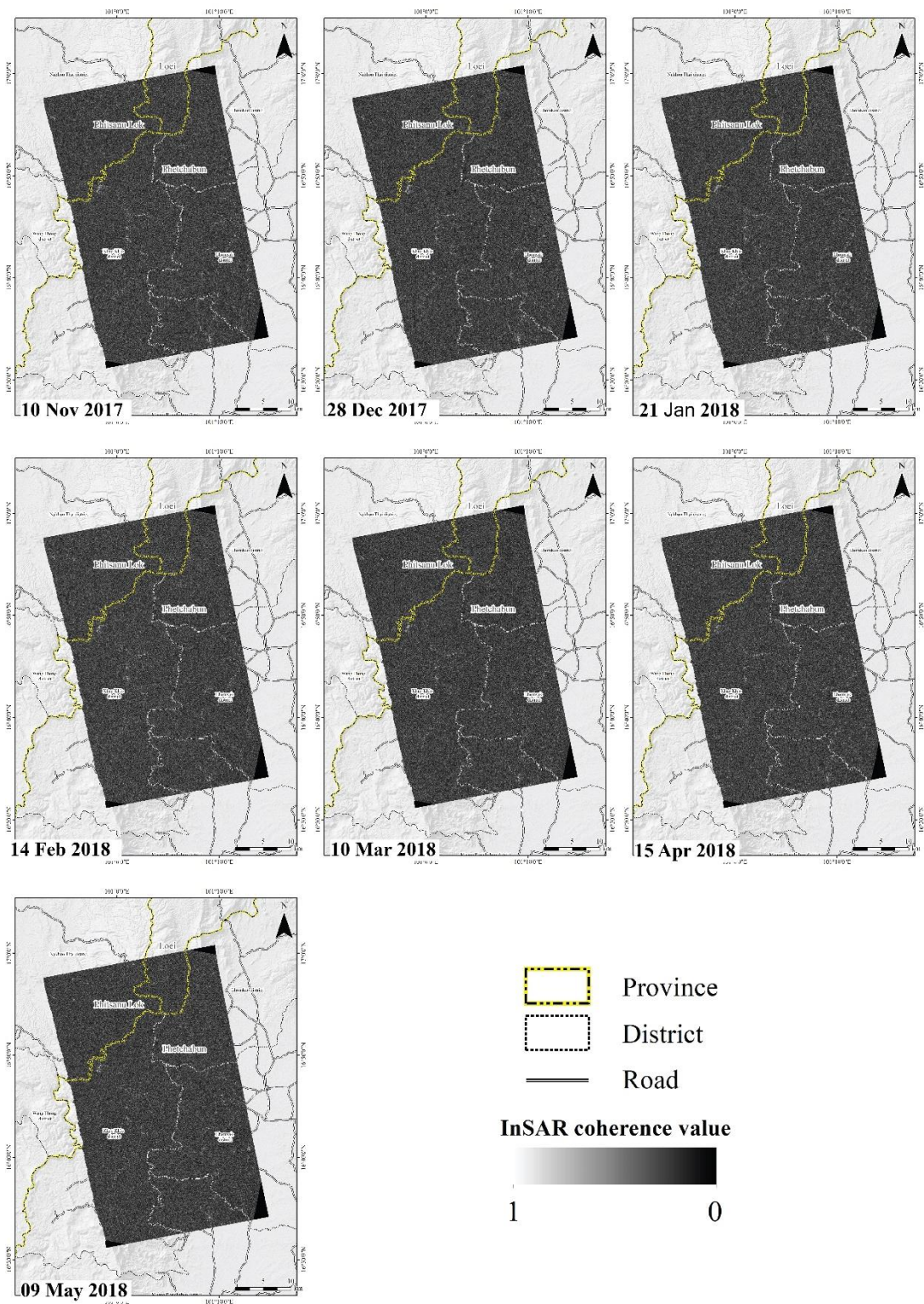**Figure 3.12** The coherence images of descending orbit between 07 February 2017 to 17 October 2017

Figure 3.13 The coherence images of descending orbit between 10 November 2017 to 09 May 2018

3.1.5 Subtract flat-earth phase or subtract topographic phase

This step eliminated phase which effect by properties of earth shape and surface. Subtract flat-earth and topographic operated for remaining only phase of earth surface displacement. Subtract flat-earth phase operated to remove flat-earth phase which obtained by scattering element on flat surface (i.e. same elevation). Flattened interferogram was eliminate only ϕflat from Equation 3.1. Subtract flat earth operated by geometric principle. This processing must apply the orbital information (the sentinel 1 position while acquired SAR data including height of satellite and perpendicular baseline), DEM and interferogram as an input data. Number of flat the Earth estimate point was defined with 501 point and degree of flat earth polynomial was defined with 3° that reasonable for study area size.

3.1.6 TOPSAR deburst

TOPSAR deburst is a final processing with SNAP. After interferogram formation including subtract flat-earth phase and removal topographic phase, all interferogram still show the seamlines between bursts. The Sentinel 1 SLC data was acquired by The IW swath mode, which separated SLC product to three sub-swaths along with slang range direction. In the addition, when the sensor motion along azimuth direction that generated a series of burst to all sub-swaths. In the order to using interferogram data, which need to merge all burst for using in PSInSAR method. The interferogram after the deburst processing (Figure 3.14) were preparedness data, which can apply to other analysis.

a)

b)
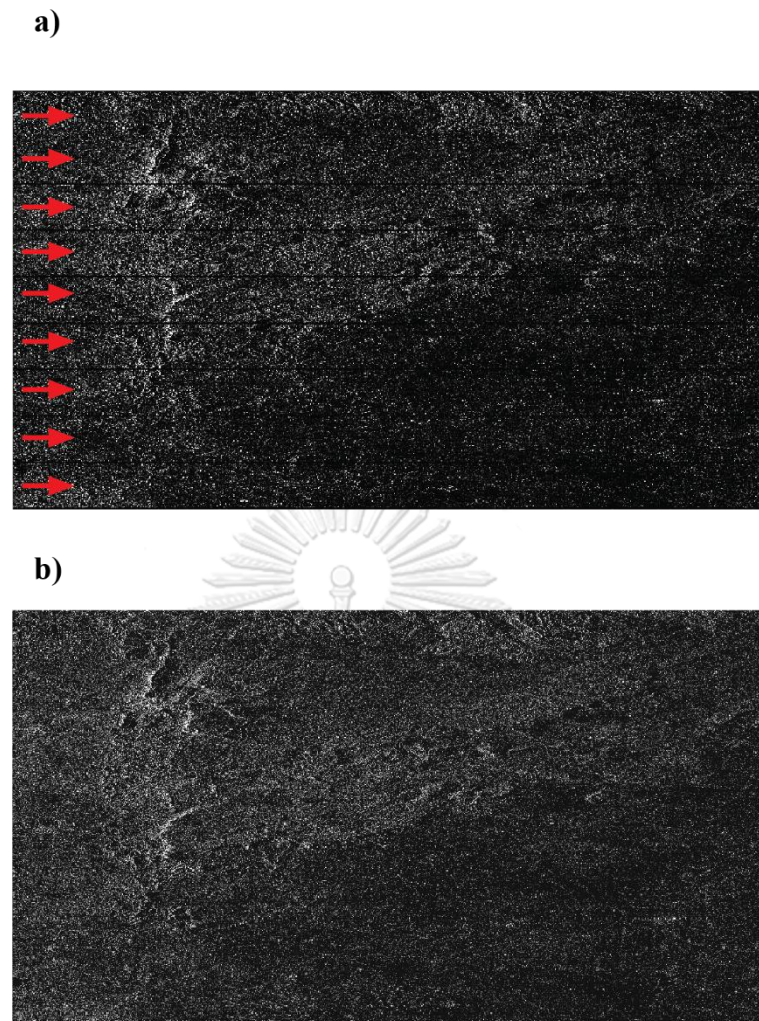
Figure 3.14 A) bursts of SAR image for this study B) SAR image deburst already

3.2 PSInSAR with StaMPS

Later interferograms were available by SNAP. StaMPS is a Permanent scatterer processor order to analysis PS pixel. Main steps of PSInSAR by StaMPS can explain by 6 step which including find the potential interferogram pixel to PS pixel, Phase unwrapping and estimate error relate with PS pixel value. The results getting by StaMPS demonstrated by position of PS pixel which contain the velocity in line of sight (VLOS). The estimate phase noise processing was the first step in the order to discover PS pixel. This step operated by iteration data pixel. All interferogram were estimated phase noise value to every pixel.

3.2.1 PS pixel selection

A few pixels of interferogram were selected to be PS pixel by their noise characteristic. The percentage of non-PS pixel was estimates in a data scene from which defined threshold of the density.

3.2.2 PS pixel filtering

This step applied for filtering selected pixels from the previous step. Due to contribution of signal from neighboring element which affect too noisy. The result from PS pixel filtering is the PS pixels containing the wrapped phase value. The wrapped phase value (W in Equation 3.2) present range of values between π to -π or 3.14 to -3.14 in radian unit (rad) (**Figure** 3.15 to 3.17 for ascending orbit and **Figure** 3.18 to 3.20).

$$\phi = W\{\ \phi_{\text{disp}} + \phi_{\text{atm}} + \phi_{\text{noise}}\ \}\ldots\ldots\ldots\text{(Eq 3.2)}$$
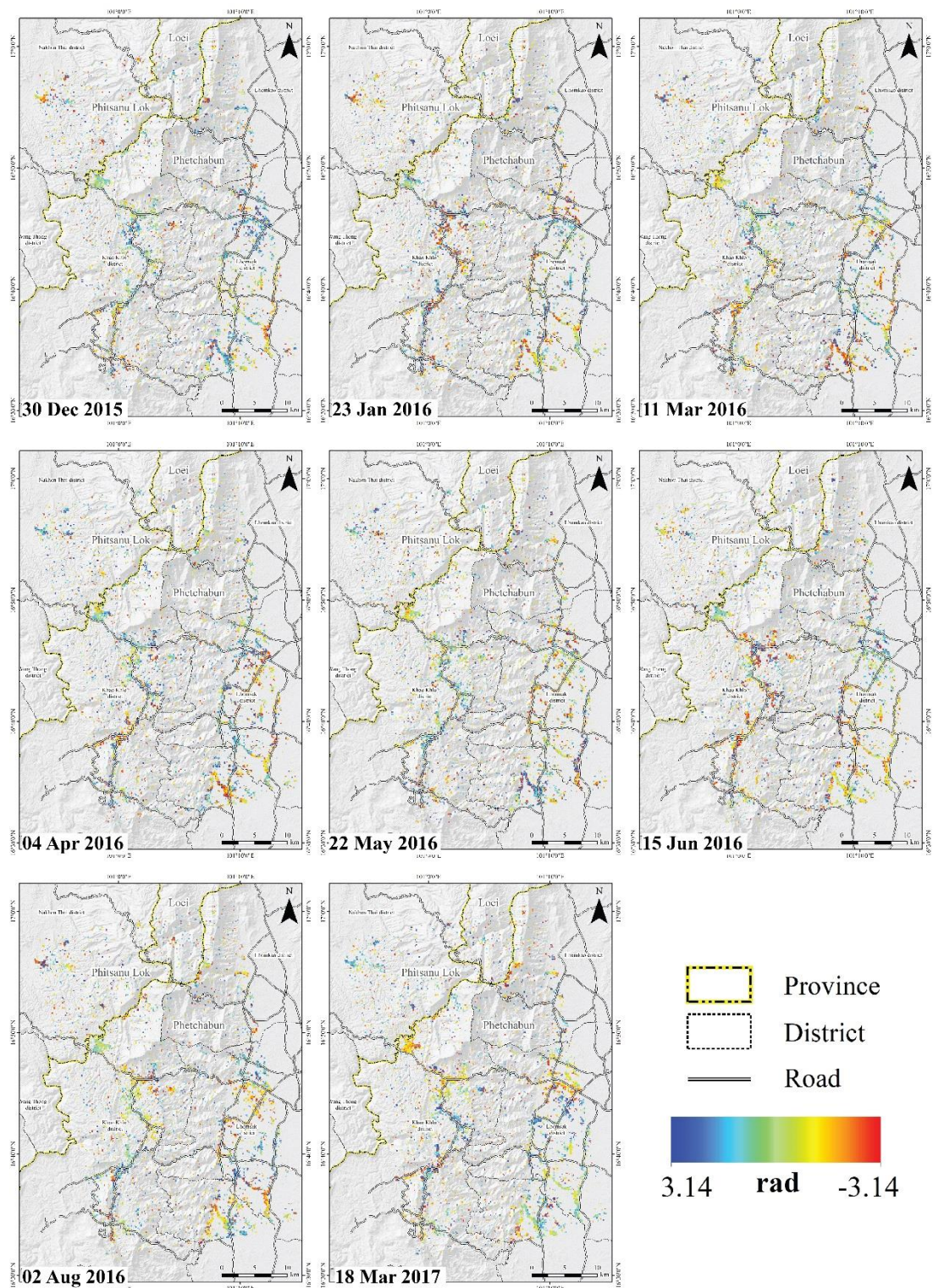
Figure 3.15 Interferogram Pixels were selected for PS points of ascending data
30 December 2015 to 18 Mar 2017
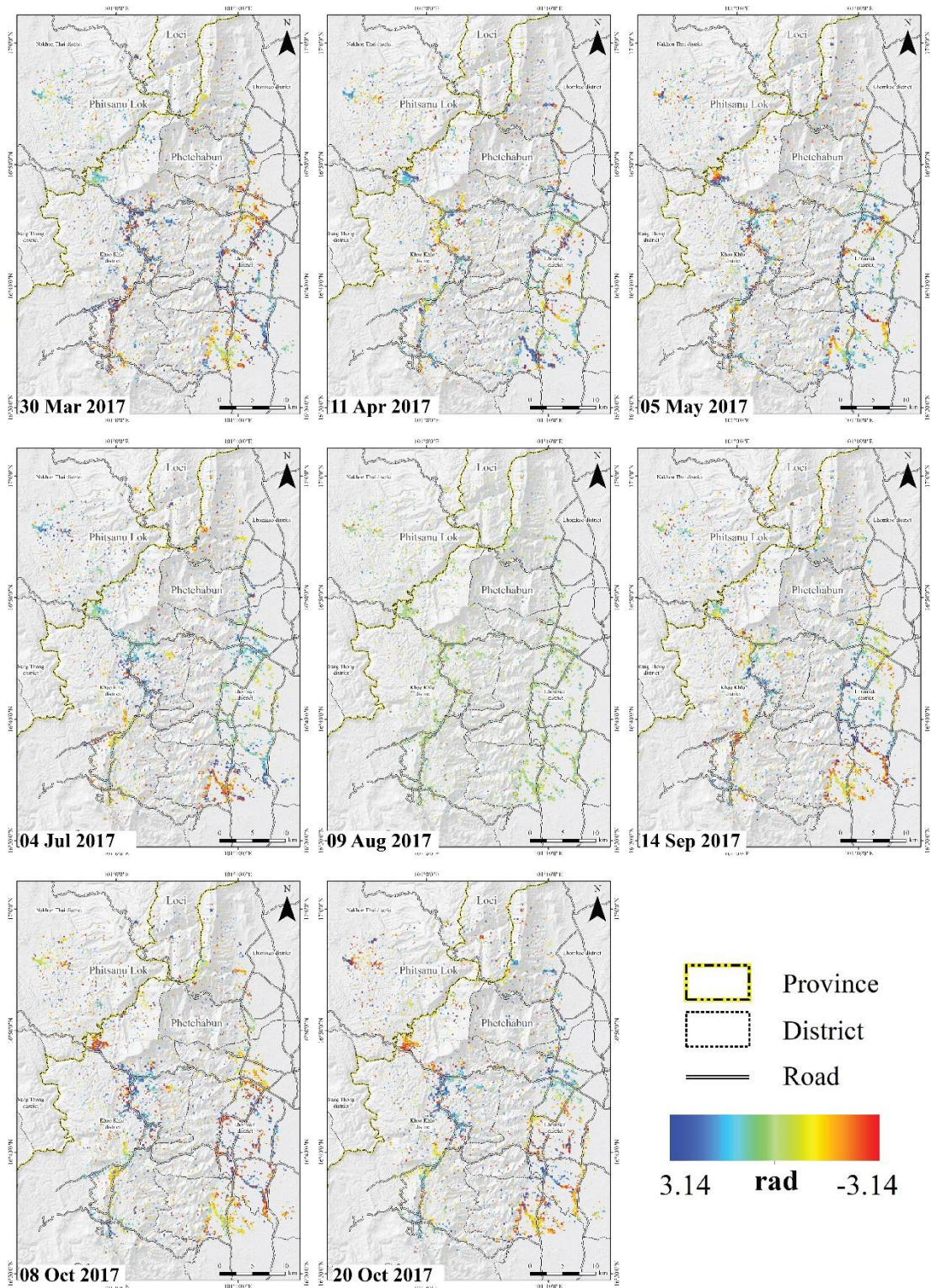
Figure 3.16 Interferogram Pixels were selected for PS points of ascending data
30 Mar 2017 to 20 October 2017
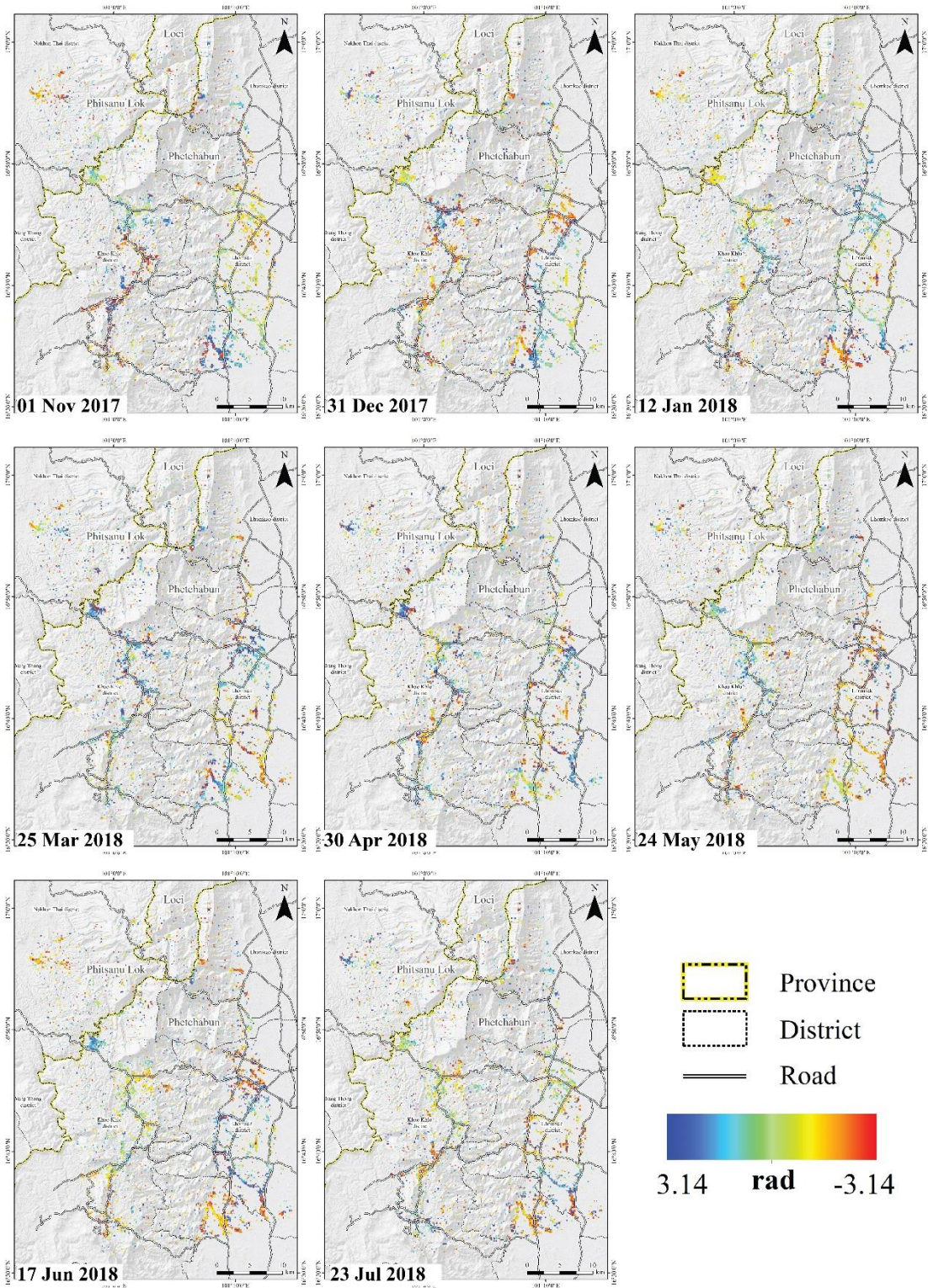
Figure 3.17 Interferogram Pixels were selected for PS points of ascending data
01 November 2017 to 23 July 2018
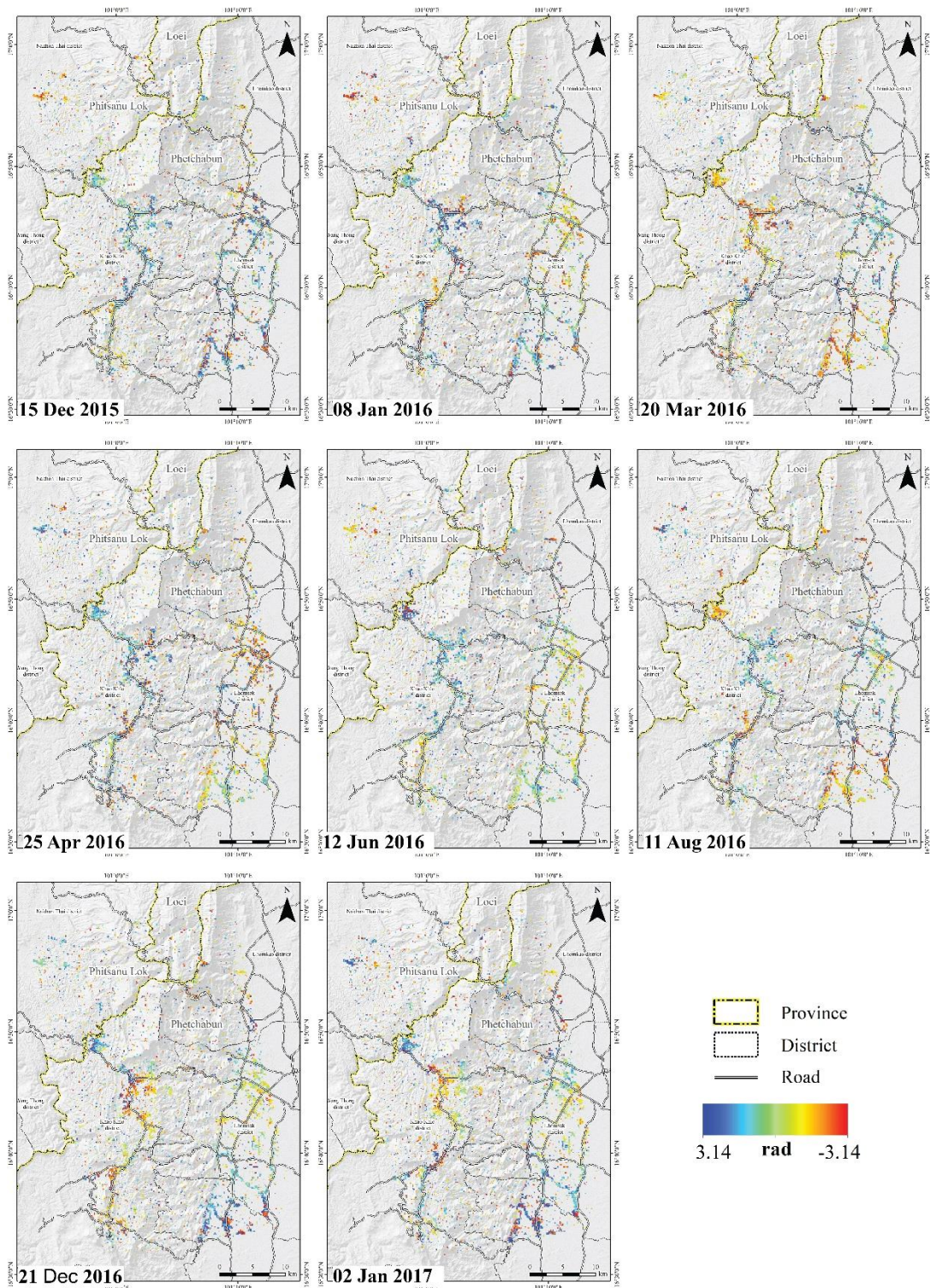
Figure 3.18 Interferogram Pixels were selected for PS points of descending data between 15 December 2015 to 02 January 2017
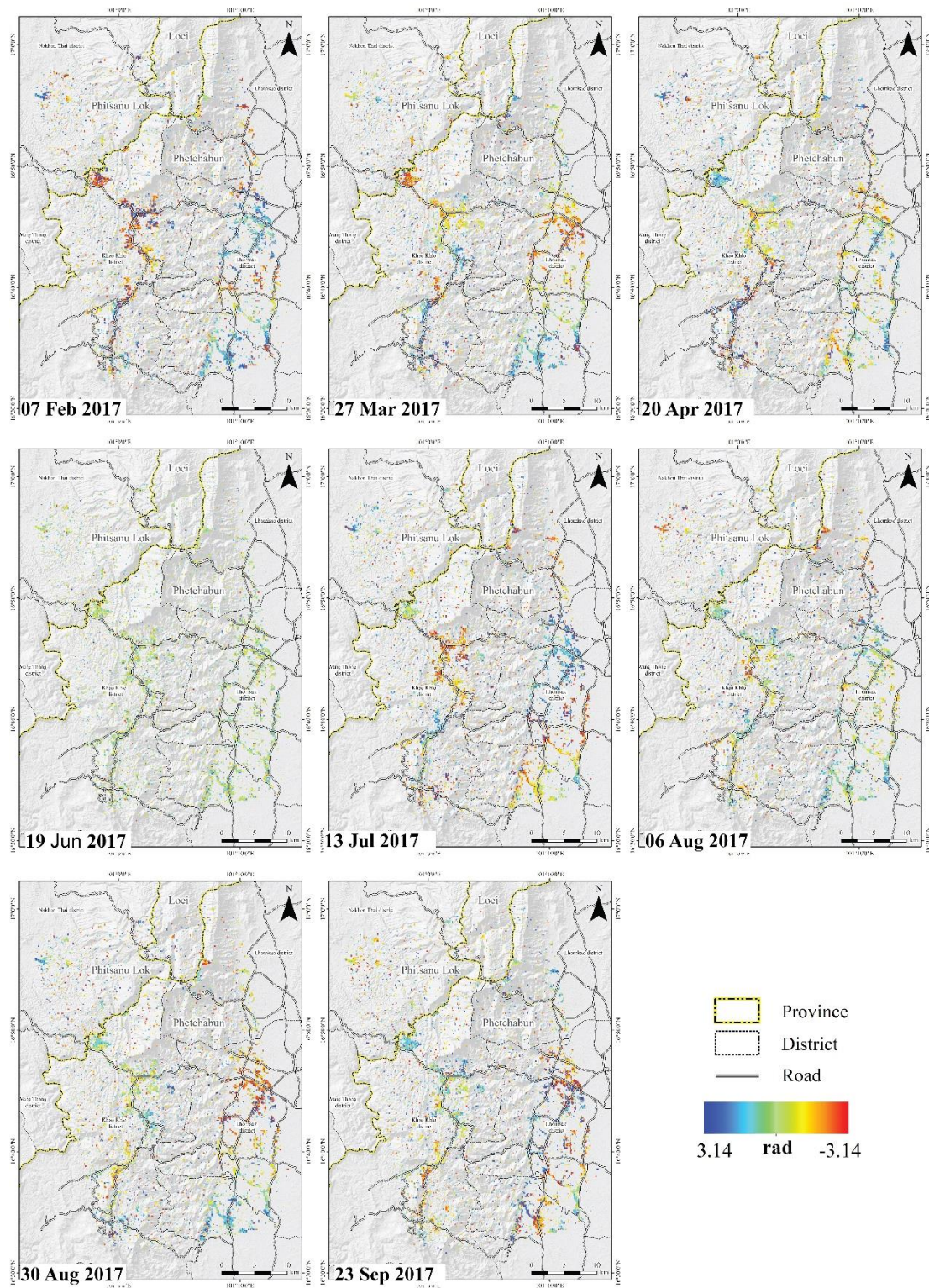
Figure 3.19 Interferogram Pixels were selected for PS points of descending data
between 07 February 2017 to 23 September 2017
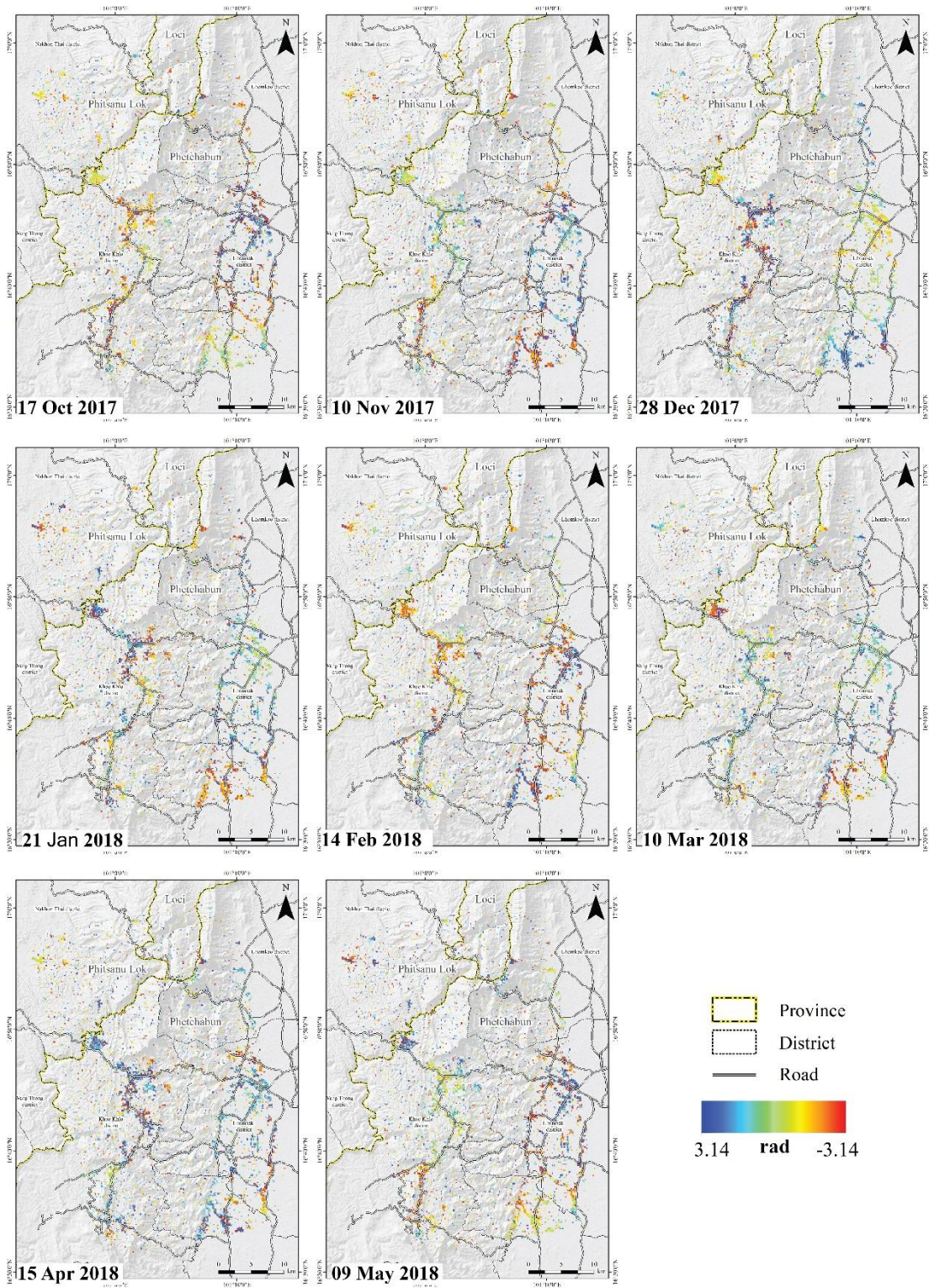
Figure 3.20 Interferogram Pixels were selected for PS points of descending data between 17 October 2017 to 09 May 2018

3.2.3 Phase unwrapping

Interferometric phase was obtained by previous process, that measured value within modulo 2π or wrapped data. Fringe of interferogram which did not unwrapping phase (Figure 3.14), which a color cycle have value between $-\pi$ to π. The unwrapping method which, using in this study was Three-dimension method. The three-dimensional unwrapping needed wrapped phase of all PS pixel. Firstly, interferometric phase was filtered phase to reduce noise by Goldstein filter algorithm. Figure 3.22 to 3.24 for ascending orbit and Figure 3.25 to 3.26 for descending orbit, demonstrated PS pixel from phase unwrapping of each image. For the ascending orbit, the range of phase value between 13 to -13 rad, the descending orbit phase value between 10 to -10 rad
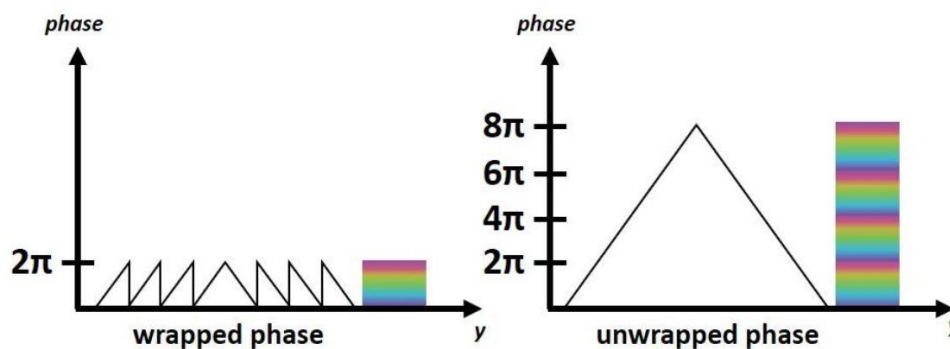
Figure 3.21 the schematic of phase unwrapped (Ferretti et al., 2007)
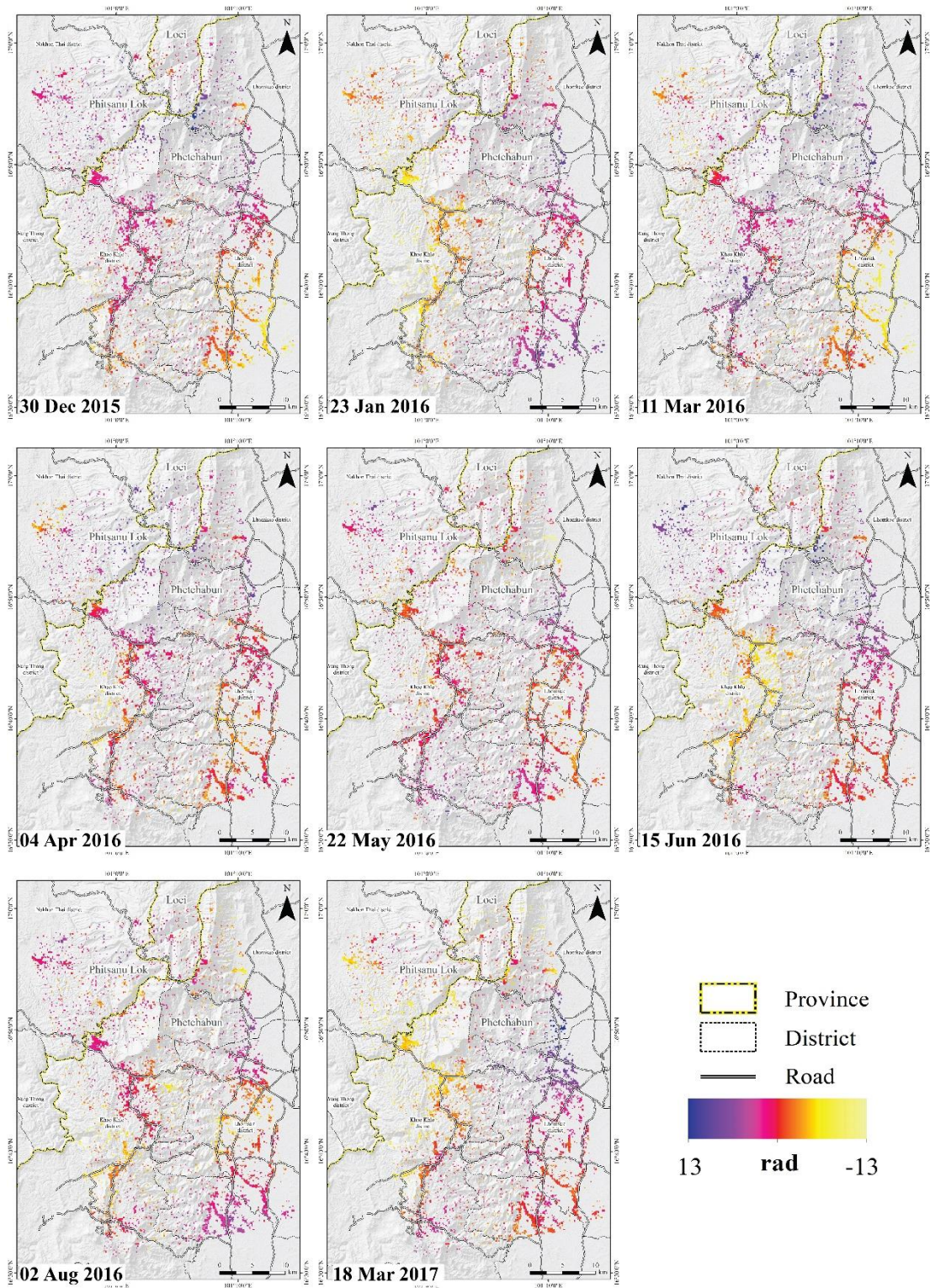
Figure 3.22 Unwrapped PS pixels of ascending orbit between 30 December 2015 to 18 Mar 2017
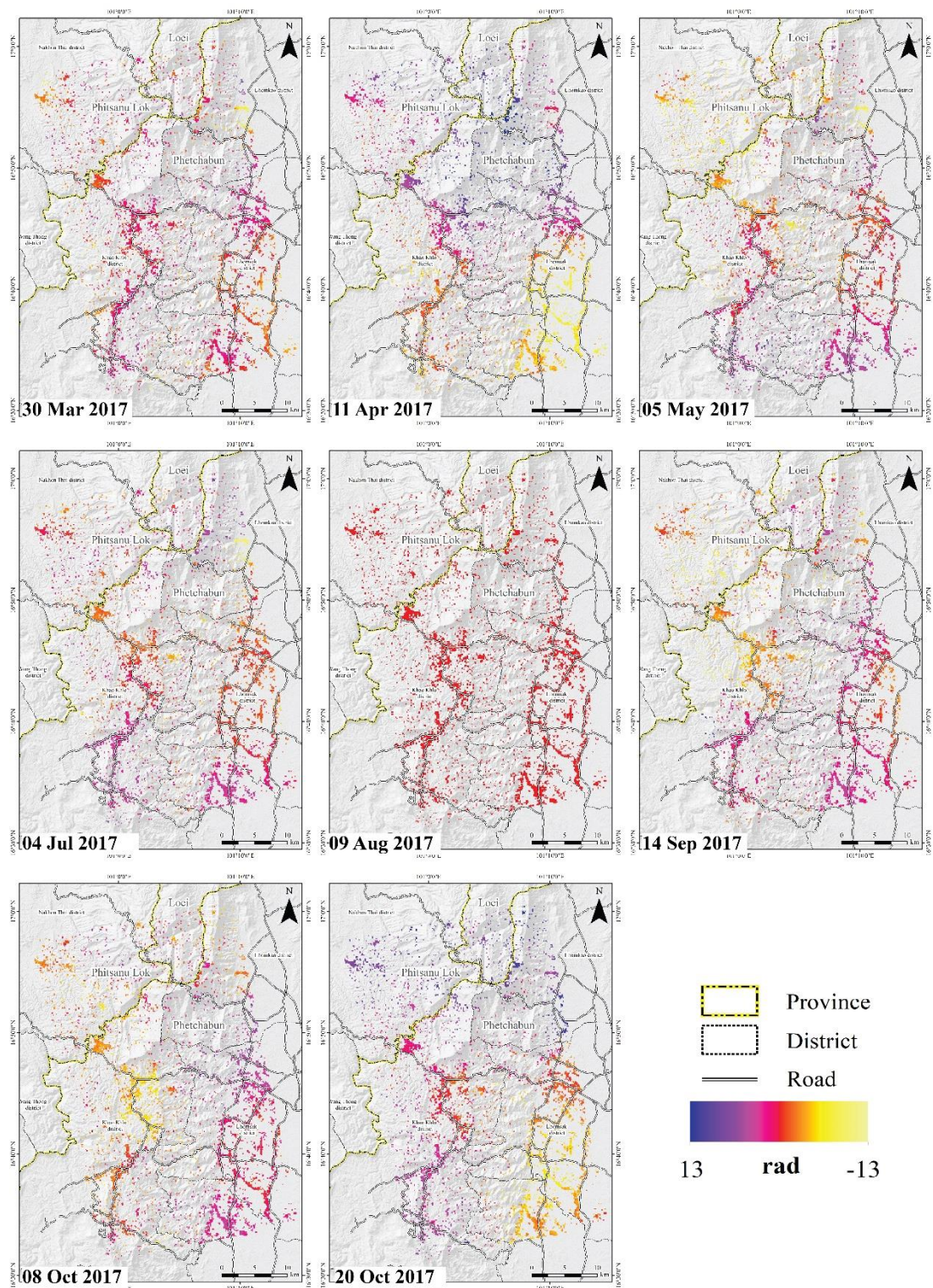
Figure 3.23 Unwrapped PS pixels of ascending orbit between 30 Mar 2017 to 20 October 2017
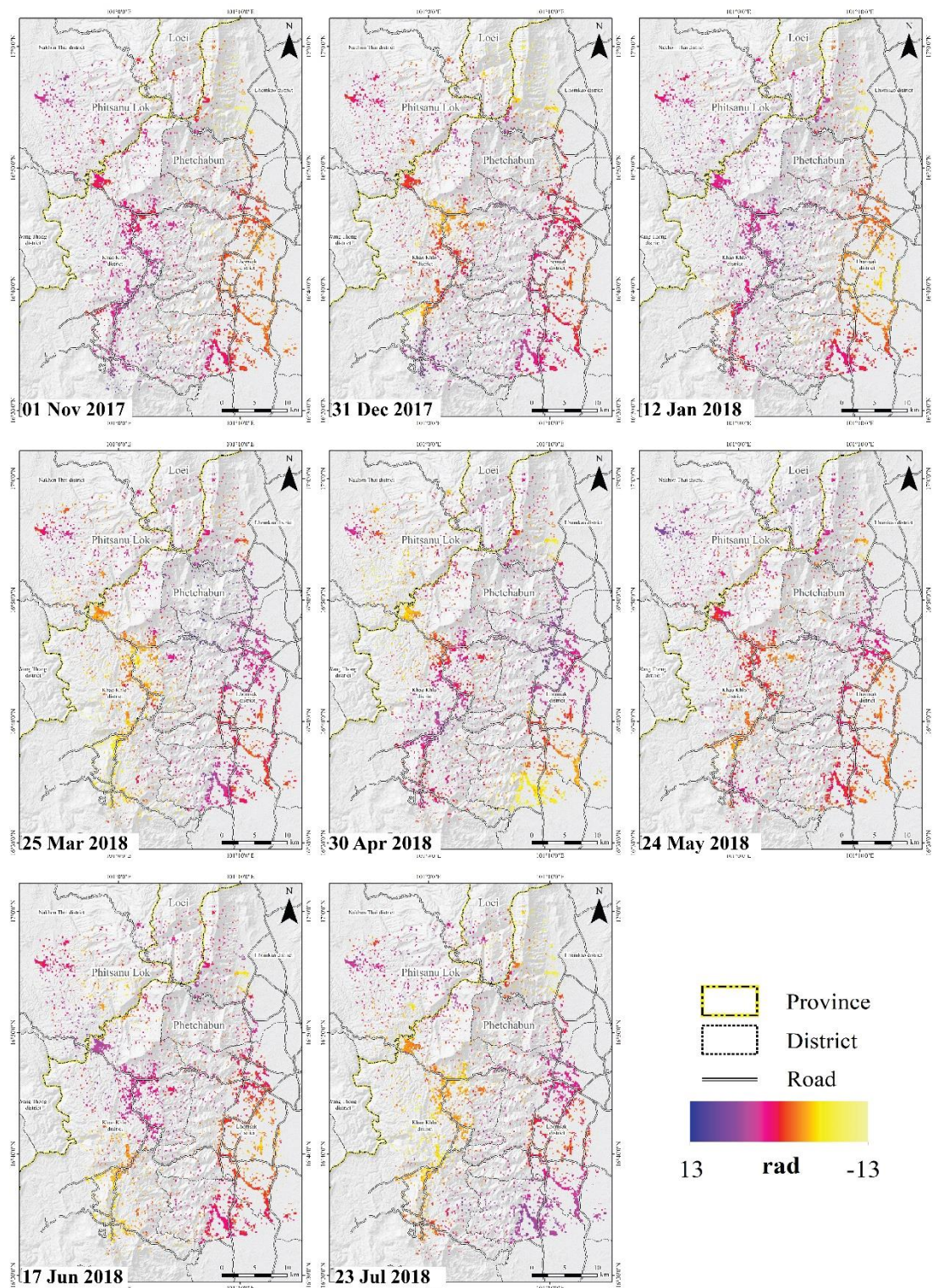
Figure 3.24 Unwrapped PS pixels of ascending orbit between 01 November 2017 to
23 July 2018
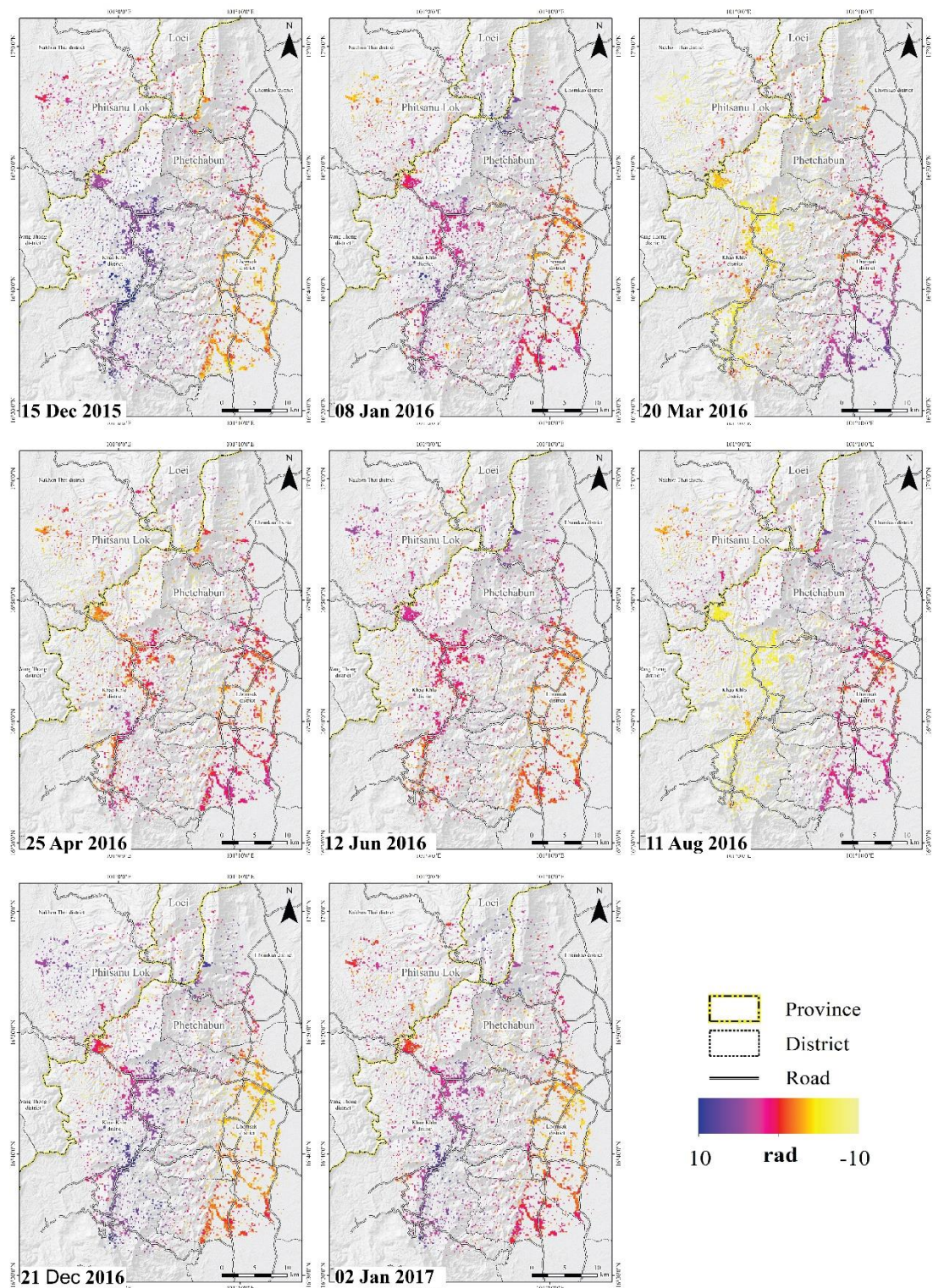
Figure 3.25 Unwrapped PS pixels of descending orbit between 15 December 2015 to 02 January 2017
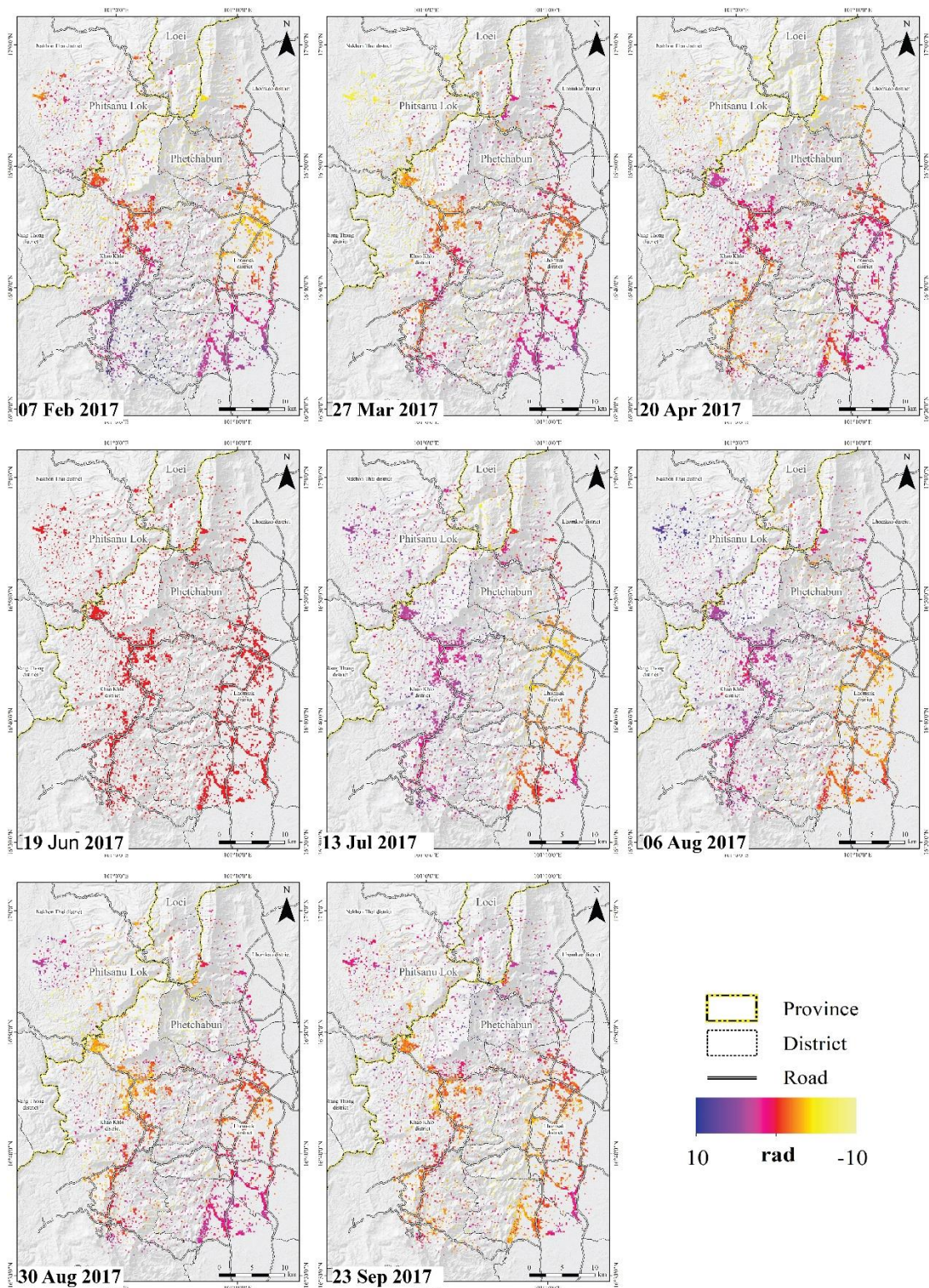
Figure 3.26 Unwrapped PS pixels of descending orbit between 07 February 2017 to 13 September 2017
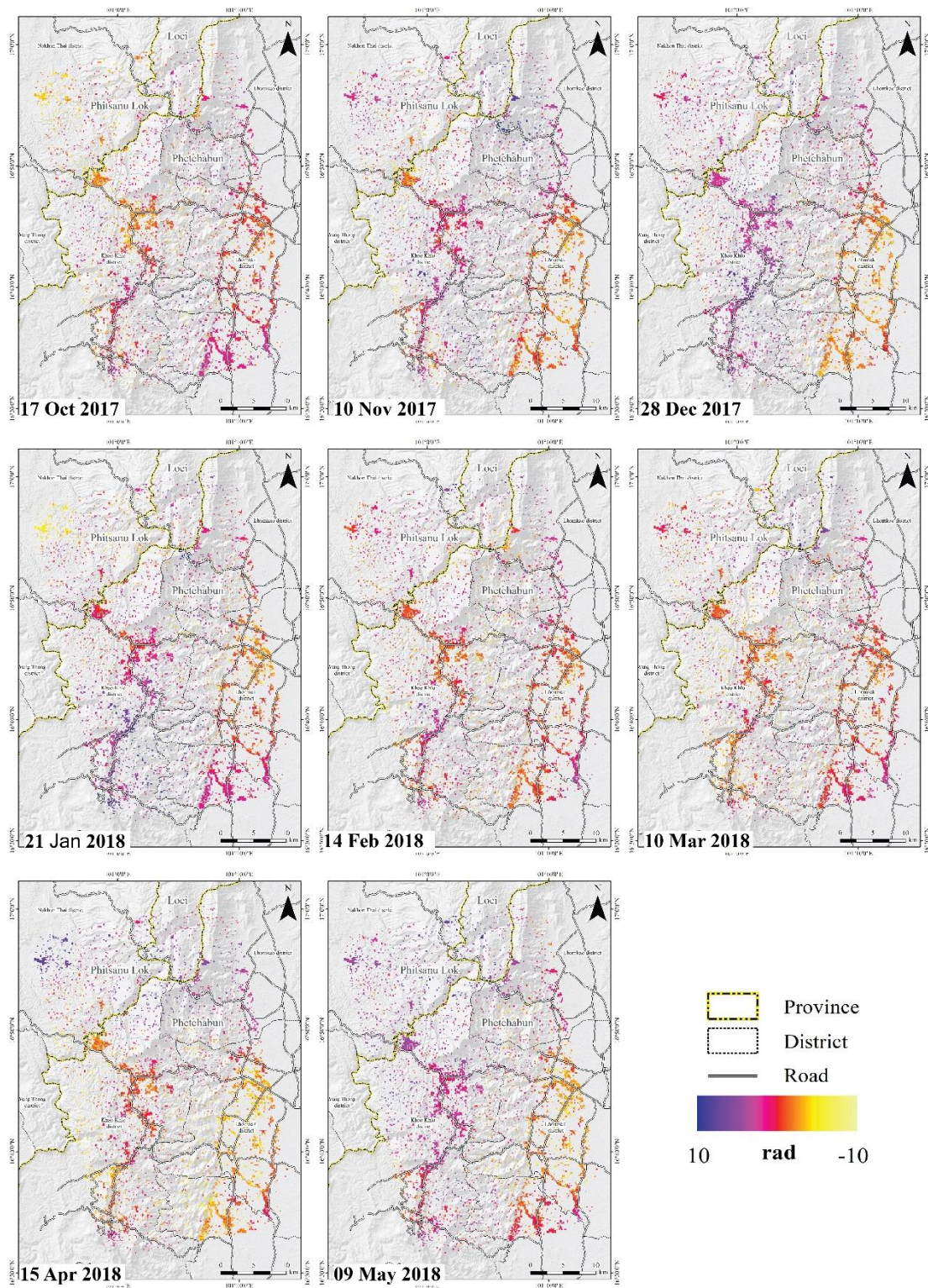
Figure 3.27 Unwrapped PS pixels of descending orbit between 17 October 2017 to 09 May 2018

3.2.4 Estimate spatially correlated look angle error

Master atmosphere and Orbit error was reduced by this step. The output of this step is PS point or PS pixel contain displacement rate. That convert by earth surface deformation in phase radian proportion with sentinel-1 wavelength. The result is defined by velocity of surface displacement along satellite LOS (mm / year). For use result from PSInSAR analysis PS point will be projected value to velocity along slope surface.

3.3 Conversion Velocity of line of sight to Velocity of slope

For investigation mass wasting by PSInSAR technique, PSInSAR results must be converted from velocity deformation along line of sight (V_{LOS}) to velocity of slope (V_{SLOPE}), that can represent mass waiting movement truly. V_{LOS} indicated to a displacement of earth surface relative with satellite LOS. Positive V_{LOS} value provided an earth surface defamation towards the satellite, but negative V_{LOS} value provided an earth surface deformation away from the satellite. Mass wasting is a phenomenon relating with movement of rock, debris and soil on a slope direction, hence mass wasting investigation must perform by slope direction. The conversion between V_{LOS} to V_{slope} is assume that the mass movement is simply parallel to the maximum slope direction. Equation 4.1 is an operator of the conversion.

$$Vslope = VLOS / C \quad\quad\quad\quad\quad (Eq\ 3.2)$$

The C value is a coefficient represents the sensitivity of the LOS vector to measure a displacement in slope direction. The C can fine by Equation 4.2, that project LOS geometry to slope plane. DEM generated slope angle and slope aspect to calculate C coefficient. Moreover, geometry of acquisition including incidence angle and the sentinel 1 ground track angle were used to fine the C. Ground track angle is a constant value related with satellite orbit direction. For incidence angle (Figure) is the angle of the intercepting between earth surface and vertical incident with wave beam.

$$C = N \times (\cos(S) \times \sin(A - 90)) + E \times (-1(\cos(S) \times \cos(A-90)) +$$

$$H \times (\sin(S))$$

$$N = \cos(90 - \theta) \times \cos(180 - \alpha)$$

$$E = \cos(90 - \theta) \times \cos(270 - \alpha)$$

$$H = \cos(\theta) \quad\text{..(Eq 3.3)}$$

Where   S = Slope angle

A = Slope aspect

θ = Incidence angle of sentinel 1

α = satellite ground track

Slope aspect and slope angle were available from ALOS PALSAR DEM with a spatial resolution 12.5 x 12.5 meters. N, E and H are the directional cosine of LOS vector. Where θ is the incidence angle of acquisition (Figure 3.28). α is the satellite ground track angle, which follow by satellite orbit direction. α angle is approximately -15º + 90º for ascending orbit and -165º + 90º. The conversion operated to each PS pixel with velocity pixel.
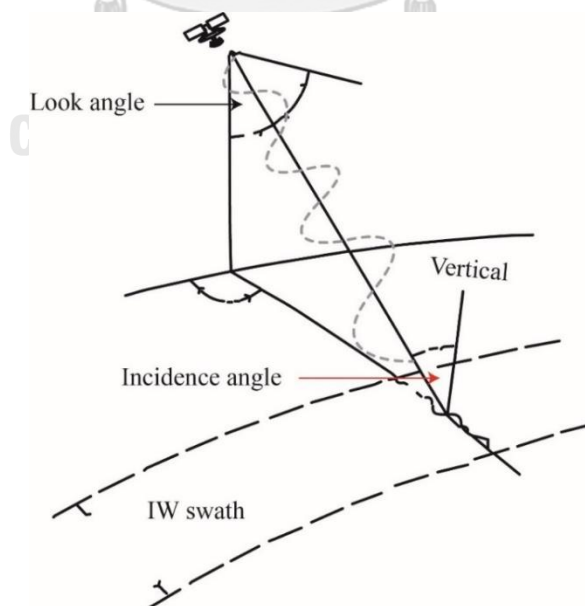
Figure 3.28 Incidence angle in the SAR image acquisition geometry
(Confuorto, 2016)

Chapter 4   RESULTS

4.1 Results of PS analysis

PSInSAR technique using StaMPS algorithm, which provided PS points on 1,400 km^2 of ascending orbit around 50,639 points and descending orbits around 56,934 points. The mean velocity of ground in LOS direction is 0.728 mm/yr for ascending and 0.328 mm/yr for descending. Figure 4.2 and 4.3 display PS point with high resolution satellite image. Mostly PS pixels are founded on the high-density human structure such building, roads, some PS point also place on area without vegetation cover.

High building distribution around study area correspond severely PS point position. Important advantage of the study area is most building located on slope area; thus, PS point can distribute on slope mostly.

LOS velocity provides from PSInSAR analysis, show displacement rate between 17.76 to -13.30 mm/year for ascending orbit and 14.87 to -15.12 mm/year for descending orbit. For both descending and ascending orbit, PS point are located rather likely area.
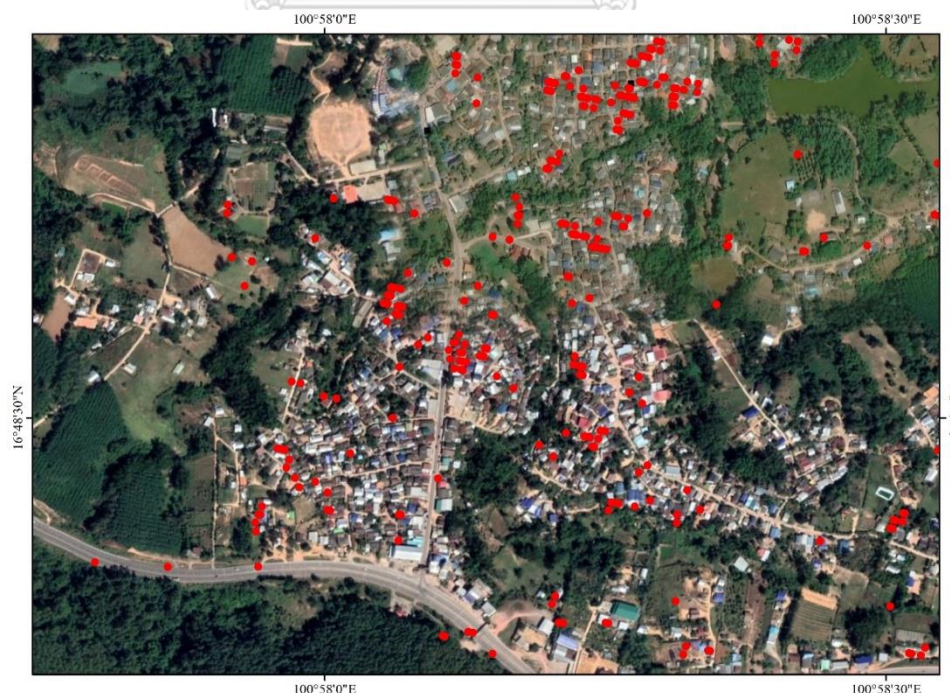
Figure 4.1 PS point containing displacement are located intensive on urban area

Khao Kho is covered by high PS point density because the area characterized by low vegetation cover and high building density. Moreover, More PS points are appeared along with Highway to Khao Kho district, especially Highway number 12. Beside the highway which characterize by human structure and outcrop is corresponded by PS selection to PS point. The other interesting area on the Phetchabun range is call Phu Thap Boek, because the area has high complex human structure. Those structure offer permanent signal and select to be PS points. Nevertheless, almost area on Phetchabun range cover by density of vegetation that effect to low number of PS point. The decorrelation of SAR image remains both temporal and spatial decorrelation, though noise was reduced.

PS point distribution get by both geometry acquisition quite provides different value and position. Those result are displacement rate relate on satellite LOS direction, so the displacement properties are move toward and outward satellite antenna (to the East and to the West). Mass movement mostly take place on slope area, consequently the conversion of LOS velocity (V_{LOS}) to slope velocity (V_{SLOPE}) is required estimate mass movement in study area.

Figure 4.2 PS point obtained by PSInSAR form StaMPS algorithm contain velocity in LOS direction, ascending orbit.
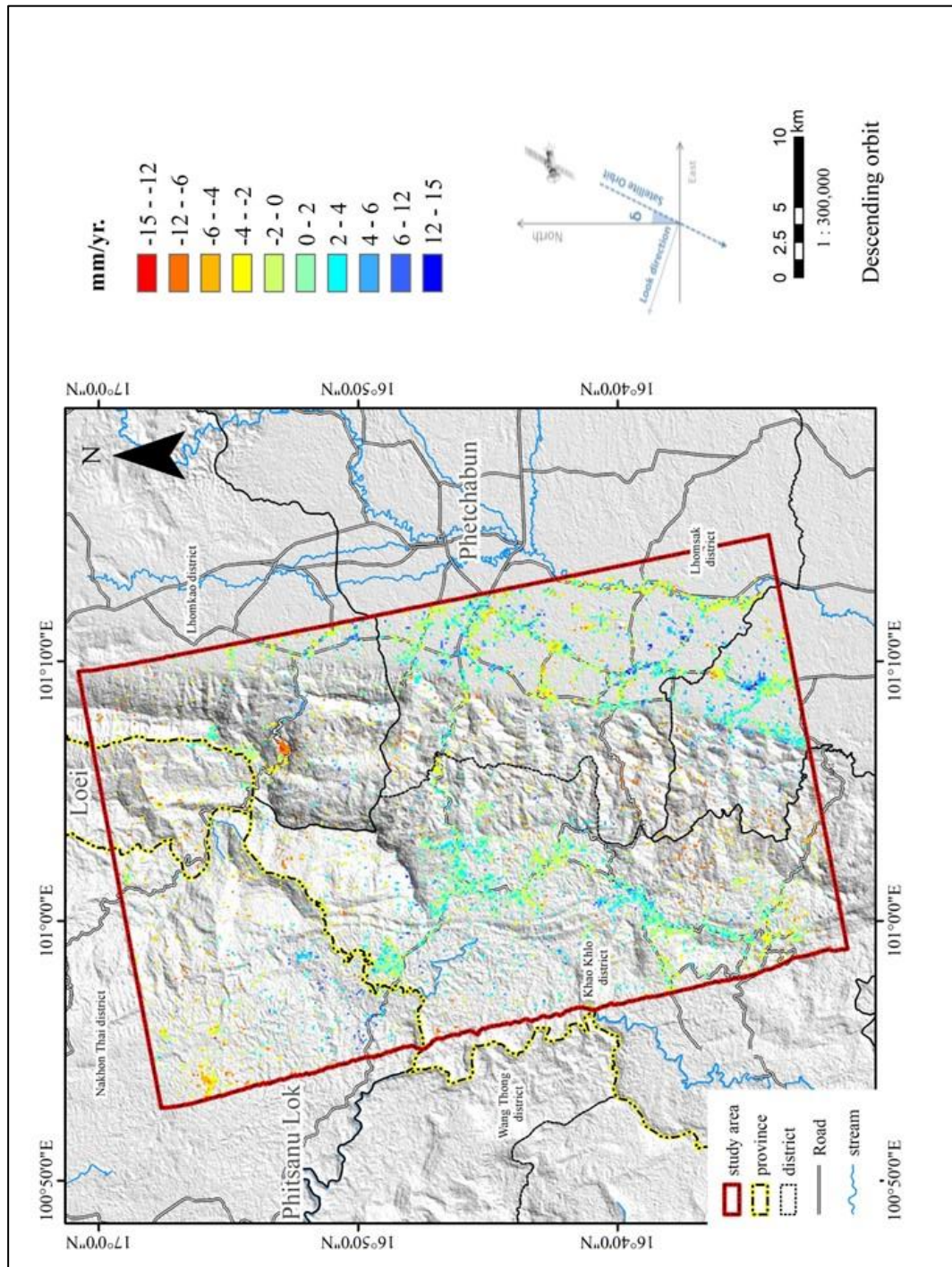
Figure 4.3 The PS point obtained by PSInSAR form StaMPS algorithm contain velocity in LOS direction, descending orbit.
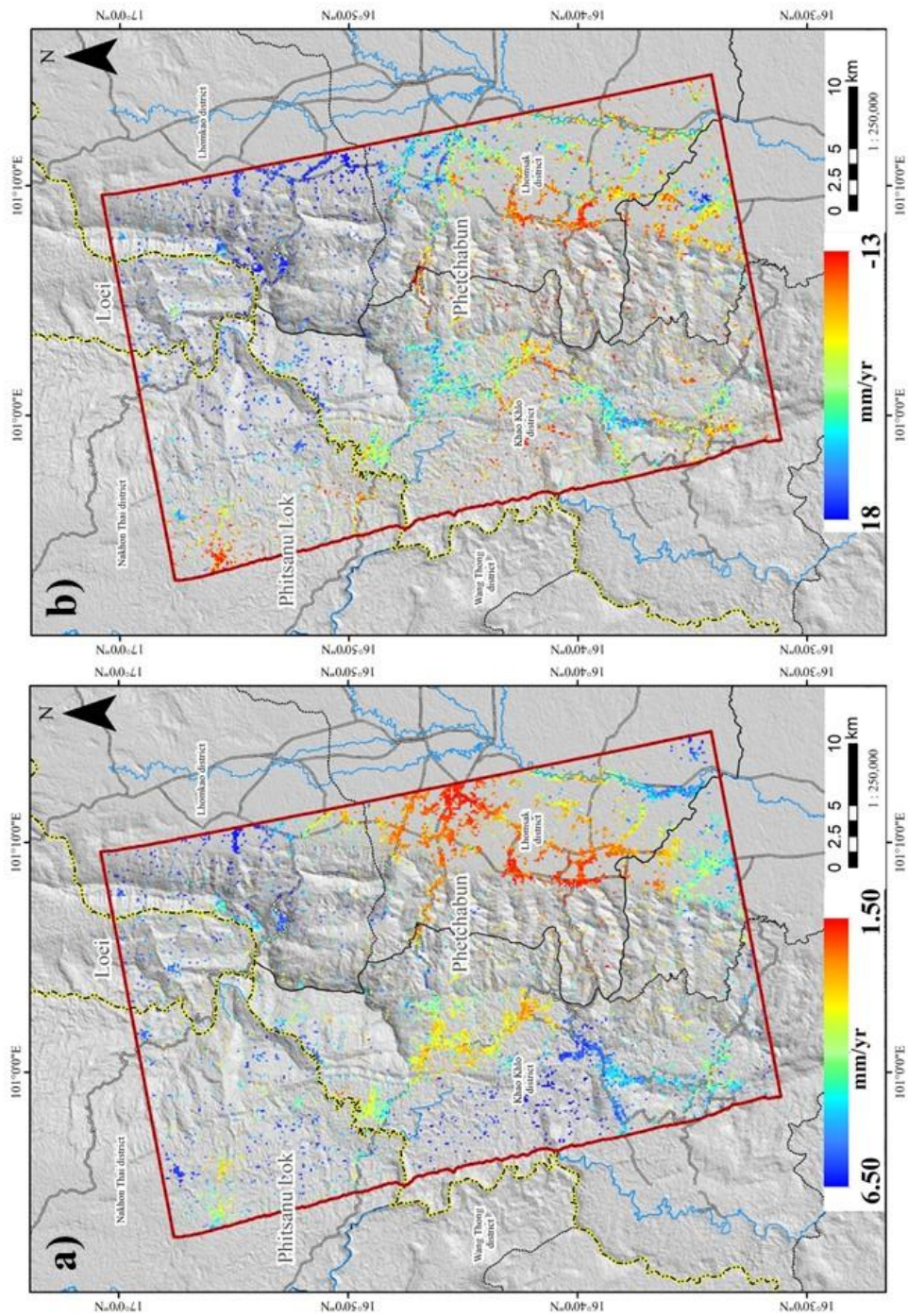
Figure 4.4 The comparison between PS point contains V$_{LOS}$ and PS result standard division of ascending orbit

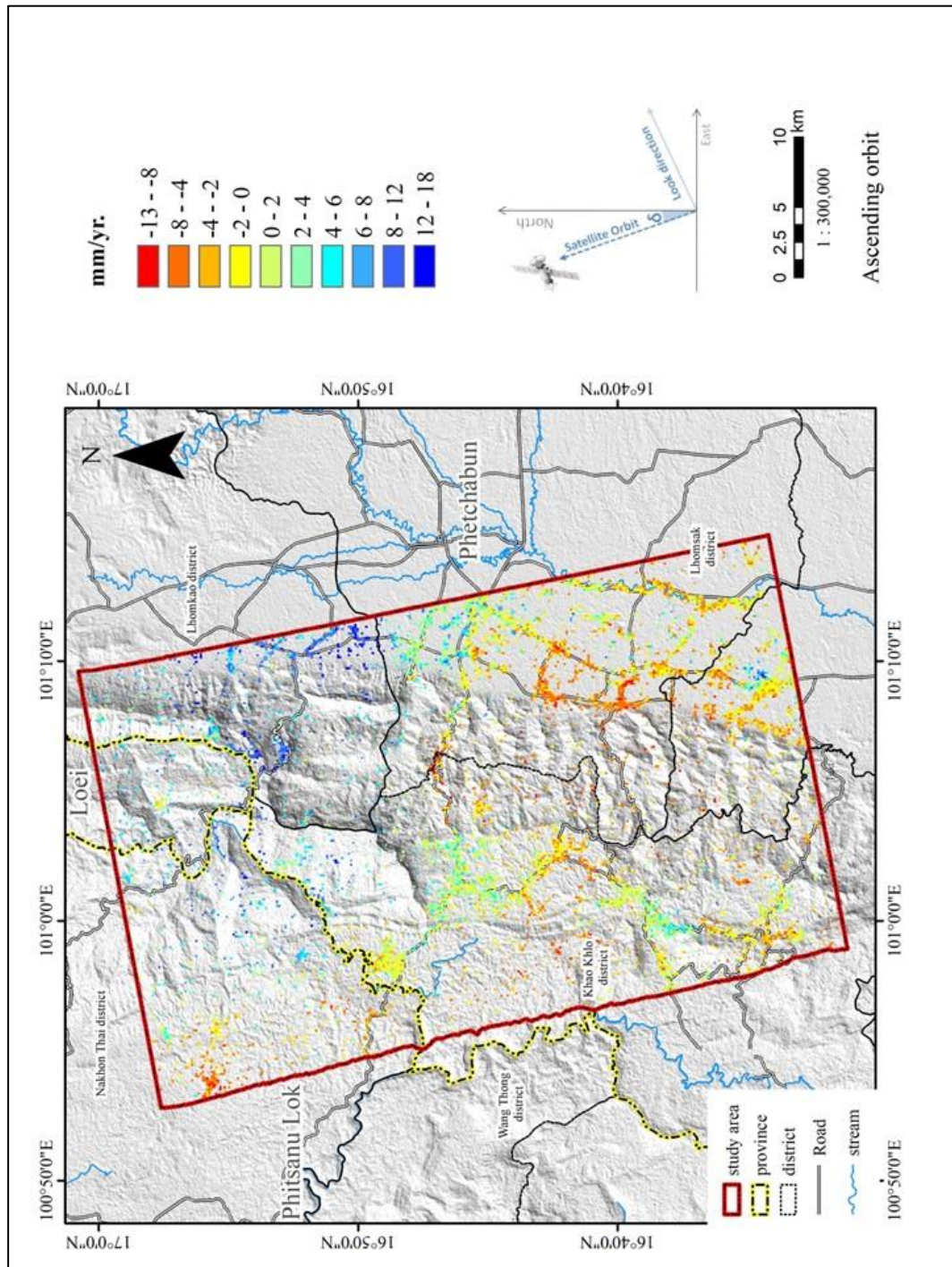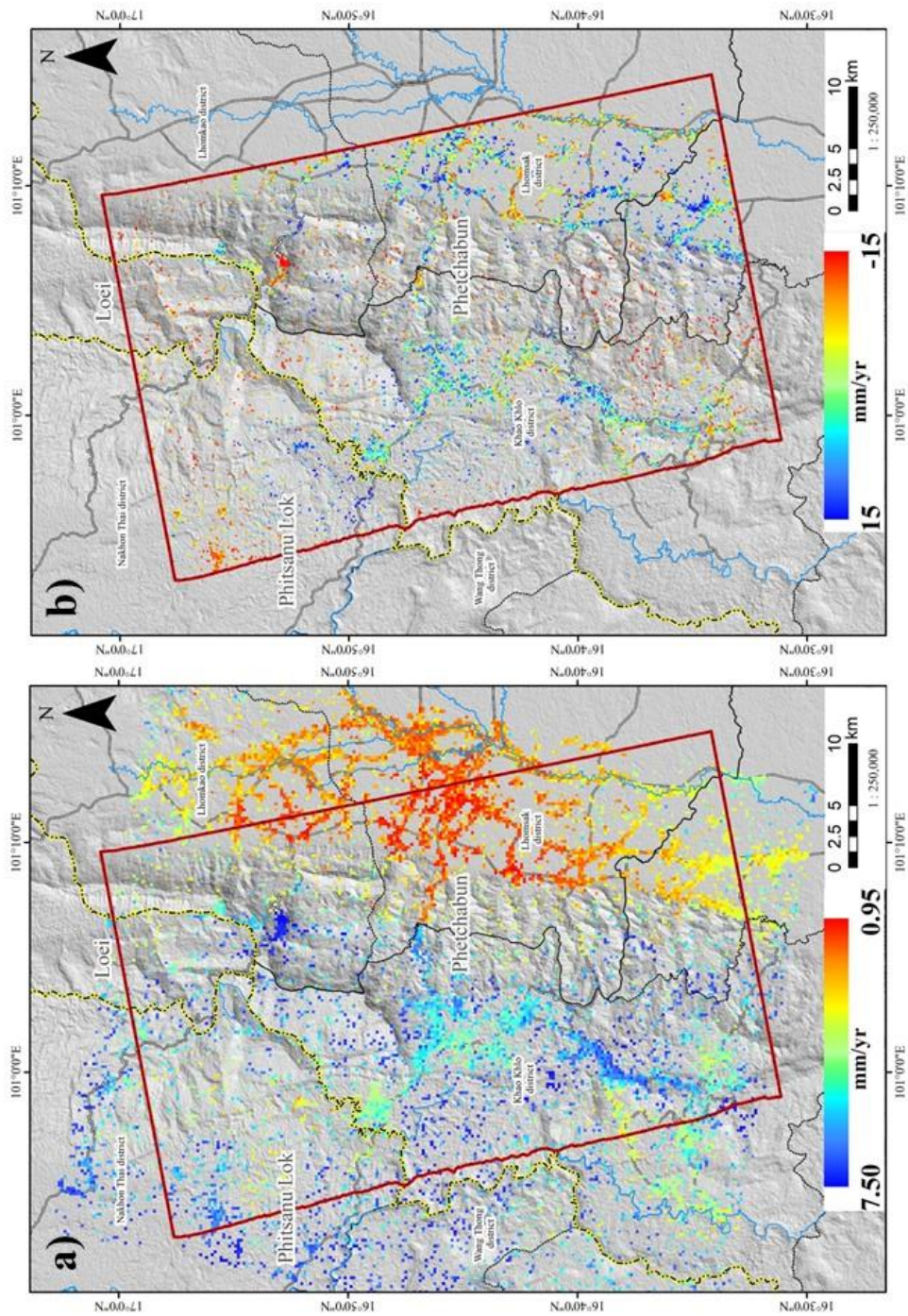**Figure 4.5** The comparison between PS point contains V_{LOS} and PS result standard division of descending orbit

4.2 The results of the conversion of V_{LOS} to V_{SLOPE}

The results of the conversion V_{LOS} to V_{SLOPE} step, which calculated together by slope aspect in degree unit, slope angle in degree unit, incidence angle and satellite ground track angle. The area properties and acquisition angle generate C-value in raster image, which use to convert geometry of displacement from LOS to slope facing. Although the conversion velocity results provide slope velocity but result still store both positive and negative value. After conversion step, V_{SLOPE} is eliminate some point and value by the positive value and slope of area. The negative value is assumed to mass wasting along slope, but the positive value might represent an uphill displacement, thus all PS point with positive value are discarded. Next, eliminating PS point on flat area (low slope). If PS point locate on flat area (slope angle < 15°), it will be deleted. Result of displacement of mass along slope or V_{SLOPE} are shown on Figure 4.8 for ascending orbit direction and Figure 4.0. Then, 2 result remain PS point around 7,352 for ascending orbit direction and 8,984 for descending orbit direction. These results correspond to the objective of this research.
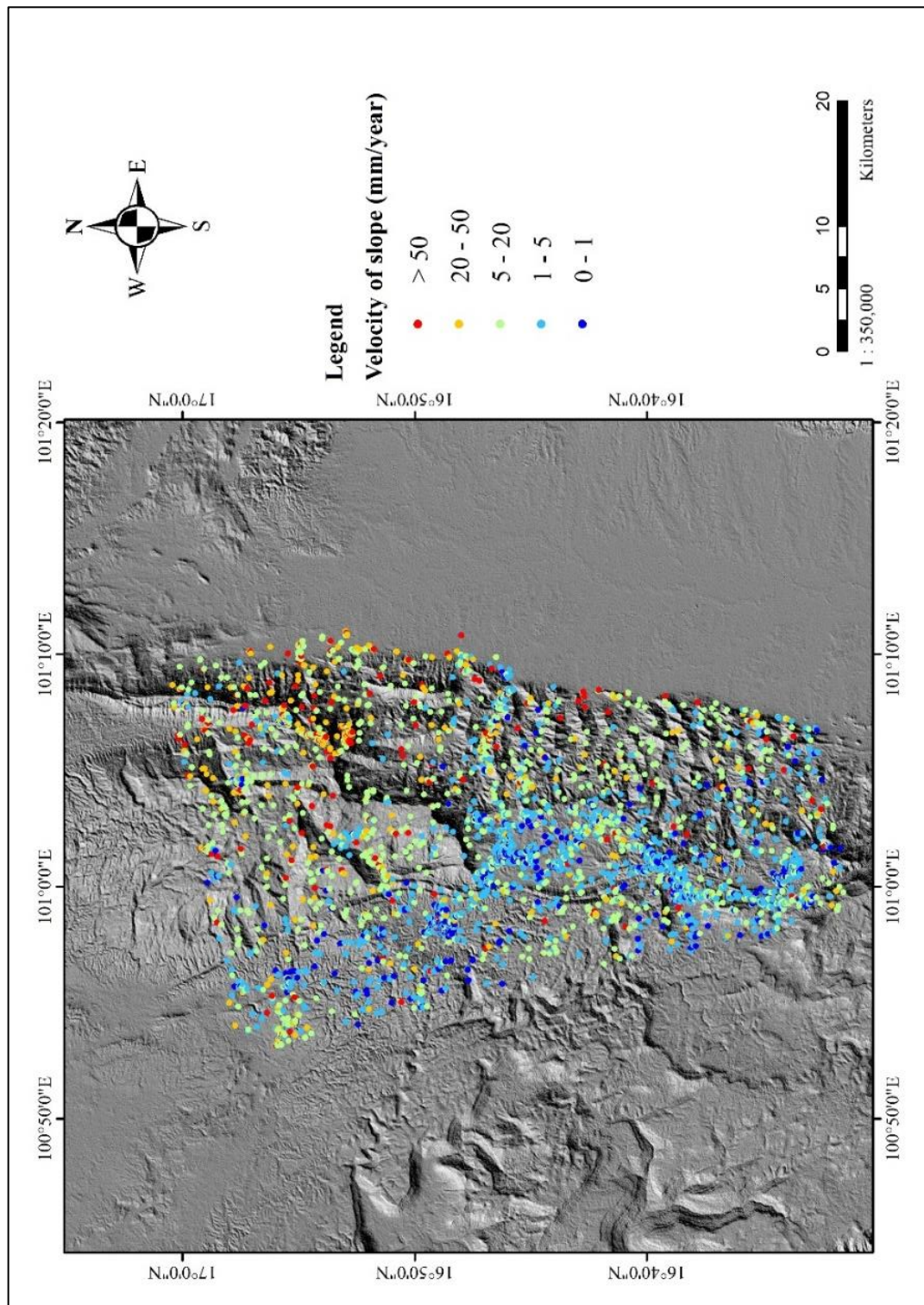
Figure 4.6 PS point contain displacement rate along slope, ascending orbit
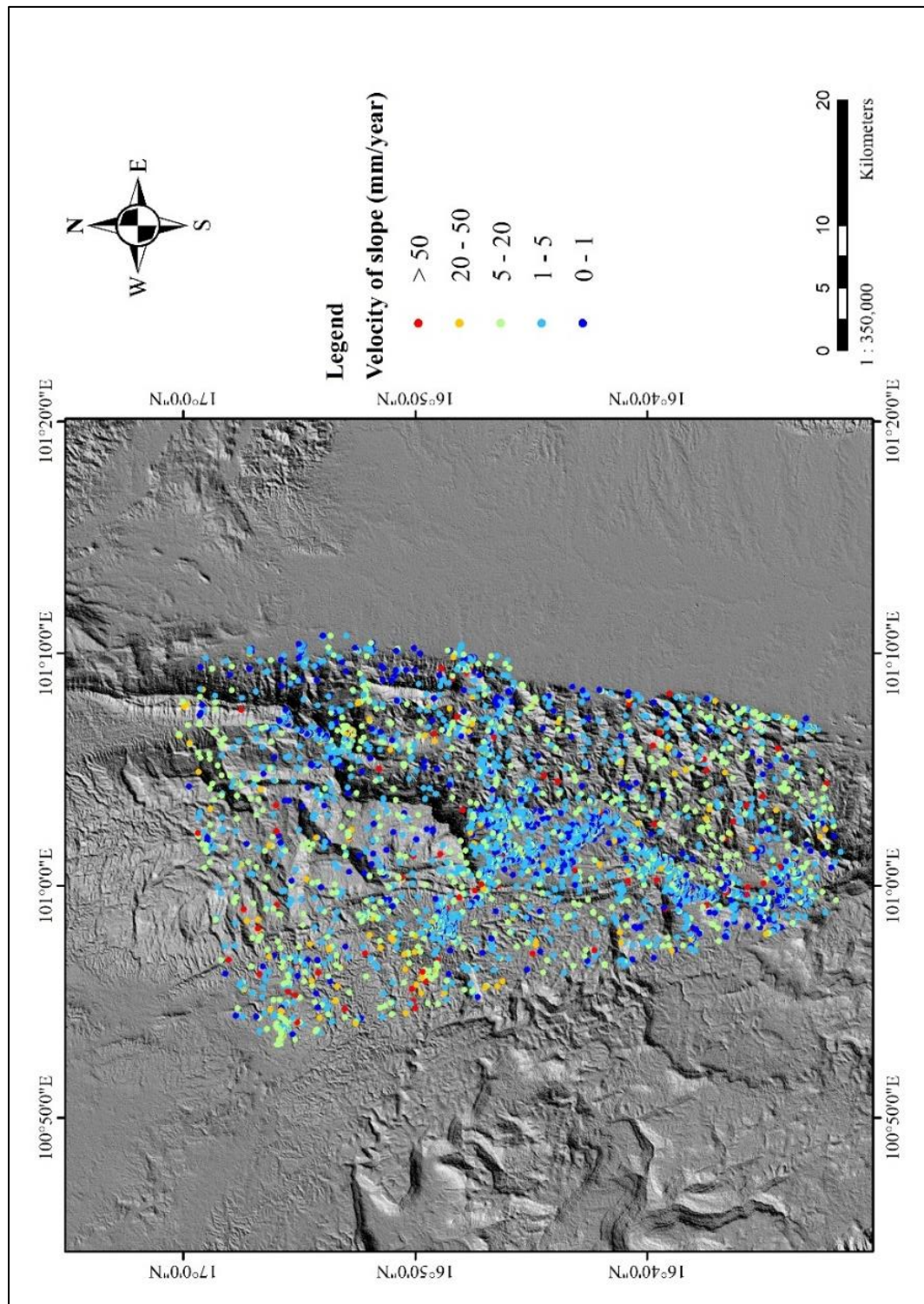
Figure 4.7 PS point contain displacement rate along slope, descending orbit.

4.3 Mass wasting classification from PSInSAR displacement rate

Mass wasting investigation can provide various terms, in this study performed 2 terms including ground displacement rate investigation and mass wasting type classification. The main result of this study obtained by time-series InSAR analysis, which is PS point and ground displacement rate (mm/year) (V_{SLOPE}). In this topic, will provide results for classify mass wasting types. According to the chapter 2, mass wasting can characterize by ground displacement rate. Figure 4.8 and Figure 4.9 show map contain with V_{SLOPE} results from both ascending and descending acquisition respectively. Some PS point will not use for classifying mass movement, because they are in plain area.

Classification from International Union of Geological Sciences Working Group on landslide, 1995 scale This working group suggested a developed slope velocity scale, which is based on Varnes (1978). They separated slope velocity to 7 classes, which velocity value and described how the movement of them (Table 4.1). All results from Chapter IV will identify types by Figure 4.8 and Figure 4.9 show classified PS points by the velocity description from International Union of Geological Sciences Working Group on landslide, 1995 scale. The dominant velocity description class is Extremely slow, there are 5,805 for ascending, 1,537 for descending orbit and very slow type, there are 1,537 for ascending 859 for descending orbit. The Slow velocity type is lower to less quantity, there are 10 for ascending and 6 for descending.

Table 4.1 The classification of mass wasting by displacement rate base on International Union of Geological Sciences Working Group on landslide, 1995 scale associated by USGS criteria.

Description	Velocity (mm/year)	Mass wasting types							
		Falls	Topple	Slides	Spreads	Flows	Debris Avalanche	Earth flow	Creep
extremely slow	< 1.6 x 10		○	○					○
very slow	1.6×10^3		○	○					○
slow	1.6×10^5		○	○	○			○	
moderate	1.6×10^7		○	○	○			○	
rapid	1.6×10^9		○	○	○	○	○	○	
very rapid	1.6×10^{11}	○	○			○	○	○	
extremely rapid	$> 1.6 \times 10^{11}$	○	○			○	○	○	
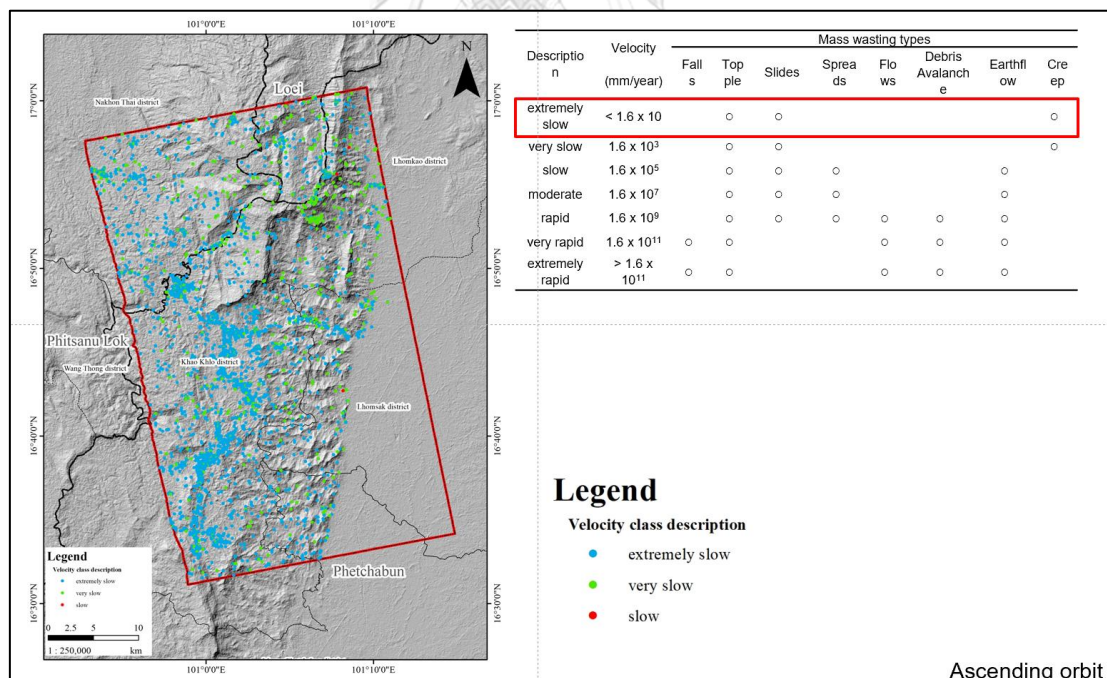
Figure 4.8 PS points were classified to 3 class of ascending orbit result

Descriptio n	Velocity (mm/year)	Mass wasting types							
		Fall s	Top ple	Slides	Sprea ds	Flo ws	Debris Avalanch e	Earthfl ow	Cre ep
extremely slow	< 1.6 x 10		○	○					○
very slow	1.6 x 10³		○	○					○
slow	1.6 x 10⁵		○	○	○			○	
moderate	1.6 x 10⁷		○	○	○			○	
rapid	1.6 x 10⁹		○	○	○	○	○	○	
very rapid	1.6 x 10¹¹	○	○			○	○	○	
extremely rapid	> 1.6 x 10¹¹	○	○			○	○	○	
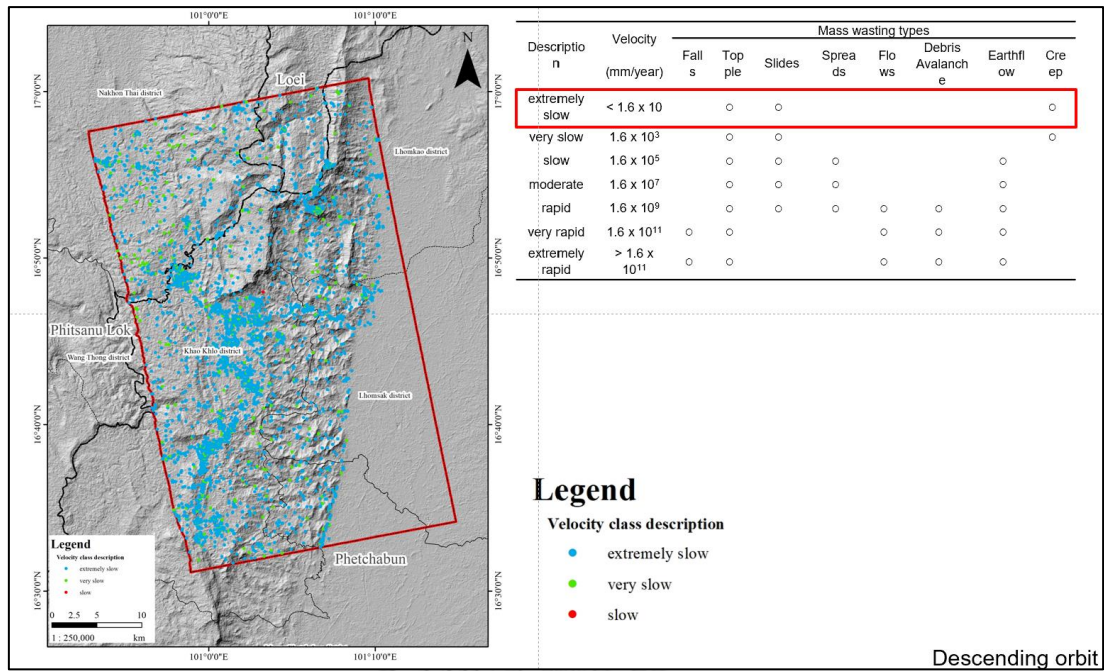
Figure 4.9 PS points were classified to 3 class of ascending orbit result
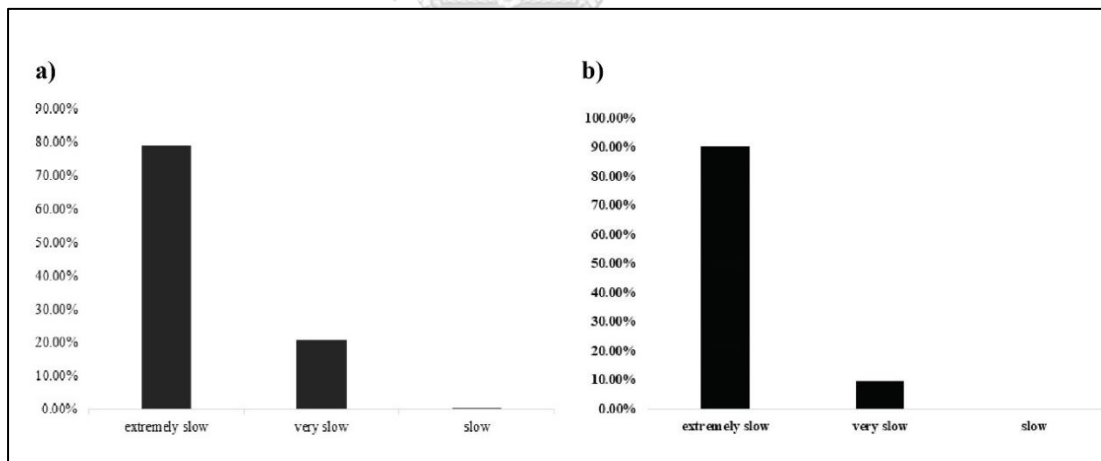
Figure 4.10 displacement rate description chart show percent for each class

Figure 4.10 present the classified mass wasting type chart from PSInSAR results. Most PS point with velocity value is represented by extremely slow to slow class. Conversely, rapid to extremely rapid class represent small number of PS point, moreover those point located alone and far from point cluster. Following defining movement velocity class, in the order to classify mass wasting type according to Chapter 2 most PS

point is classified to "soil Creep" from the result of both ascending and descending orbit.

Chapter 5   DISCUSSION

5.1 V_{slope} PS points result compare with landslide susceptibility map

Landslide susceptibility of DMR provides area and the spatial probability of a mass wasting event. The statistical model was applied and integrated GIS application and the geographic data. The method for the DMR susceptibility map is the Frequency Ratio (FR), which assess and evaluate the susceptibility map with GIS data obtained by field surveying, rainfall record, and interpreted data (landslide scar). The landslide susceptibility map published by the DMR, there are five susceptibility levels of the landslide: very low susceptibility (blue color), low susceptibility (pink color), medium susceptibility (light orange), high susceptibility (orange), very high susceptibility (yellow color).

This study, PS points from the result in Chapter IV overlay with the DMR landslide susceptibility map. For the comparison of PS points result of ascending orbit, which shows quantity PS point setting on susceptibility zone. The extremely slow PS point is the largest number of all PS points for Ascending and Descending orbit. Those points are in low susceptibility area of about 3,268 for Ascending orbit (Figure 5.4) and 4,256 for Descending orbit (Figure 5.5), because the location of the Extremely slow points, which are mostly concentrated in urban areas. The PS point distribution map displaying the continuity and density of those along buildings or road in Khao Kho district. Another reason is the area characterized by low-slope terrain, is considered relatively stable in terms of mass wasting occurrences. Therefore, landslide susceptibility of DMR and displacement investigate by PSInSAR result are correspondence for extremely slow both ascending and descending orbit. While PS points containing the Slow displacement are a largest number on low susceptibility zone, that about 598 slow displacement PS point and 468 PS point on medium susceptibility zone. Although amount of slow and extremely slow PS points for each susceptibility zone are similar, but the ratio for each susceptibility zone has differential between extremely slow and very slow displacement rate. The percentage of Very slow PS point on High susceptibility zone is about 19 %, but the percentage of

extremely slow PS point on High susceptibility zone is only 4 %. That describing, region with high displacement rate might be in high mass wasting susceptibility zone.
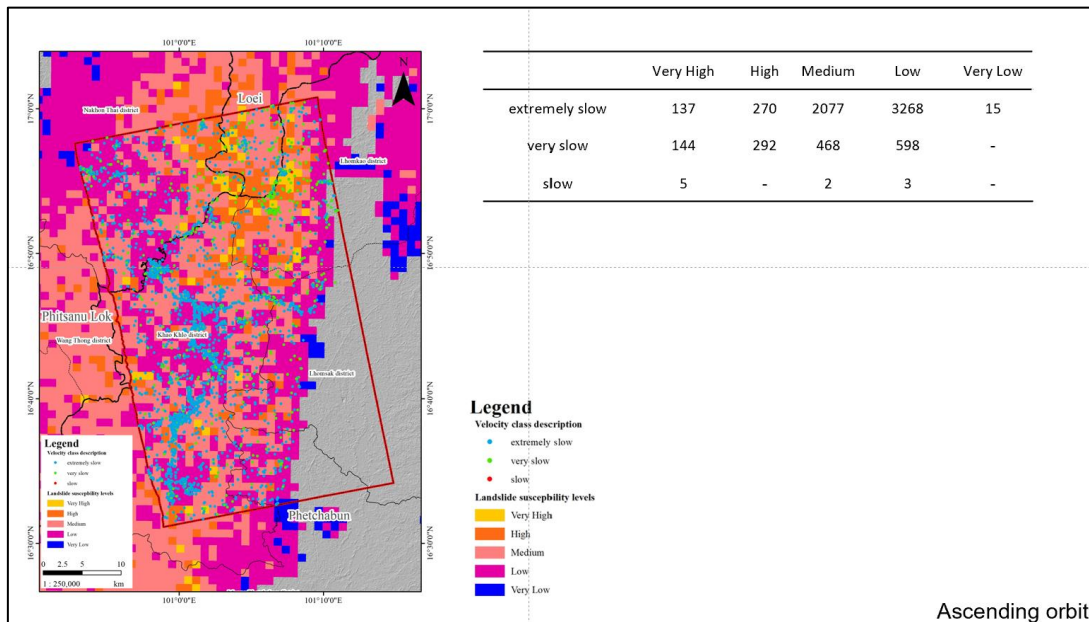

	Very High	High	Medium	Low	Very Low
extremely slow	137	270	2077	3268	15
very slow	144	292	468	598	-
slow	5	-	2	3	-

Figure 5.1 The displacement rate classified PS point of ascending orbit overlay the landslide susceptibility map of DMR

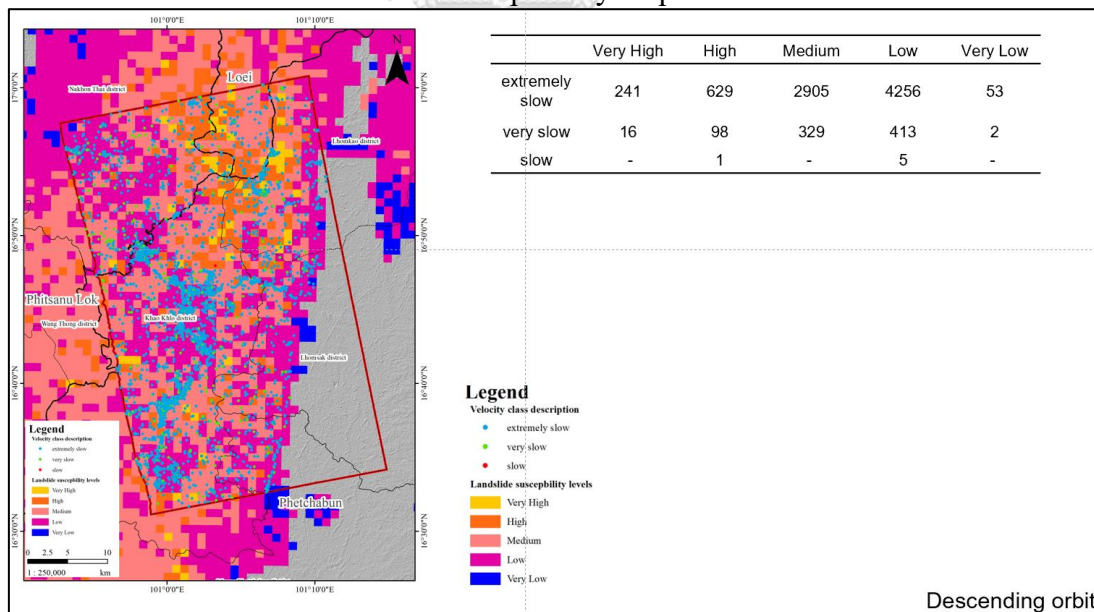|	Very High	High	Medium	Low	Very Low
extremely slow	241	629	2905	4256	53
very slow	16	98	329	413	2
slow	-	1	-	5	-

Figure 5.2 The displacement rate classified PS point of descending orbit overlay the landslide susceptibility map of DMR,

When comparing the results obtained from this study with the susceptibility of debris flow and debris flood in Nam Ko sub-catchment

studied by Yumuang (2006). Debris flow and Debris flood in Nam Ko sub-catchment are compared them with the PS points obtained from the PSInSAR analysis (Figure 5.6) and (Figure 5.7). For the ascending orbit, there are 115 PS points in Nam Ko area, with most of the PS points classified as "extremely slow," with an average velocity about 11 mm/yr. in the other hand, for the descending orbit, there are 218 PS points, with most of them also classified as "extremely slow," with an average velocity about 27 mm/yr. The considering PS points distribution, for the ascending orbit, there are very few PS point and most of them located in the low susceptibility areas, and some points falling into the very low susceptibility level, and only some located at the "moderate" level. However, a higher density of PS points is found in the stream areas, which, according to Yumuang (2006)'s susceptibility map, are classified stream and around as high and very high susceptibility areas. On the other hand, the PS points obtained from the descending orbit provide 218 PS points, which show a distribution along the slopes similar with ascending orbit, but with a higher density are located at Nam Ko reservoir more than PS points from ascending orbit.

Figure 5.3 PS point of ascending orbit plotting with debris flow and debris flood susceptibility map of Yumuang (2006)

Figure 5.4 PS point of descending orbit plotting with debris flow and debris flood susceptibility map of Yumuang (2006)

5.2 V$_{slope}$ PS points result compare with slope stability map

Chansorn et al. (2023) assessed the stability of slopes within the Huai Nam Phung subbasin in Thailand using a hydrological model to evaluate landslide events. One part of this study shown the slope stability map, that result including stable and unstable area calculating by groundwater levels during period of interesting and physical characteristics of study area. It was found that on October 30, 2017, there was the unstable slopes, with up to 80% of the total slope area being unstable. This was confirmed by comparing it with records of 63 landslide occurrences in areas with slope stability less than 1.0.

When comparing the results obtained from Chansorn et al. (2023) with V$_{slope}$ PS points, as shown in Figure 5.8 and Figure 5.9, it involves comparing the PS points that have been evaluated and reclassified already, both in the ascending and descending orbits. For the ascending orbit, there were a total of 648 PS points, with an average value of -82 mm/yr. However, there was a significant standard deviation of up to 476 mm/yr., because of a considerable difference between the average value and the maximum displacement, while, for result from the descending orbit, there were 821 PS points, with an average of 11 mm/yr and a standard deviation of 37 mm/yr.

It can be observed that the PS points, both in the ascending and descending orbits, exhibit a distribution pattern in the western part of Huai Nam Phung, which cover Phetchabun mountain range. In the mentioned area, it has been evaluated as an unstable region, particularly in Phu Thap Boek, which has recorded landslide incidents, as will be discussed in the next section.
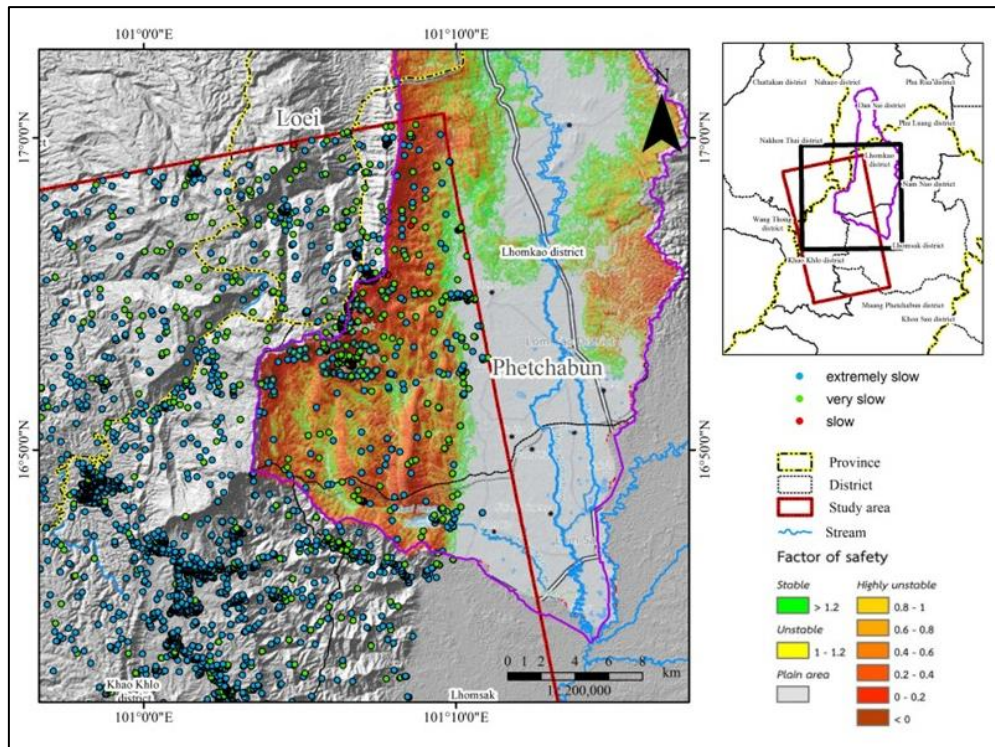
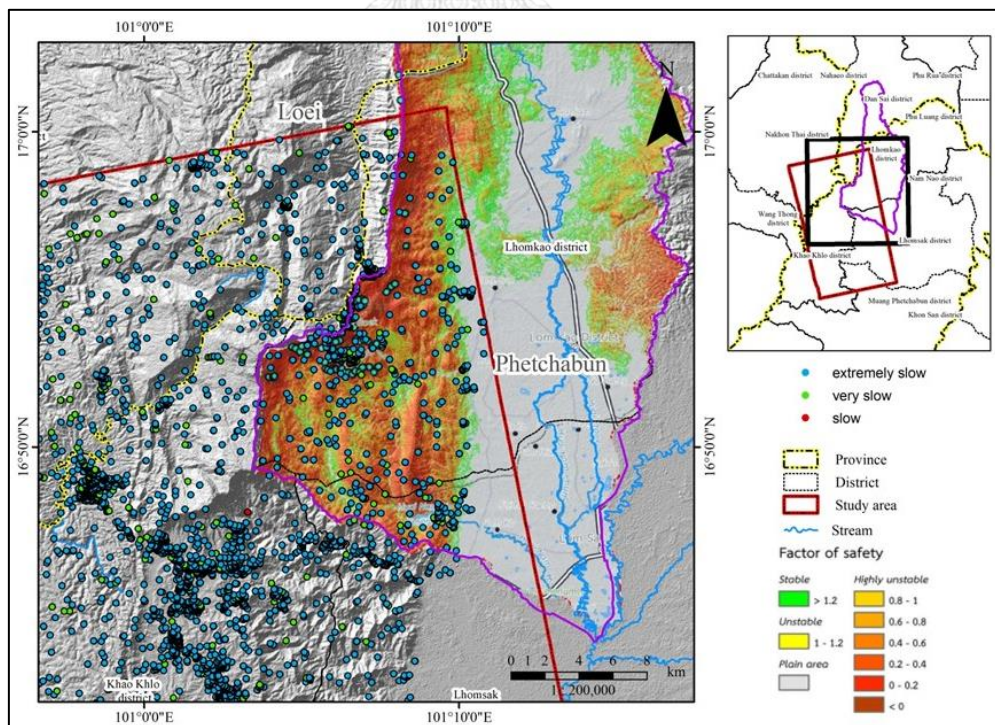**Figure 5.5** PS point of ascending orbit plotting with slope stability by
Chansorn et al., (2023)

Figure 5.6 PS point of descending orbit plotting with slope stability by
Chansorn et al., (2023)

5.3 PSInSAR results comparison with the Landslide inventory from Thailand Department of Mineral Resources

Landslide inventory of DMR is record of landslide and interpret from landslide scar, represent by point data. Figure 5.10 and Figure 5.11 show the distribution of Landslide inventory map in the study area are dense around the south of Phu Thap Boek Mountain. The PSInSAR results plotting with landslide inventory show not related, because the landslide inventory collected by landslide evidence which locate on steep slope surface but PSInSAR appearing on human structures on Phu Thap Boek. That described the limitation for using PSInSAR to update landslide inventory, PSInSAR is not sustainable for detection the mass wasting inventory occurring out of urban areas or less human structures. On the other hand, PSInSAR is suitable for detection though investigation the mass wasting in urban areas.
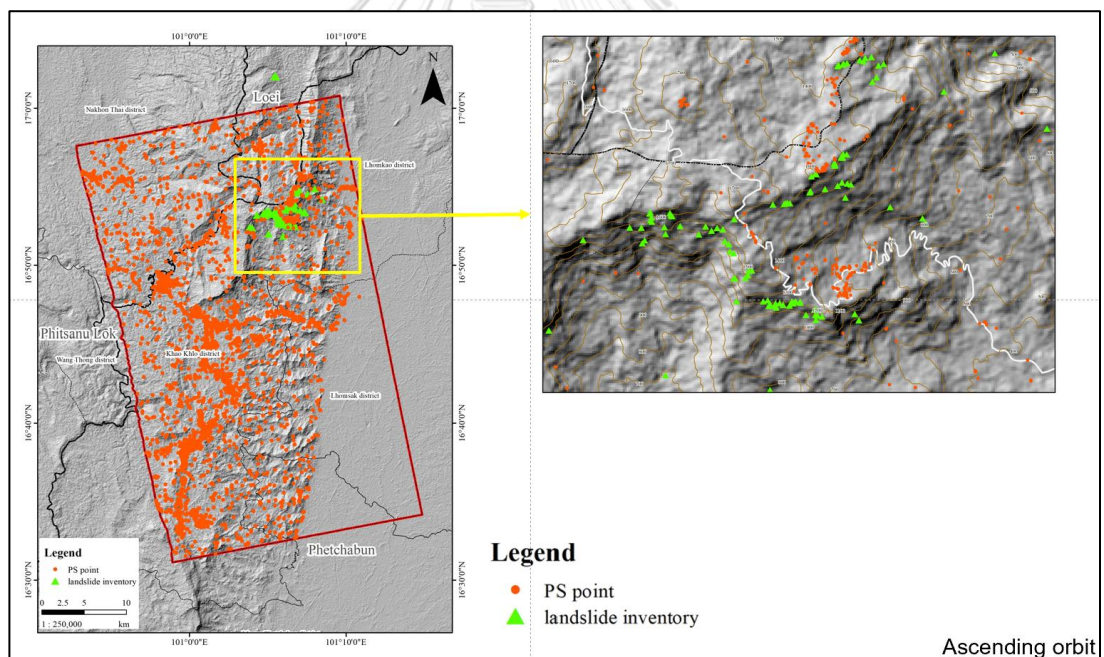

Figure 5.7 PS point of ascending orbit plotting with landslide inventory point collected by DMR and showing data on Phu Thap Boek area
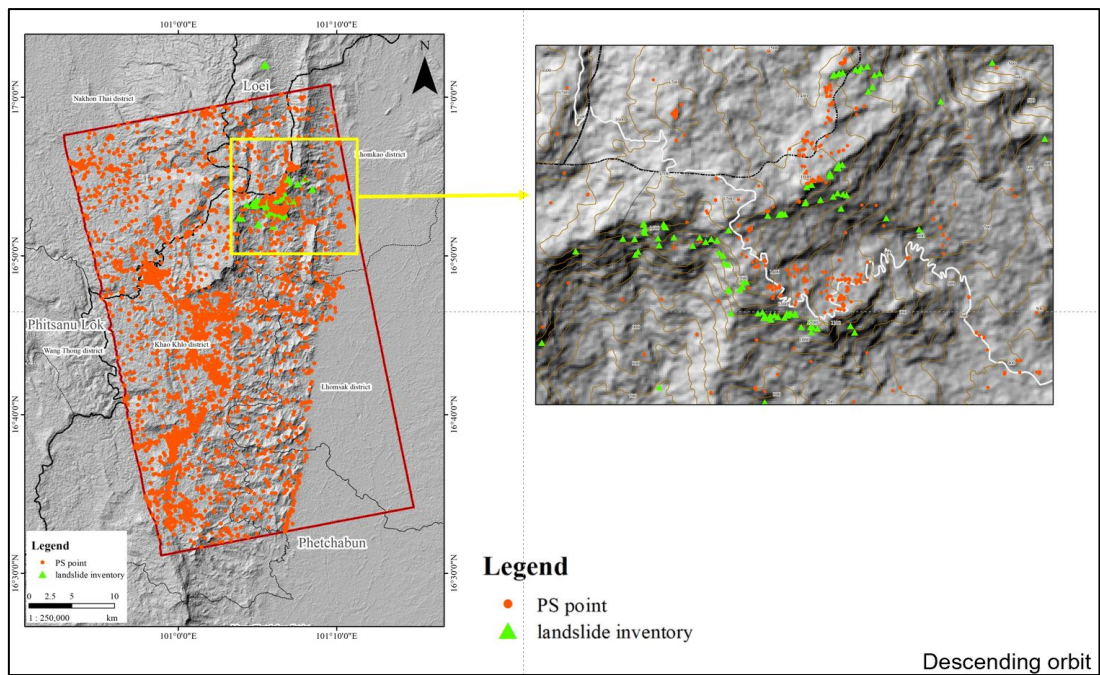
Figure 5.8 PS point of descending orbit plotting with landslide inventory point
collected by DMR and showing data on Phu Thap Boek area

REFERENCES

VITA

NAME   Nuttavit Kumvijairat

DATE OF BIRTH   03 Jan 1995

PLACE OF BIRTH Bangkok, Thailand

INSTITUTIONS   Bangpakok Wittayakom School 2007 - 2013
ATTENDED   Bachelor of Science (Geoinformatics), Faculty of
                    Geoinformatics 2013 - 2016

HOME ADDRESS   81/584 Prachautid Rd., Trung Khru, Bangkok,
                    10140